Naval Oceanographic Office

Stennis Space Center
MS 39522-5001

Technical Report
TR 306
June 1992

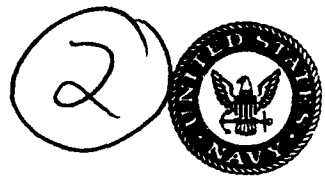

TR 306

CHARACTERIZATION OF THE BOTTOM SEDIMENT VELOCITY-DEPTH RELATIONSHIP FOR THE SOMALI BASIN AND THE ARABIAN SEA

NELSON J. LETOURNEAU

ACOUSTICS DIVISION

Approved for public release; distribution is unlimited.

Prepared under the authority of
Commander,
Naval Oceanography Command

FOREWORD

Knowledge of the geoacoustic parameters of the sea floor is required for accurate prediction of sound propagation in bottom-limited areas. This technical report discusses the acquisition of wide angle bottom reflection data and the development of bottom sediment velocity versus depth curves and functions from these data in the Somali Basin and the Arabian Sea.

ROBERT Y. BELT
Captain, U.S. Navy
Commanding Officer

REPORT DOCUMENTATION PAGE

Form Approved
OMB No. 0704-0188

1. AGENCY USE ONLY (Leave blank)	2. REPORT DATE	3. REPORT TYPE AND DATES COVERED
	June 1992	

4. TITLE AND SUBTITLE

Characterization of the Bottom Sediment Velocity-Depth Relationship for the Somali Basin and the Arabian Sea

5. FUNDING NUMBERS

6. AUTHOR(S)

Nelson J. LeTourneau

7. PERFORMING ORGANIZATION NAME(S) AND ADDRESS(ES)

Naval Oceanographic Office
Stennis Space Center, MS 39522-5001

8. PERFORMING ORGANIZATION REPORT NUMBER

TR 306

9. SPONSORING/MONITORING AGENCY NAME(S) AND ADDRESS(ES)

Commander, Naval Oceanography Command
Stennis Space Center, MS 39529-5000

10. SPONSORING/MONITORING AGENCY REPORT NUMBER

11. SUPPLEMENTARY NOTES

12a. DISTRIBUTION/AVAILABILITY STATEMENT

Approved for public release;
distribution is unlimited.

12b. DISTRIBUTION CODE

13. ABSTRACT (Maximum 200 words)

In the study and modeling of sound propagation of the ocean bottom, one of the most important parameters is the velocity of sound versus depth in the bottom. To provide this parameter in the Somali Basin and the Arabian Sea, each area was sampled with velocity-depth measurements by the wide-angle bottom reflection method. Sediment surface sound velocity and bottom water sound velocity were collected as supporting data. From these data, instantaneous velocity functions and velocity-depth functions were derived using the method of Houtz et al. (1968, 1970) and Bachman and Hamilton (1980). Data from groups of stations were used to derive a representative function for an area or line of stations. Based on the results of the analysis, a minimum number of representative functions were derived for the larger area. In the Somali Basin, a maximum of three functions adequately characterizes the relationship for the area. In the Arabian Sea, due to the physiography, four functions are needed to characterize the relationship throughout the area. In the course of the work, a close relationship of sediment surface velocity and depth was noted. This was verified by plotting the sediment surface sound velocity versus depth and fitting these data with a least-squares line. A correlation coefficient was used to verify the relationship. (continued on reverse)

14. SUBJECT TERMS

Arabian Sea, Somali Basin, Bottom Sediment, Wide Angle Reflection, Layer Thicknesses, Average Velocity, Instantaneous Velocity, Velocity-Depth Relationship, Velocity Ratio, Reflectivity

15. NUMBER OF PAGES

144

16. PRICE CODE

17. SECURITY CLASSIFICATION OF REPORT	18. SECURITY CLASSIFICATION OF THIS PAGE	19. SECURITY CLASSIFICATION OF ABSTRACT	20. LIMITATION OF ABSTRACT
UNCLASSIFIED	UNCLASSIFIED	UNCLASSIFIED	SAME AS REPORT

REPORT DOCUMENTATION PAGE (CON.)

Block 13 (Continued):

This relationship is believed to be due to the water included in the samples cored, thus the bottom water velocity versus depth was plotted and fitted with a least-squares line. The slope of the lines for the sediment velocity versus depth and the bottom water velocity versus depth are compared. In both the Somali Basin and the Arabian Sea, the two quantities are nearly identical. Thus, it is concluded that the sediment surface sound velocity is definitely a function of depth in deep water areas.

CHARACTERIZATION OF THE BOTTOM SEDIMENT VELOCITY-DEPTH RELATIONSHIP FOR THE SOMALI BASIN AND THE ARABIAN SEA

A DISSERTATION SUBMITTED TO THE GRADUATE DIVISION OF THE UNIVERSITY OF HAWAII IN PARTIAL FULFILLMENT OF THE REQUIREMENTS FOR THE DEGREE OF

DOCTOR OF PHILOSOPHY

IN

GEOLOGY AND GEOPHYSICS

MAY 1991

By

Nelson J. LeTourneau

Dissertation Committee

Frederick Duennebier, Chairman
Pow F. Fan
Murli H. Manghnani
Gregory Moore
Alexander Malahoff

We certify that we have read this dissertation and that, in our opinion, it is satisfactory in scope and quality as a dissertation for the degree of Doctor of Philosophy in Geology and Geophysics.

DISSERTATION COMMITTEE

Chairperson

ABSTRACT

Two relatively large ocean areas, the Somali Basin and the Arabian Sea, were sampled to determine the bottom sediment velocity versus depth relationship. The sampling method was that described by Clay and Rona (1965) and Le Pichon et al. (1968). This method employs a sonobuoy as the receiver and a ship towing a seismic source moving away at a constant speed and course. The method is known as the variable angle or the wide-angle bottom reflection technique (WABR). The result is a series of layer thicknesses and associated layer average velocities. These interval thicknesses and velocities are then converted to instantaneous velocity-time functions relating velocity to one-way travel time from the sediment surface and then to a velocity versus depth function in the manner described by Houtz et al. (1968, 1970) and Bachman and Hamilton (1980).

In each area, individual station instantaneous velocity-time curves are compared to each other to detect anomalous locations; then instantaneous velocity-time curves developed from groups of stations are used to determine curve variations in terms of compass direction or position. Velocity versus depth functions are derived from the instantaneous velocity-time functions and these also are examined for consistency of the function with respect to area or compass direction.

From this analysis, a minimum number of velocity versus depth functions is chosen to characterize the two large areas, and these are compared to the results of previous investigators of specific areas to ensure general agreement and consistency. These functions differ from each other in the sense that they describe the velocity-depth relationship of the sediments for specific depositional environments and indicate the gradients that might be expected for such areas. They may also be used to gain insight and to generalize on the velocity-depth relationship of the sediments in other ocean areas of similar depositional environment.

TABLE OF CONTENTS

APPENDICES

LIST OF FIGURES

LIST OF FIGURES (CON.)

LIST OF TABLES

ACKNOWLEDGEMENTS

The author gratefully acknowledges the encouragement and support of the Naval Oceanographic Office in this work and the help of many of the personnel of this organization who assisted in the acquisition and processing of the data. I thank the members of my dissertation committee for their time, patience and helpful suggestions. A special thanks to Dr. W.M. Adams, who opened doors long closed and got me on track again.

INTRODUCTION

A. OBJECTIVES

The problem of accurately modeling the world's ocean areas is an overwhelming task requiring nearly unlimited resources and time. Given the resources and time available, the problem can be made tractable by determining the critical parameters in specific areas and then characterizing large areas of generally similar type. That is the approach used in this study. A number of velocity versus depth measurements, sufficient to cover uniformly the area of interest, were made using the sonobuoy technique as described by Clay and Rona (1965) and Le Pichon et al. (1968). The sonobuoy technique is referred to in this thesis as the Wide-Angle Bottom Reflection method (WABR). WABR is particularly useful in this application due to the fact that it requires only one vessel, it can be done while underway and it is relatively inexpensive. The method requires minimal ship support, allowing numerous other oceanographic measurements to be made from the same vessel.

Specific velocity-depth measurements are compared to each other for variation in the relationship with respect to distance and direction throughout the area of interest. In this manner, subareas of similar velocity-depth relationship can be determined and characterized by an average relationship for the subarea. A large ocean area is then characterized by one or a minimum number of velocity-depth relationships.

The Naval Oceanographic Office (NAVOCEANO) employed the USNS WILKES for surveying in the Indian Ocean from the late 1970's to the mid-1980's. The availability of ship time on this vessel and general interest in the geology of the Arabian Sea and the Somali Basin made these two areas a natural choice for this study. The two areas, along with the bottom physiography and the WABR station locations, are depicted in figures 1 and 2. The WABR measurements are referred to as stations, even though the measurement is made over a distance of 9 to 10 nautical miles, for ease in cataloging and for giving specific locations for the measurement. The point used as a location for the measurement in this report is that point where the sonobuoy was deployed into the water.

B. BACKGROUND

Somali Basin

The Somali Basin is defined by the area bounded on the north by the Carlsberg Ridge, on the west by the east coast of Somali, Kenya and Tanzania, on the south by the Comoros Islands and Madagascar and on the east by the Seychelles and Mauritius Plateau.

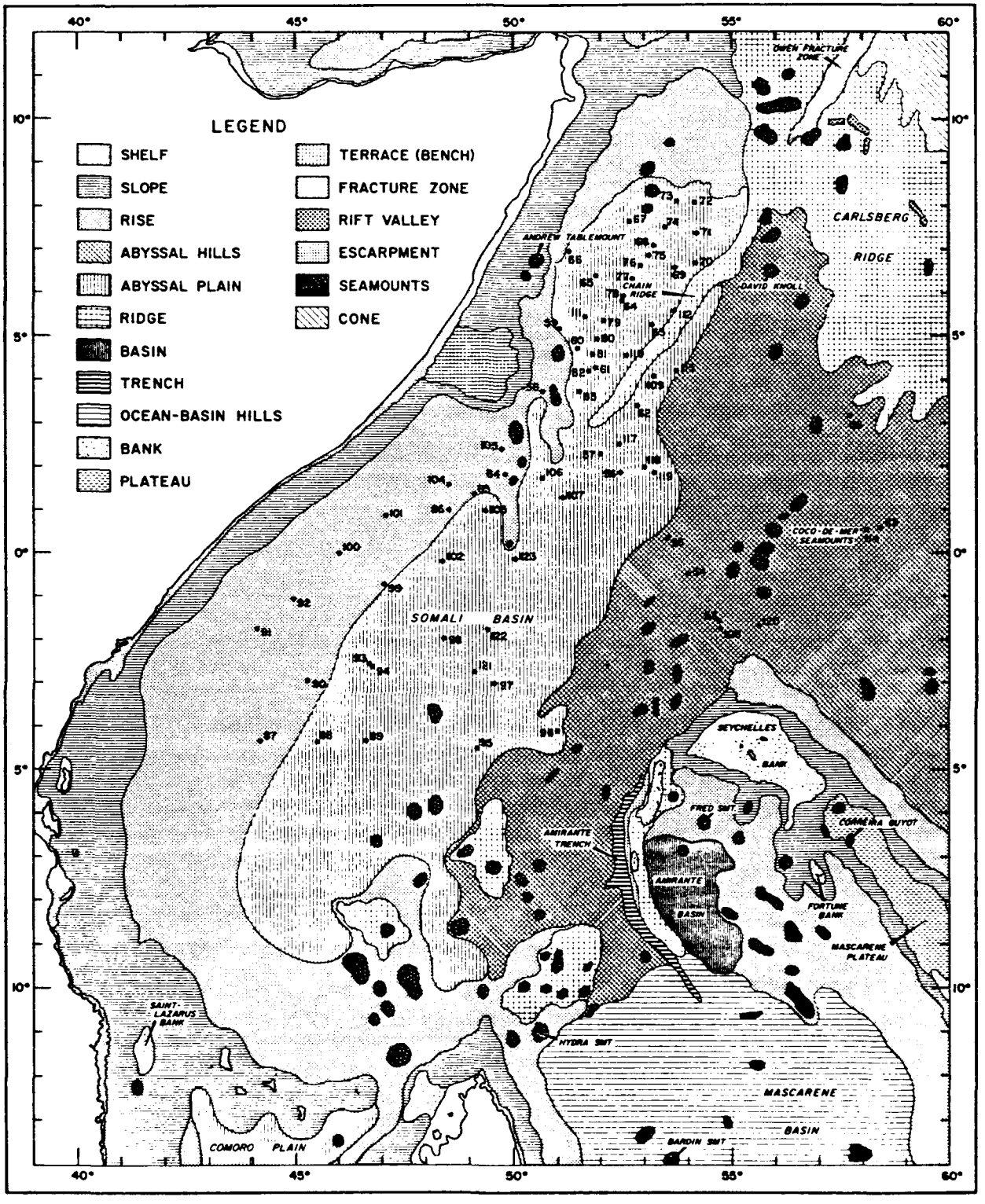

Figure 1. Somali Basin Physiography and Station Locations.

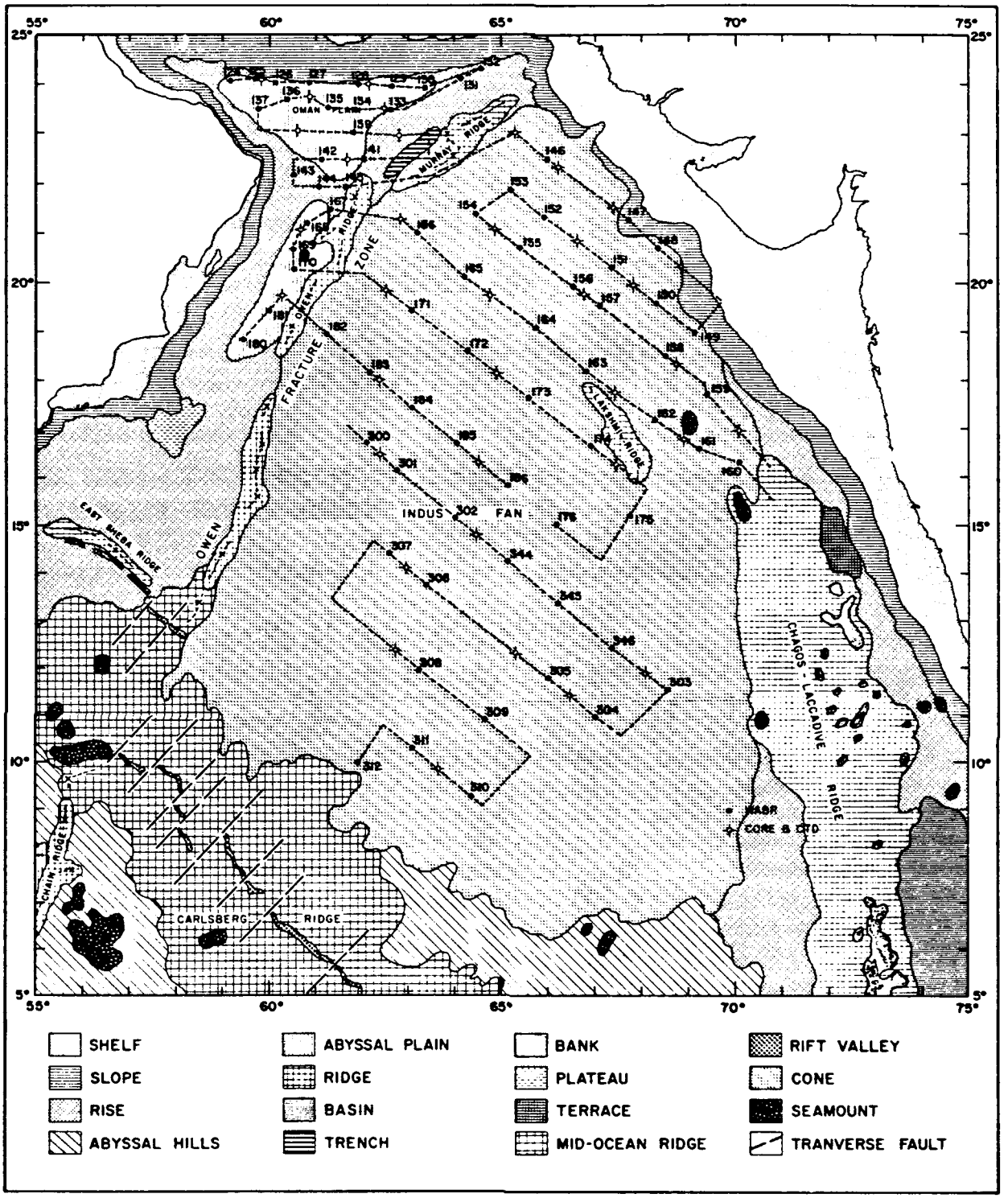

Figure 2. Arabian Sea Physiography and Station Locations.

Five cruise legs were devoted to the Somali Basin, during which a total of 70 usable stations were chosen to take advantage of the physiography and to provide for adequate coverage of the area. These stations are superimposed on the physiography of the Somali Basin, as indicated in figure 1. Station numbers refer to successive WABR stations taken by NAVOCEANO. Along with the interval velocity measurements, 45 usable cores and 57 sound velocity, salinity, temperature, depth (SVSTD) measurements were made, and continuous seismic profiles were taken on each leg.

Considerable seismic profiling in the Somali Basin was conducted by Ewing et al. (1969) and Bunce et al. (1967), as well as refraction profiling by Francis et al. (1966); however, only a small number of interval velocity measurements were previously available as noted by Hamilton (1980). Good discussions of the area are given in Francis et al. (1966), Bunce et al. (1967) and Davies and Francis (1964). The physiography of the Somali Basin is illustrated in figure 1. The Somali Basin is made up of several relatively isolated abyssal plains, abyssal hills or swales, continental rise areas of the African Coast, the Mascarene Plateau and the Carlsberg Ridge. In the northern portion of the basin, Chain Ridge separates two abyssal plain areas and almost pinches out the western of the two plains against the African Continental Rise. A larger abyssal plain extends southward, and a smaller abyssal plain with swales exists to the north and east of the Seychelles Islands. Bunce et al. (1967) pointed out that the depth to basement abruptly changes at the southern edge of Chain Ridge at approximately 3° 30' S latitude, and that the northern and southern parts of the Somali Basin are very different. The northern part has a deep basement covered with thick, mostly uniformly stratified terrigenous sediments, and it has a distinct geoid low and large negative gravity anomalies. This geoid low and the large gravity anomalies are believed to be the result of the superposition of a continental edge effect anomaly and the fracture zone effect (Cochran, 1988).

The southern part of the Somali Basin has a shallow basement with high relief covered with stratified flat-lying sediments filling the basement depressions, with isolated hills of basement material rising above the abyssal plain deposits. The basin is believed to have been formed during the southward movement of east Gondwanaland with the northern basin being the third of a series of oceanic basins, the other two being the Mozambique Basin and the Southern Basin, separated by long transform faults (Cochran, 1988). According to DuToit (1937) Madagascar was displaced from the African Coast in the large crustal movement in which India separated from Africa leaving the Seychelles Islands behind. Cochran (1988) suggested that the original Northern Basin was split apart by the movement cited by DuToit and that Chain Ridge formed along the new boundary. In a study of sea floor age and fracture zone trends as constraints on continental reconstruction by Burroughs, an investigator

(Sowerbutts) relates development of the East African Rifts with the southeastward movements of the continents out of the present day Somali Basin area (Burroughs, 1977). Burroughs disputed the age relation but not the concept. The development of ridges, scarps and volcanoes cited by various investigators of the Somali Basin is typical of the present-day development of these features in the East African Rift system, matching the definition of fracture zones by Menard and Chase (1970).

Burroughs (1977) suggested that turbidites make up a negligible portion of the sediments in the Somali Basin. However, other investigators have suggested that a large portion of the sedimentary section in both the Northern and Southern Basins is due to turbidite flows. Bunce et al. (1967) ran profiles in both basins and attributed much of the sediment section to turbidity flows based on the clearly defined stratification in the uppermost sequence. This sequence occurs in both basins and is underlain by a generally acoustically transparent sequence, and then by a third sequence which shows some stratification. NAVOCEANO seismic profiles are in complete agreement with the conclusions by Bunce (1967). Sediments in the Northern Basin are on the order of 2.0 seconds of two-way travel time thick and the uppermost section, thickly stratified, is on the order of 0.75 seconds thick. In the Southern Basin, the total sediment thickness is less than that of the Northern Basin, on the order of 1.5 seconds of two-way travel time. The uppermost sequence is about 0.5 seconds thick, which is about the same proportion relative to the deeper sediments as in the Northern Basin. The sediment section of the Continental Rise is considerably thicker than that in both of the Basins and heavily stratified sequences of 1 second or more of travel time are found here. (See figure 3.) Thus, it is estimated that turbidity flows contribute at least 30% and possibly as much as 40% of the sedimentary section, with the African Coast considered to be the primary source of these sediments.

Arabian Sea

The Arabian Sea is bounded on the north by the southern extremes of Iran and Pakistan, on the east by India, on the west by the Arabian Peninsula and on the south by the Carlsberg Ridge. Four cruise legs were devoted to the study of the Arabian Sea area over a period of 3 years. The inadequacy of the WABR method in shallow water, due to the strong overriding multiples, precluded work on the continental shelf in this area, as in the Somali Basin. The intractability of the seismic methods in the ridge provinces, due to multipath returns, left only the deltaic fan and abyssal plain areas for study.

The physiography of the Arabian Sea is dominated by the huge Indus Cone, the deltaic outpouring of the Indus River and the resting place for the erosion products from the highlands of India and Pakistan. Multichannel seismic investigations by Societe Nationale Elf Aquitain Petroleum have shown that there

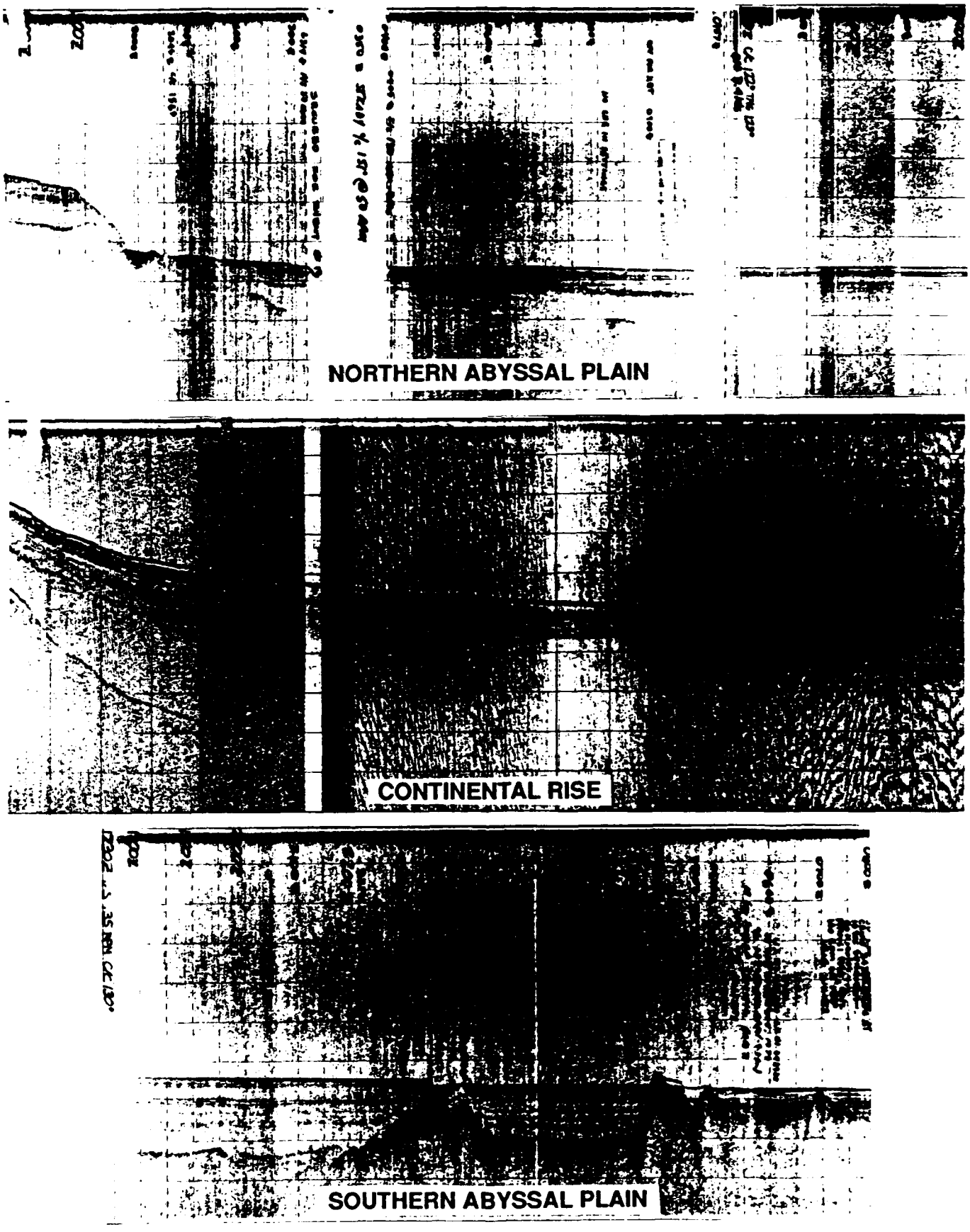

Figure 3. Illustration of Seismic Vertical Profile Records in Somali Basin.

is a thickness of more than 35,000 feet (10,370m) of sediment at the head of the Indus Cone. The remainder of the basin includes a small triangular abyssal plain known as the Oman Abyssal Plain, a long, narrow abyssal plain between the Murray Ridge-Owens Fracture Zone and the continental shelf of the Arabian Peninsula (known as the Owens Abyssal Plain), as well as surrounding ridges and the Chagos-Laccadive Plateau. (See figure 2.) The southern edge of the Indus Cone is bounded by the Carlsberg Ridge, the northern extension of the Mid-Ocean Ridge. The western edge of the Cone is bounded by the Murray Ridge, extending from the shelf of Pakistan, and the Owen Fracture Zone, extending just to the east of Socotra. The eastern boundary of the Cone is formed by the shelf of India and the Chagos-Laccadive Plateau. The continental shelves of Pakistan, Iran and Oman, along with the Murray Ridge, form the boundaries of the Oman Abyssal Plain. The two abyssal plains and the Cone are the subject of study in this area.

The Oman Abyssal Plain and the Owens Abyssal Plain are part of the Arabian Plate, while the Indus Fan is part of the Indian Ocean Plate. White and Ross (1979) demonstrated that the northern wall of the Oman Abyssal Plain is the frontal portion of a huge accretionary wedge of sediments resulting from the underthrusting of the Oceanic Plate. White and Klitgord (1976) have described the imbricated fold structure in this accretionary wedge and the continued filling in of the interfold basins by detritus from the Makran Coast. The basin itself is part of the Arabian oceanic plate thrusting northward. Their multichannel work show the basin to have a thick sequence, thickening to the north and abruptly terminating against the imbricated wedge. Our east-west seismic lines start just south of the frontal fold and progressed southward. Thus, our seismic records show only the flat-lying abyssal plain deposits.

An exhaustive study of the Indus Fan was recently published by Kolla and Coumes (1987). Kolla extensively studied the Indus Cone for some time and some of the data used in his reports is from the cruises undertaken for this study. A definitive study of the surficial sediments of the Indus Cone was published by Kolla et al. (1981). In that study, they divide the fan into upper, middle and lower regions based on the 3.5 KHz and seismic profile characteristics. Two prominent features in the Indus Fan are the Lakshmi Ridge and the Chagos Lacadive Ridge. It was against the Lacadive Ridge that we delineated the eastern edge of our survey. Naini and Kolla (1981) note that there are somewhat higher velocity basal sedimentary layers following the structural trends of the basement in the upper and middle regions. They believe these layers are pelagic, while the upper sedimentary layers have been deposited by turbidity currents.

I. INSTRUMENTATION FOR DATA COLLECTION

The wide-angle bottom reflection method (WABR) requires a shipborne sound source, a sonobuoy to receive the reflected signals, a radio receiver to pick up the transmissions from the sonobuoy and a recording device to record the received data. The sound source used on the USNS WILKES was a 90-kilojoule sparker system consisting of three 30-kilojoule units fired simultaneously. The three sparkers were towed behind the ship, about 75 feet aft, with each individual sparker consisting of two plastic-coated solid conductors in a ladder-type arrangement held a foot apart by plastic spacers. (See figure 4.) A hydrophone streamer was also towed behind the ship for simultaneous vertical seismic profiling. The sonobuoys used during most of the survey were U.S. Navy-type AN/SSQ-41A as depicted in figure 5. In later stages of the work, AN/SSQ57A-type sonobuoys were used. The radio receiver in the system was a Watkins-Johnson model 8730 A with two band selections, 0-30 MHz and 30-600 MHz, and a Yagi log periodic antenna with an antenna preamplifier. The raw data from the receiver were recorded on one FM and one AM channel of a Hewlett-Packard model 4968A precision instrumentation eight-track tape recorder and paralleled to a Teledyne seismic amplifier model 24220. The filtered and amplified output was displayed on a Raytheon model 1811 line scan recorder. A second Raytheon recorder recorded the vertical reflection profile data from the hydrophone streamer array during the WABR measurement.

Along with the WABR system, the ship carried other types of instrumentation to obtain data to support the velocity-depth measurements. Navigation equipment included the Magnavox model 706 satellite receiver units, which later were replaced with Magnavox 1107 units. For water column data, a Bisset-Berman (Plessey) model 9040 sound velocity, salinity, temperature, depth (SVSTD) unit was used during the earlier part of the work, and later replaced with a Neil Brown Model Mark 111 conductivity, temperature, depth (CTD) unit. Supporting core data were obtained with a 2000-pound modified Ewing corer with a 20 foot barrel. Underway total magnetic field intensity data were collected using a Geometrics model G801 marine proton precession magnetometer towed 250 meters behind the ship. Bathymetric measurements were continuously made while underway, employing a Harris model 853D 12-KHz Narrow-Beam Echo Sounder manufactured by General Instruments Corporation. This system produces a beam pattern having a beam angle of 2 2/3 degrees and is pitch and roll stabilized electronically using the ship's Mark 19 gyrocompass for stable reference. A subbottom profile was obtained with an Edo 3.5-KHz unit. Expendable bathythermograph data (XBT) were collected periodically using XBT T-7 probes (750-meter depth) and a Sippican Mark 2A recorder. The reliability of this system was enhanced by its simplicity; therefore, it supplied a large quantity of data. The instrumentation used was standard throughout the industry and was returned to the

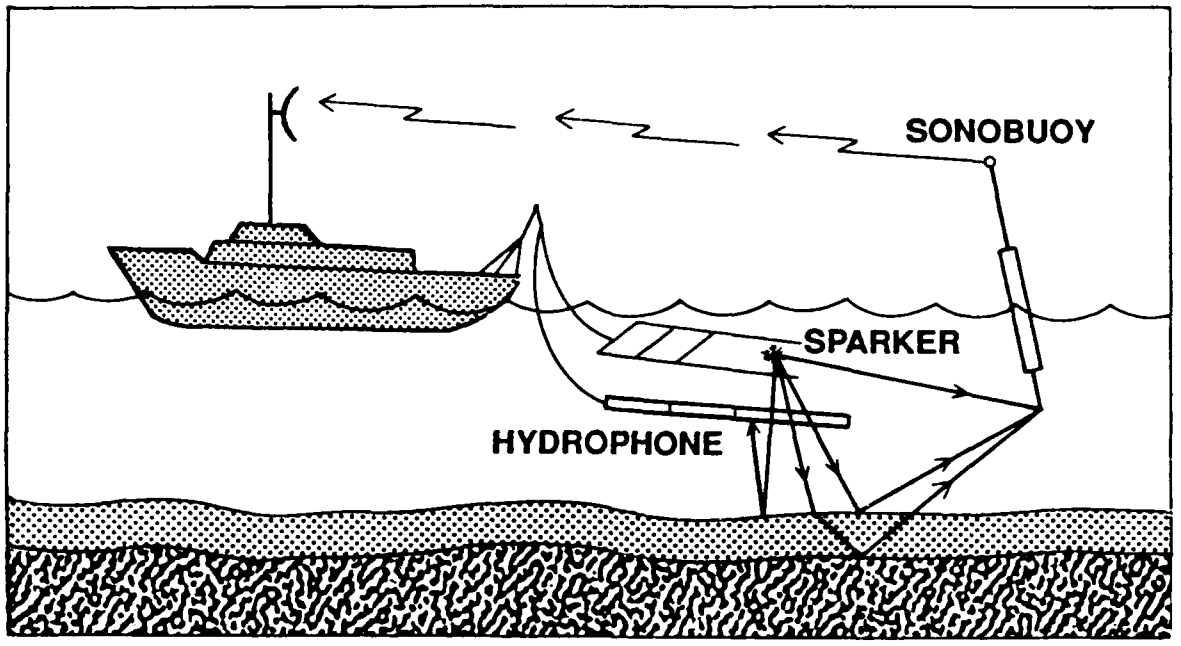

(a) Illustration of Both Vertical Profiling and Wide-Angle Bottom Reflection.

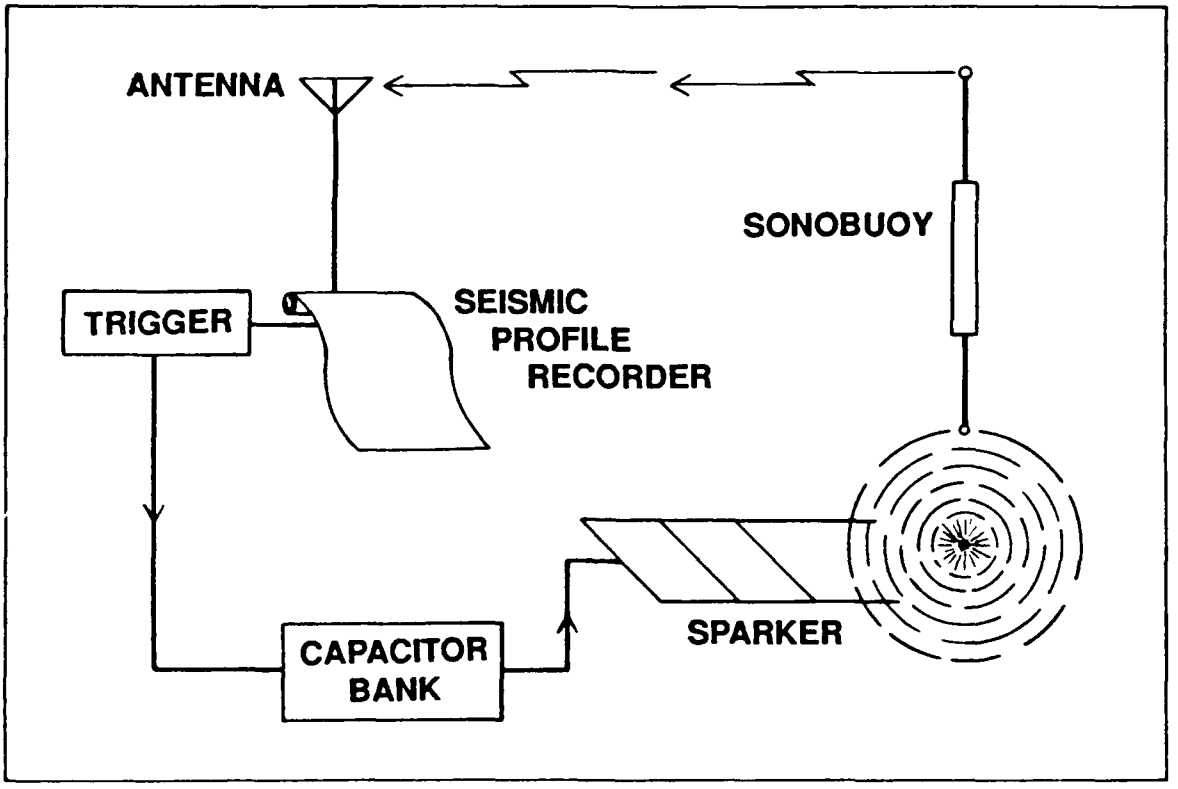

(b) Block Diagram of a Typical System.

Figure 4. Illustration of Seismic Profiling System.

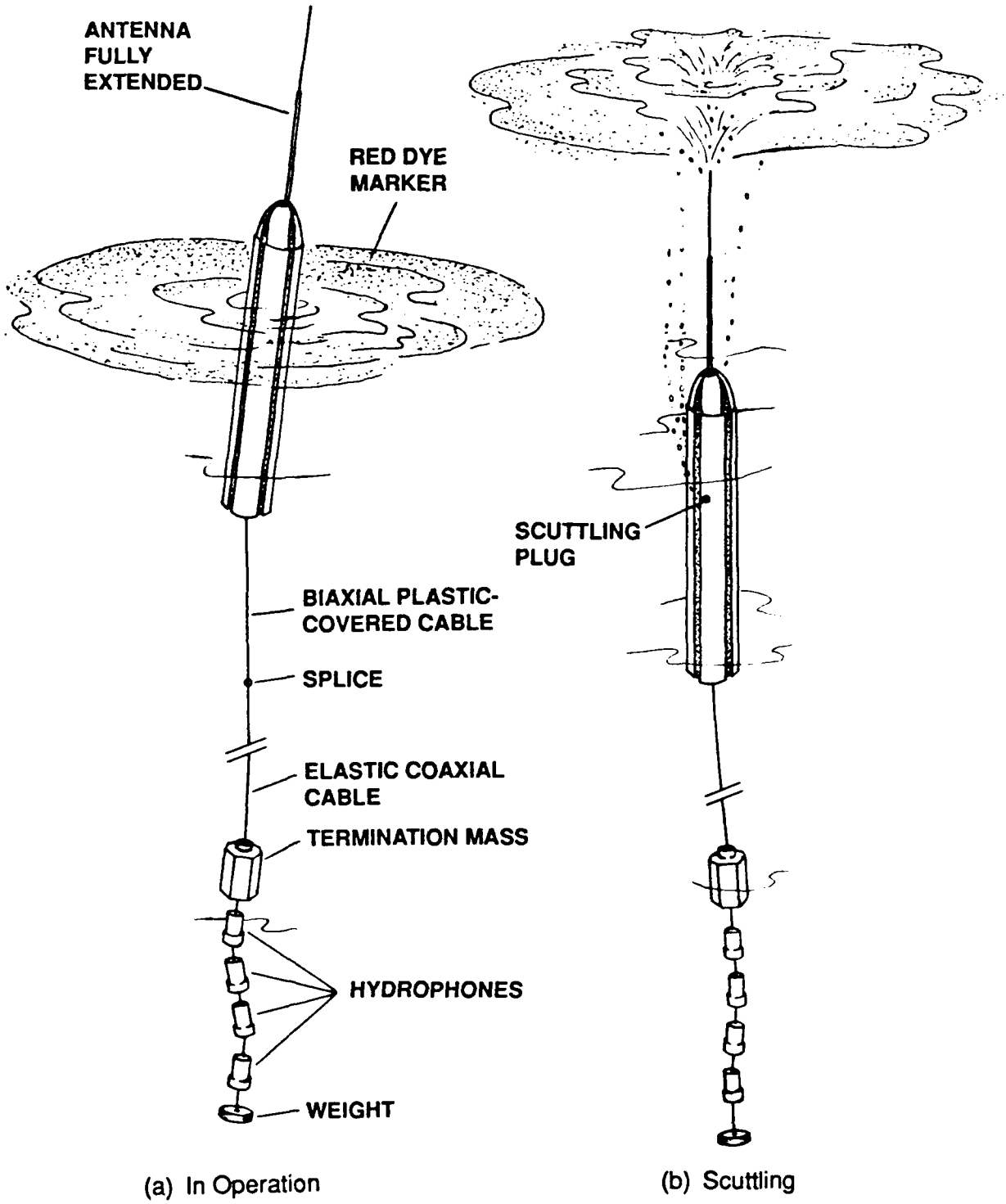

Figure 5. Illustration of Navy Sonobuoy Type AN/SSQ-41A.

manufacturer or to NAVOCEANO laboratories periodically for calibration and maintenance. A rigorous preventative maintenance program was carried on aboard the ship and the calibration of the instruments checked prior to each cruise. Most sonobuoys do not transmit true amplitudes and since travel times are the primary consideration in this study rather than amplitudes, the accuracy of the timing systems of the recorders is of prime importance. The recorders are controlled by crystal oscillators with an accuracy of five parts per million, and these were monitored by two rubidium frequency standards aboard the ship.

Data are easily reproducible from the raw data on magnetic tape, from the original visible recordings or from the 35-mm film copies made of all of the seismic records. The interval velocities and the thicknesses obtained for each station by the Dix (1955) method have been tabulated and are being published as a NAVOCEANO Basic Data Report. This publication will include all of the stations taken through 1988.

II. DATA ACQUISITION AND PROCESSING

Several other methods of obtaining seismic velocity data were considered for this study. The two-ship wide-aperture method was evaluated but was discarded due to the costs involved and the difficulty of obtaining two ships for a project over such large areas and requiring so much ship time. Multi-channel reflection methods are highly desired for the increased detail and the much greater discrimination of layer thicknesses, but the level of effort and costs of using this method were beyond the means of the project. Also, since the bulk of the work was in water depths greater than 3000 meters, the work was beyond the capabilities of the average multi-channel system. Refraction methods would have been as suitable as the WABR method as far as costs and ship time were concerned, but the requirement of large sources rich in low frequencies necessitates explosives, giving rise to a myriad of regulations and conditions aboard Navy ships. The availability of sonobuoys at minimal cost to NAVOCEANO and the need for only one ship made WABR the method of choice.

The data used for the characterization of the two ocean areas were acquired over a period from 1979 to 1985 and required nine cruise legs for the task. Cruise legs were multi-disciplinary and the tracks were planned to accommodate other disciplines, yet have the opportunity to take measurements in a systematic manner so that stations would be located to take advantage of physiography. Wide-angle reflection measurements were the primary purpose of the cruises in the Arabian Sea and the tracks were designed specifically for this purpose. A series of tracks was chosen to obtain uniform coverage of the region while maintaining tracks along depth contours to minimize the variation in water depth along the track.

The WABR technique is a marine adaptation of the Dix (1955) X^2-T^2 method developed for land exploration. The X^2-T^2 method is used to determine interval velocities and thicknesses and has been discussed by Clay and Rona (1965), Le Pichon et al. (1968) and Houtz et al. (1968). During our underway data acquisition, the ship towed a sparker which fired every 10 seconds. One or more hydrophone streamers were also towed, generally at a speed of 8 to 9 knots. Seismic vertical profile data were recorded on two analog paper recorders. One recorder, the primary recorder, was operated at a 10-second sweep, recording data from the entire time period between shots to maintain a continuous unbroken record of the bottom when going from shelf areas to abyssal depths and vice versa. The second recorder was operated at a 4-second sweep with a sweep delay eliminating most of the water column data but expanding the subbottom. (See figure 6.)

To make a wide-angle measurement the ship is slowed to approximately 5 knots and the 2 seismic recorders are switched to a 4-second sweep, firing the sparker at a 4-second rate. The

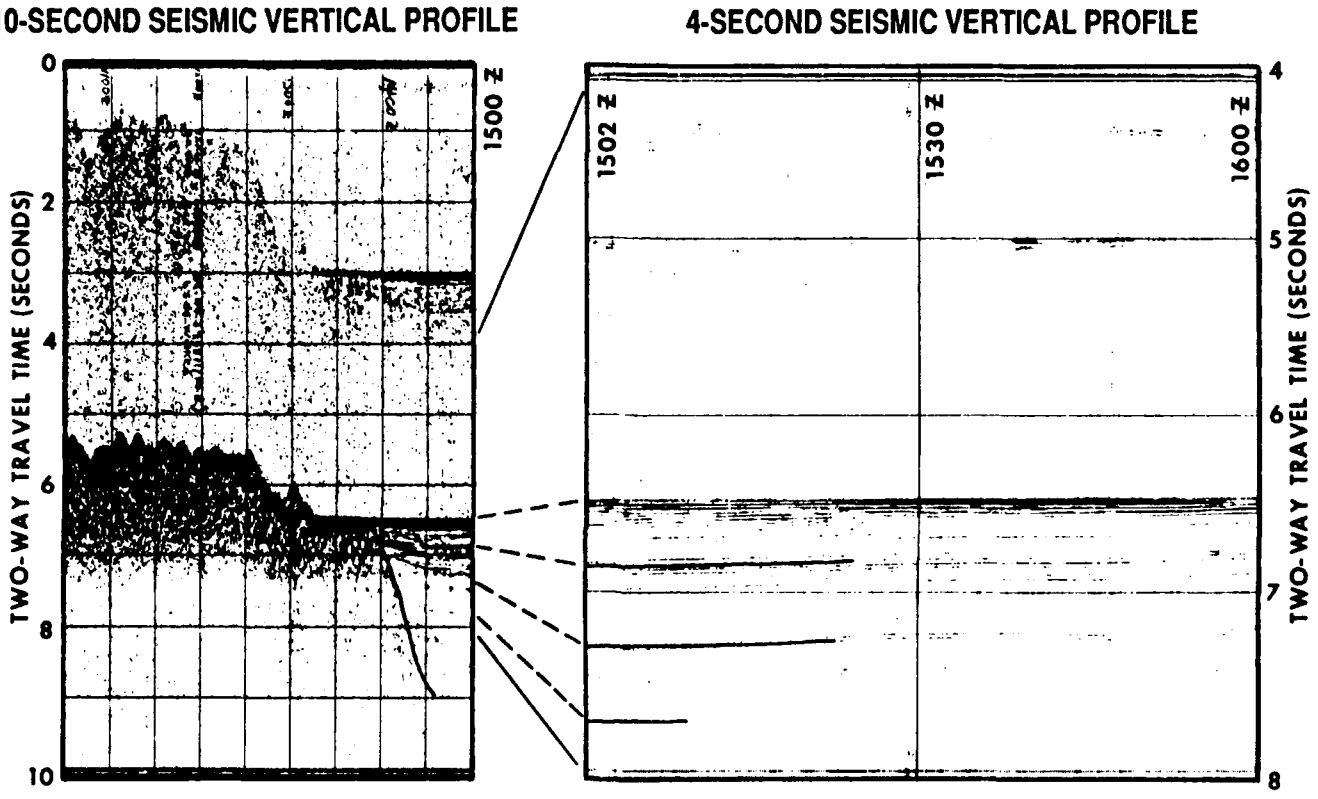

Figure 6. Illustration of 10-Second and 4-Second Vertical Profile Records.

signal input to the second recorder is switched from the hydrophone streamer to the sonobuoy receiver output. In this manner, the first seismic recorder continues to record seismic vertical profile data while the second recorder now records data from the sonobuoy (figure 7). A 4000-Hz reference signal from the second line scan recorder was put on an FM channel of the tape recorder and the sparker trigger pulse was put on an AM channel. A voice-recorded header message was put on AM channel eight with information on the time, place and conditions of the WABR run. The ship is slowed to 5 knots in order to spread the wide-angle reflection record over a longer time interval for a given distance covered, which aids in picking horizons. The firing rate is increased in order to maintain data density with 4 seconds being the maximum firing rate of our system. The 3.5-KHz subbottom profiler is turned off to prevent interference, but the 12-KHz narrow-beam echo sounder continues to operate. A sonobuoy is deployed over the fantail, and the ship is run at a constant speed and course for the duration of the measurement. The run is continued for 1 1/2 to 2 hours, depending on sonobuoy transmission quality for a distance of 9 to 10 nautical miles. The tape recorder was shut down after a voice annotation at the end of the run and the ship returned to normal underway operation.

Wide-angle reflection measurements were often taken just prior to arrival on core station or immediately upon departure from a station so that the core and CTD data could be associated with the measurement. At sea, cores were cut to manageable lengths of 4 to 5 feet, x-rayed and then velocity measurements were taken with a velocimeter, based upon study of the x-ray photographs. The measurements were made in two directions at right angles to each other with both measurements perpendicular to the length of the core. X-rays were taken of the cores in order to aid in determining layer boundaries and locate inclusions such as large shell fragments, pebbles, worm holes, etc. Once boundary layers were determined, velocity measurements were taken at the top and bottom of the layer and uniformly throughout. All of these data were returned to NAVOCEANO at Stennis Space Center, Mississippi, where the data processing was performed.

To keep from damaging or otherwise defacing the continuous seismic records, working paper records were made from the tapes. In rare cases where no tape recording was obtained or the tape recording was poor or faulty, full-size photographs of the wide-angle reflection record were made. Working reflection records were made by playing the tapes back through the same model seismic amplifier and line scan recorder as were used on the ship. The recorded 4000-Hz reference signal was used as a speed reference for the line scan recorder and the recorded trigger pulse was used to sychronize the line scan recorder to the tape recorder, just as the original line scan recorder and tape recorder were synchronized on the ship. The resulting record is an exact duplicate of the original.

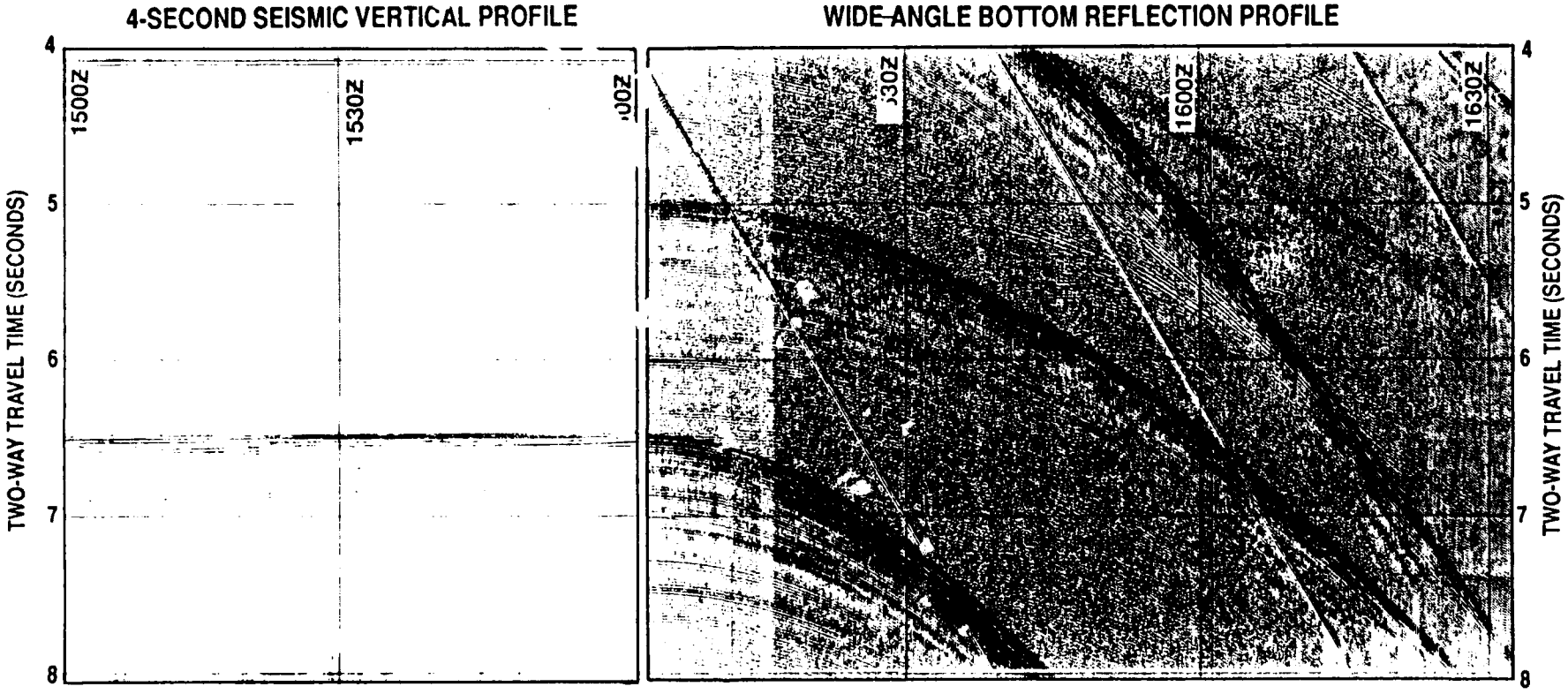

Figure 7. Illustration of WABR and Simultaneous Vertical Profile Records.

Processing to obtain velocities was done as follows: Using the seismic vertical profile record made during the station, coherent reflections were picked out and transferred to the working record. The trace of the direct wave and the trace of the arrivals from the reflections were enhanced with color pencil as shown in figure 8. Travel times of the direct wave and each of the reflected arrivals were measured from the record and tabulated on a form as illustrated in figure 9. The near-surface water sound velocity, at the sparker depth and the sonobuoy hydrophone depth, was obtained from CTD data and used to calculate the distance from source to receiver based on the direct wave travel time. These data were input to a computer program written by Michael McGlaughlin of NAVOCEANO and later slightly modified by the author. (See appendix C.)

The program calculates the squares of the arrival times and distances, and uses the least-squares method to fit the best straight line to the plotted X^2-T^2 values. A coefficient of correlation (COC) calculated to determine the degree of fit was also found useful in determining "picking" errors and numerical transpositions in entering the data into the computer. The correlation coefficient is defined as "the square root of the ratio of the explained variation to the total variation." It is a measure of the goodness of fit between the assumed equation and the data. If the Dix conditions of horizontal and parallel layers are met, the plot of the X^2-T^2 values is a straight line. The correlation coefficient would then be 1.0, and lower values indicate that either the conditions were not met or there are errors or noise in the data set. No fit of more than two data points is ever perfect; however, exceptionally good fits will achieve a COC of 0.99997 or 0.99998. As an example, an error of 0.2 seconds in arrival time will affect the fourth decimal place and result in a coefficient of 0.9996 or 0.9997. Checking the poor correlation coefficients most often resulted in detecting errors in picking travel times or transposition errors. Poor course maintenance or variations in speed show up as waves in the X^2-T^2 plot or bunching up of the data points. A disconcerting characteristic of our computer plotting routines is that COCs are rounded off at the fifth decimal place, thus resulting in coefficients of 1.0.

After establishing the straight line fit, the computer program then goes through the Dix calculations and determines interval velocities and interval thicknesses. The program outputs the X^2-T^2 plot and a tabulation of the input data with the resulting interval velocities and thicknesses as shown in figures 10 and 11. As noted earlier, the correlation coefficients indicated as 1.0000 in figure 11 have been rounded off at the fifth decimal and are actually on the order of 0.99998.

The velocimeter measurements made at sea are later corrected for temperature and pressure at NAVOCEANO's core lab. The procedure used for making the corrections is included as appendix B. The measurements for each core were averaged over a

depth interval of 30 centimeters. In the tabulation of station layer thicknesses and layer velocities, the initial thickness (0.000) and associated velocity is that obtained from the core analysis.

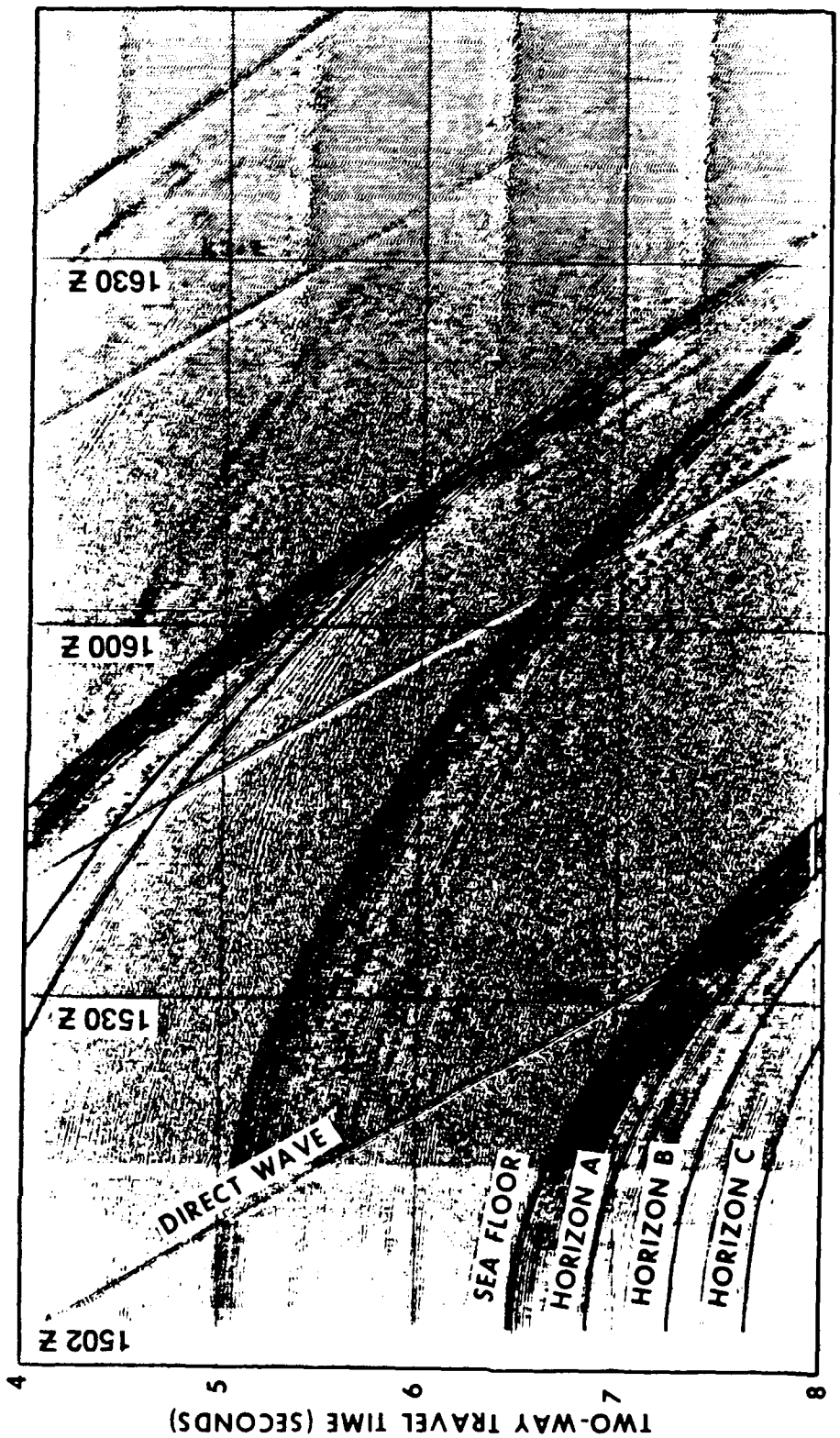

Figure 8. Illustration of Enhanced WABR Record.

TRAVEL TIME TABULATION

STATION NO. 85

CRUISE NO. 343916 LEG NO. 30 JULIAN DATE 271 SHIP USNS WILKES

AREA INDIAN OCEAN LATITUDE 01° 21.5' N LONGITUDE 049° 06.3' E

SONOBUOY: CONSEC. NO. 30 - 36 REPORT NO. _____

SHIP'S RUNNING TIME FROM SONOBUOY IN MINUTES	DIRECT WAVE TRAVEL TIME IN SECONDS (ONE-WAY)	DISTANCE SHIP TO SONOBUOY IN KM.	TWO-WAY REFLECTION TIME (SECONDS)				
			SEA FLOOR	HORIZON A	HORIZON B	HORIZON C	HORIZON D
	t	x	t	t	t	t	t
0.0	0.000		6.248	6.503	6.905	7.260	
8.5	0.840		6.296	6.550	6.957	7.313	
17.1	1.740		6.482	6.732	7.120	7.457	
24.1	2.456		6.717	6.960	7.322	7.660	
29.6	3.015		6.955	7.177	7.527	7.853	
34.1	3.461		7.170	7.389	7.733	8.033	
38.2	3.900		7.385	7.605	7.945	8.215	
41.9	4.265		7.600	7.810	8.112	8.395	
45.1	4.600		7.792	8.000	8.295	8.563	
48.3	4.925		8.000	8.200	8.485	8.740	
51.2	5.220		8.190	8.395	8.660	8.905	
54.0	5.507		8.385	8.577	8.838	9.070	
56.6	5.785		8.568	8.755	9.008	9.228	
59.1	6.025		8.740	8.928	9.172	9.375	
63.9	6.510		9.085	9.252	9.490	9.675	
68.3	6.955		9.425	9.595	9.805	9.970	
72.5	7.390		9.765	9.930			
76.4							
80.1							
83.6							
87.0							
90.3							
93.5							

Figure 9. Travel Time Tabulation Sheet.

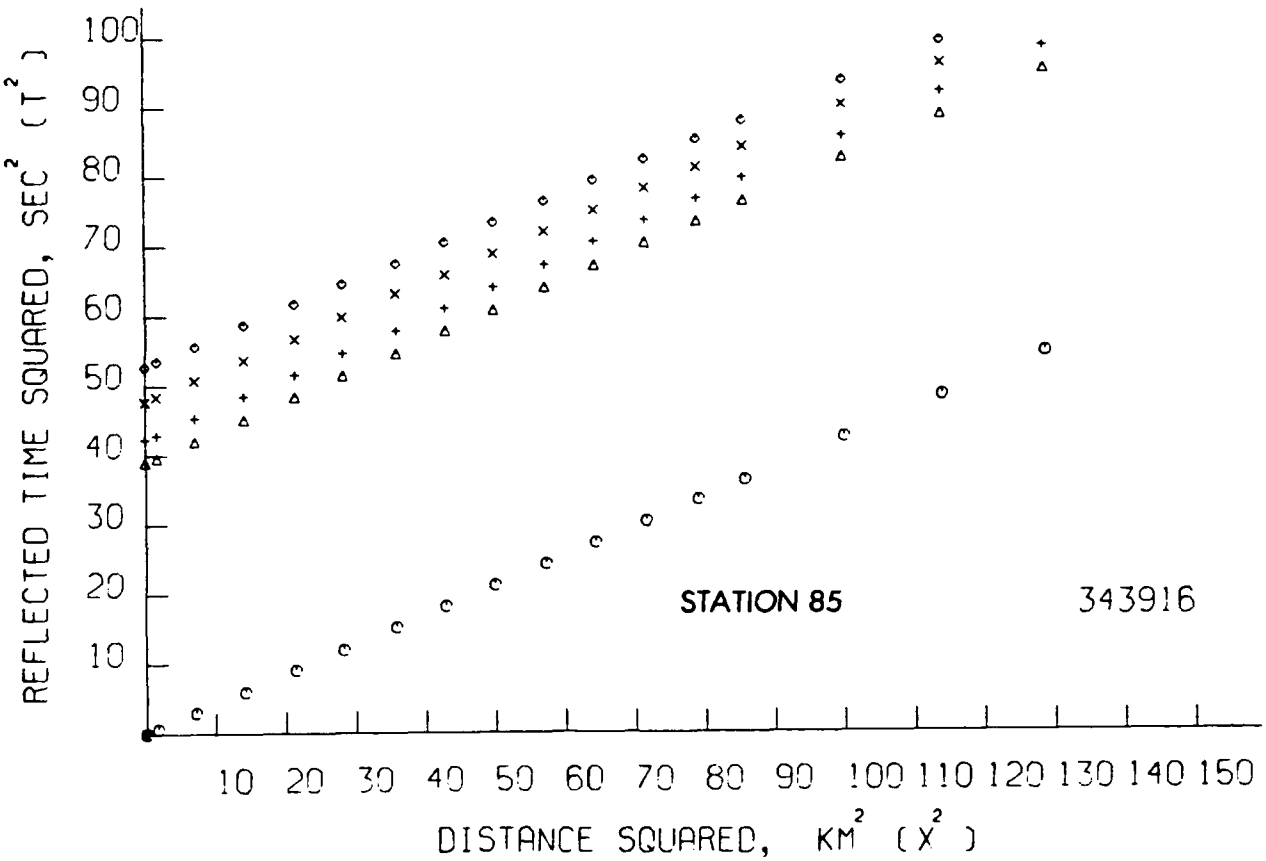

Figure 10. Computer Plot of X^2-T^2 Values.

SONOBUOY STATION NO. 85 AREA INDIAN OCEAN

SHIP WILKES 3939;6 LEG 30 DATE 271/79 LATITUDE 1.22 N LONGITUDE 49.06 E

DIRECT WAVE TRAVEL TIME (ONE WAY) IN SECONDS		DISTANCE SHIP TO SONOBUOY IN KM.		2-WAY REFLECTION TIME (SECONDS)											
				SEA FLOOR 1		HORIZON A 2		HORIZON B 3		HORIZON C 4		HORIZON D 5		HORIZON E 6	
T	T^2	X	X^2	T	T^2	T	T^2	T	T^2	T	T^2	T	T^2	T	T^2
.000	.000	.000	.000	6.248	39.038	6.503	42.289	6.905	47.679	7.260	52.708	.000	.000	.000	.000
.840	.706	1.289	1.663	6.296	39.640	6.550	42.903	6.957	48.400	7.313	53.480	.000	.000	.000	.000
1.740	3.028	2.671	7.134	6.482	42.016	6.732	45.320	7.120	50.694	7.457	55.607	.000	.000	.000	.000
2.450	6.002	3.761	14.143	6.717	45.118	6.960	48.442	7.322	53.612	7.660	58.676	.000	.000	.000	.000
3.015	9.090	4.628	21.419	6.955	48.372	7.177	51.509	7.527	56.656	7.853	61.670	.000	.000	.000	.000
3.461	11.979	5.313	28.224	7.170	51.409	7.389	54.597	7.733	59.799	8.033	64.529	.000	.000	.000	.000
3.903	15.210	5.986	35.838	7.385	54.538	7.605	57.836	7.945	63.123	8.215	67.486	.000	.000	.000	.000
4.255	18.190	6.547	42.860	7.600	57.760	7.810	60.996	8.112	65.805	8.395	70.476	.000	.000	.000	.000
4.603	21.160	7.061	49.858	7.792	60.715	8.000	64.000	8.295	68.807	8.563	73.325	.000	.000	.000	.000
4.925	24.256	7.560	57.152	8.000	64.000	8.200	67.240	8.485	71.995	8.740	76.388	.000	.000	.000	.000
5.220	27.248	8.013	64.203	8.190	67.076	8.395	70.476	8.660	74.996	8.905	79.299	.000	.000	.000	.000
5.507	30.327	8.453	71.457	8.385	70.308	8.577	73.565	8.838	78.110	9.070	82.265	.000	.000	.000	.000
5.785	33.466	8.880	78.854	8.568	73.411	8.755	76.650	9.008	81.144	9.228	85.156	.000	.000	.000	.000
6.025	36.301	9.248	85.532	8.740	76.338	3.928	79.709	9.172	84.126	9.375	87.891	.000	.000	.000	.000
6.510	42.380	9.993	99.857	9.085	82.537	9.252	85.600	9.490	90.060	9.675	93.606	.000	.000	.000	.000
6.955	48.372	10.676	113.975	9.425	88.831	9.595	92.064	9.805	96.138	9.970	99.401	.000	.000	.000	.000
7.390	54.612	11.348	128.578	9.765	95.355	9.930	98.605	.000	.000	.000	.000	.000	.000	.000	.000

VELOCITY (0 TO 1) 1.512 KM./SEC. COC = 1.0000
THICKNESS (0 TO 1) 4.722 KM.
VELOCITY (1 TO 2) 1.525 KM./SEC. COC = 1.0000
THICKNESS (1 TO 2) .194 KM.
VELOCITY (2 TO 3) 1.846 KM./SEC. COC = 1.0000
THICKNESS (2 TO 3) .371 KM.
VELOCITY (3 TO 4) 2.041 KM./SEC. COC = 1.0000
THICKNESS (3 TO 4) .362 KM.

Figure 11. Computer Data Tabulation Sheet.

III. DATA INTERPRETATION

The WABR method estimates a velocity versus depth relationship where the depth is expressed in terms of layer thickness and the velocity is an average velocity for the layer. Investigators in this area prefer to express this as a parameterized relationship in terms of velocity versus one-way travel time, called an instantaneous velocity function. Acoustic modelers prefer to work in terms of velocity versus depth. Thus, after obtaining the interval velocities and thicknesses for each of the WABR measurements, as described in the section on data acquisition and processing, the next step is to derive instantaneous velocity curves for each station. This is accomplished by making plots of the interval velocity data versus one-way travel time from the sediment surface to the midpoint of the interval. A curve is then fit to the plotted data points. This method was discussed by Houtz et al. (1968, 1970), Hamilton et al. (1974) and Bachman and Hamilton (1980) and was closely followed in this work.

As noted by these authors, interval velocity measurements have the drawback of modeling reality as constant velocity layers, thus yielding first-order discontinuities that may not exist, leading to erroneous reflection coefficients. Hamilton et al. (1974) and Bachman and Hamilton (1980) have pointed out the importance of sediment surface velocities to the acoustic community and how these data provide anchor points in the velocity versus one-way travel time plot. To provide these data in this study, sediment surface velocities were obtained from cores as noted earlier.

The process used to derive instantaneous velocity-time functions was to compute the one-way travel time from the sediment surface to the midpoint of each layer, based on the average layer velocities obtained from each layer. These travel times are plotted versus the corresponding interval velocity. Two additional programs were written by Sara Windsor (pers. com. 1982), with some adaptation and modification by the author. One program converts individual layer thicknesses and velocities to velocity versus one-way travel time to layer midpoint, plots the data points, and fits each of three curves (linear, parabolic, and exponential) to the points by the least squares method. Presently, both linear and parabolic curves are commonly used by modern investigators such as Houtz et al. (1968, 1970) and Bachman and Hamilton (1980). The exponential curve was tried because of the consideration that many geologic processes, such as erosion and deposition, tend to be exponential in nature and compaction might follow the same trend. A correlation coefficient was calculated for each curve fit so that the best fitting type of curve may be determined. The curve is forced through a sediment surface velocity point by weighting this data point. (See appendix D.)

In the second program, data from several stations are then combined on the same graph and again fit with each of the three different curves and correlation coefficients calculated. Each curve is forced through the average surface sediment velocity of all of the stations included in the run. (See appendix E.) It should be noted that in spite of heavy weighting of the surface velocity data point, the best fit curve often resulted in a slightly different surface velocity due to skewing of the line or curve by the remaining data points. The author felt that this was acceptable, even though the surface velocity is a directly measured quantity because of the possible errors involved in the core sample velocity measurements and a reasonable validity given to the other data points. An example of a single station plot and a group station plot is given in figure 12.

Of the 70 stations in the Somali Basin, 80% of the velocity versus one-way time data were best fit by a parabolic curve and the remaining 20% were best fit by a linear curve. The criteria for fit was the correlation coefficient. The coefficient of correlation is a measure of how well a linear or other equation describes the relationship between the variables. A COC of 1.0 is a perfect fit. Of those stations best fit by a parabolic curve, the difference in the correlation coefficients between parabolic and linear fit was at the most 0.01 and most often on the order of 0.005. Thus, it would be reasonable to assume a linear function for one-way travel time plots for the areas investigated. The exponential curve was the best fit by correlation coefficient in only one case out of all cases, and it was thus assumed that the speculation concerning the exponential nature of compaction was not justified.

Plotting the interval velocity at the midpoint of the layer is valid only if the layer has a constant velocity or if the velocity increases linearly with depth. If the best curve fit is parabolic, then the linear conditions are not met and the position in the layer at which the interval velocity is assigned must be corrected. Houtz et al. (1968) made an analysis of the error involved in placing the interval velocity at the layer midpoint when the velocity increases in the layer as a second-order function. The error analysis determines that the correction for the interval velocity position in the layer is $E = Cdt^2/12$, where C is the constant in the parabolic curve fit given by $V = At^2+Bt+C$ and dt is the interval thickness in terms of one-way travel time. Thus, when the correlation coefficient indicates that the best fit is the parabolic curve, the position of the interval velocity in the layer is corrected by the factor E, replotted and refit with a parabolic curve for the resultant "Instantaneous Velocity Curve" of Houtz et al. (1968) and Hamilton et al. (1974). An example of instantaneous velocity curves derived using data from one station and data from numerous stations is presented in figure 12.

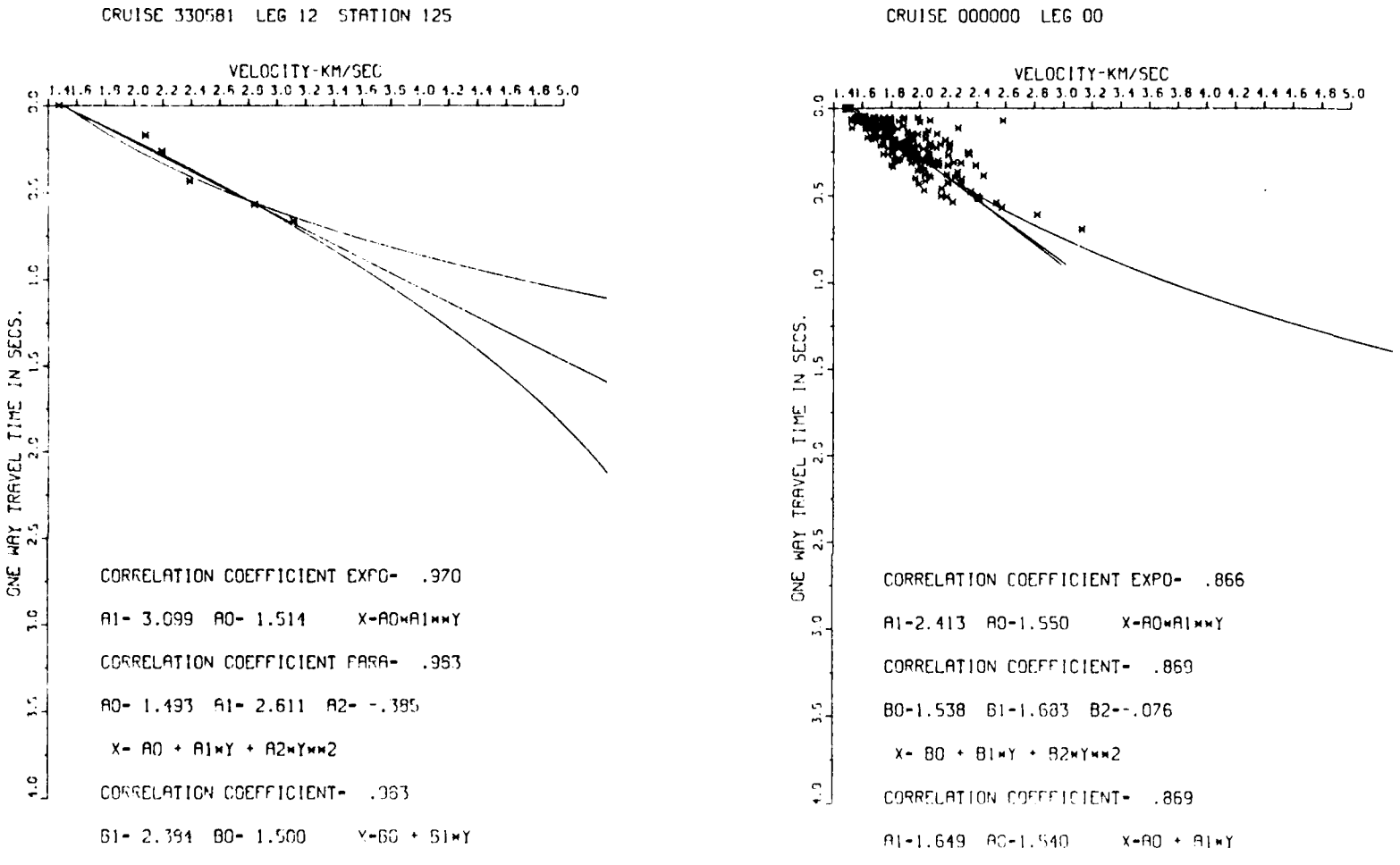

Figure 12. Example of Single and Group Station Data Plots and Curve Fits.

A function for depth in terms of one-way travel time from the sediment surface is derived by integrating the instantaneous velocity function:

$$V = at^2+bt+c$$

$$\int V\,dt = D = et^3+ft^2+gt+H$$

where V is the velocity and the integral of velocity, D, is the depth from the sediment surface. The constant of integration H is zero since the depth must be zero at time equal zero. We now have expressions for velocity and depth in terms of one-way travel time. These can be related by setting up a table for the values of velocity and depth obtained from the two equations when the same values of time are inserted into the equations and the values for V and D calculated.

t	V	D
0.1	i	j
0.5	k	l
1.0	m	n
1.5	o	p
2.0	q	r

Corresponding pairs of velocity and depth values (i,j;k,l;m,n; o,p) are plotted and fit with a curve by least squares resulting in a curve and function expressing the velocity in terms of depth.

$$V' = s+uD+wD^2$$

The program used to derive the velocity-depth function is given in appendix F. The estimate of error for the resultant velocity-depth function is the sum of the errors in each step of the process. The error in the WABR process has been estimated by Le Pichon et al. (1968) at $\pm$ 80m/s. The standard estimate of error in the instantaneous velocity process is approximately 120 m/s and in the velocity-depth process is approximately 10 m/s. Thus the cumulative error is approximately 210 m/s.

With very few exceptions, seismic penetration was about 1.2 seconds; therefore, measurements and plots are limited to the upper 1000 to 1500 meters of the sediment. Some individual stations have only two data points: a surface velocity and one-layer velocity. Other stations have as many as eight data points. For those stations with very few data points, it was not possible to derive a velocity-depth function without a great deal of speculation. Thus, groups of stations from an area were used to derive a velocity-depth function which was representative of that particular area. As an example, a velocity-depth function for the northernmost portion of the abyssal plain between Chain Ridge and the African Continental Rise was derived using stations 67 through 76; thus 40 or more data points were

used to derive the representative velocity-depth function. The use of groups of stations for deriving the velocity-depth functions was followed to derive functions for entire abyssal plains, portions of abyssal plains, east-west and north-south trending lines through abyssal plains and continental rise areas. These functions are compared to each other in order to determine whether or not significant differences exist between the velocity-depth functions of the various areas. A discussion of the two regions and the variations of their velocity structures follows.

A. SOMALI BASIN

A list of the stations in this area, along with layer interval velocities and thicknesses, is given in table 3. There were insufficient data points to derive an instantaneous velocity function for three areas, namely: the continental rise north of 3° 30'S, the abyssal plain area east of Chain Ridge and the abyssal plain area to the north and east of the Seychelle Islands. Instantaneous velocity-time functions and velocity-depth functions were obtained for eight groupings of stations: (1) north-south line in the northern abyssal plain, (2) east-west line in the northern abyssal plain, (3) north-south line in the southern abyssal plain, (4) east-west line in the southern abyssal plain, (5) all abyssal plain stations, (6) all continental rise stations, (7) all northern abyssal plain stations, and (8) all southern abyssal plain stations.

In comparing the north-south line to the east-west line in the northern abyssal plain, we find that the velocity gradient decreases with depth on the east-west line while the gradient is more nearly constant on the north-south line (figure 13). The same comparison in the southern abyssal plain (figure 14) shows just the opposite of this situation, a decreasing gradient in the north-south line and a more nearly constant gradient in the east-west line. In the southern abyssal plain, both lines show the same initial gradients and velocities down to 400 meters where the curves begin to diverge. A comparison of all of the abyssal plain stations to all of the continental rise stations shows a similar feature (figure 15). Both curves are essentially the same down to a depth of about 600 meters at which point the curve for continental rise stations begins to show a greater decrease in gradient. A velocity-depth curve from a function derived using all 70 of the Somali Basin stations is also presented in figure 15 for comparison.

A comparison of the velocity-depth curve and function for the northern abyssal plain stations to the southern abyssal plain stations indicates that both curves show essentially the same gradient to approximately 350 meters, where the gradient for the northern abyssal plain begins to decrease more rapidly than does that for the southern abyssal plain. The two curves are slightly offset due to a small difference in surface sediment velocity. The velocity-depth curve for all of the abyssal

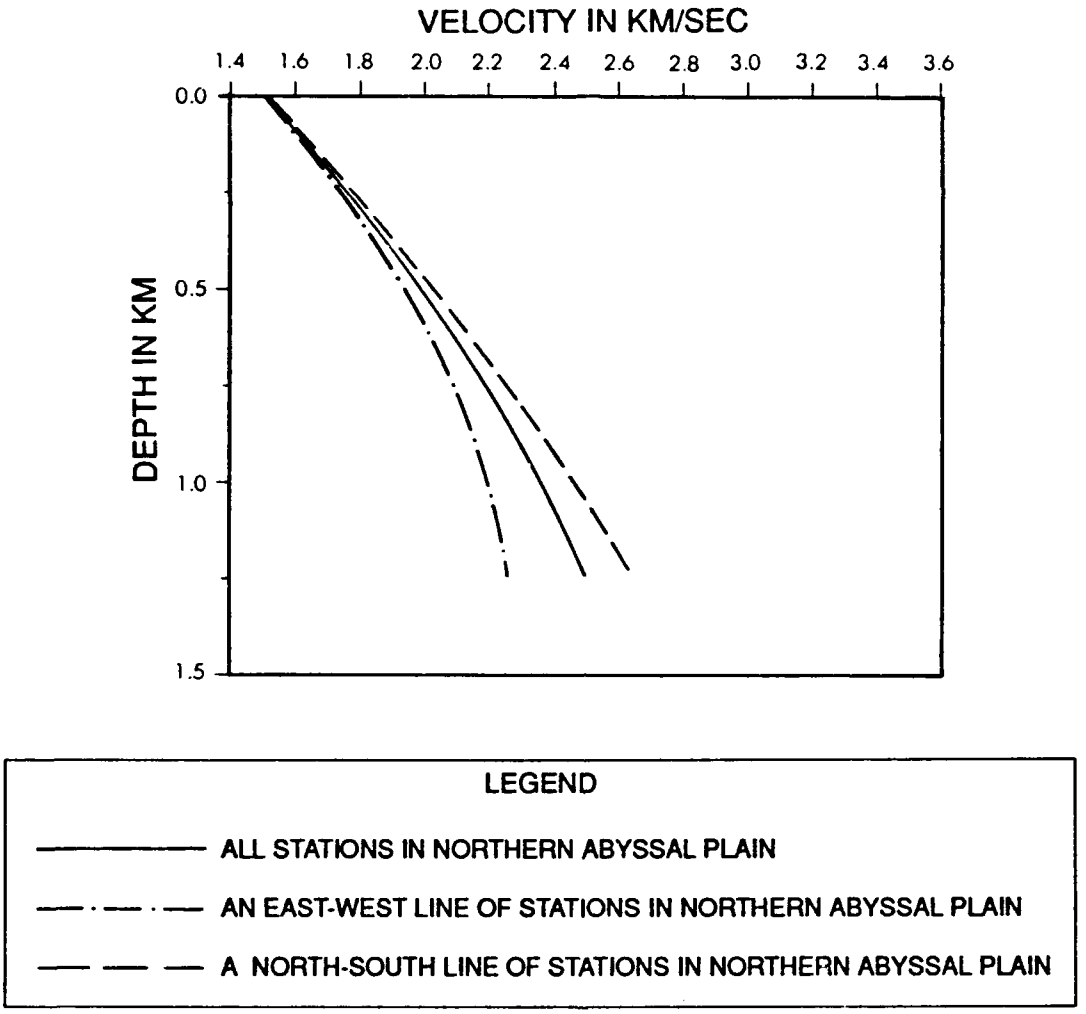

Figure 13. Velocity-Depth Curves For E-W Versus N-S Lines in the Northern Abyssal Plain.

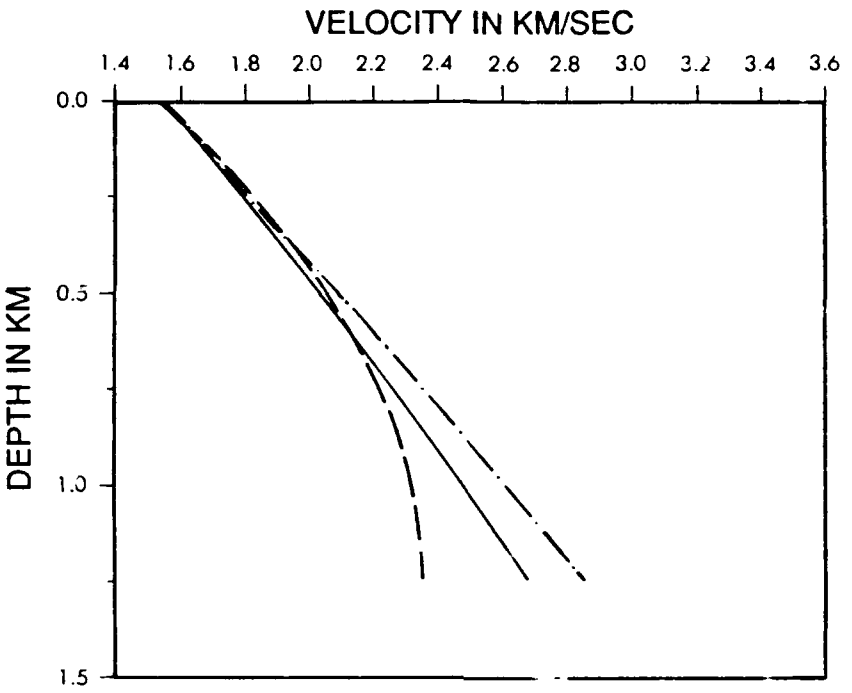

LEGEND

——————— ALL STATIONS IN SOUTHERN ABYSSAL PLAIN

—·——·—— AN EAST-WEST LINE OF STATIONS IN SOUTHERN ABYSSAL PLAIN

— — — A NORTH-SOUTH LINE OF STATIONS IN SOUTHERN ABYSSAL PLAIN

Figure 14. Velocity-Depth Curves For E-W Versus N-S Lines in the Southern Abyssal Plain.

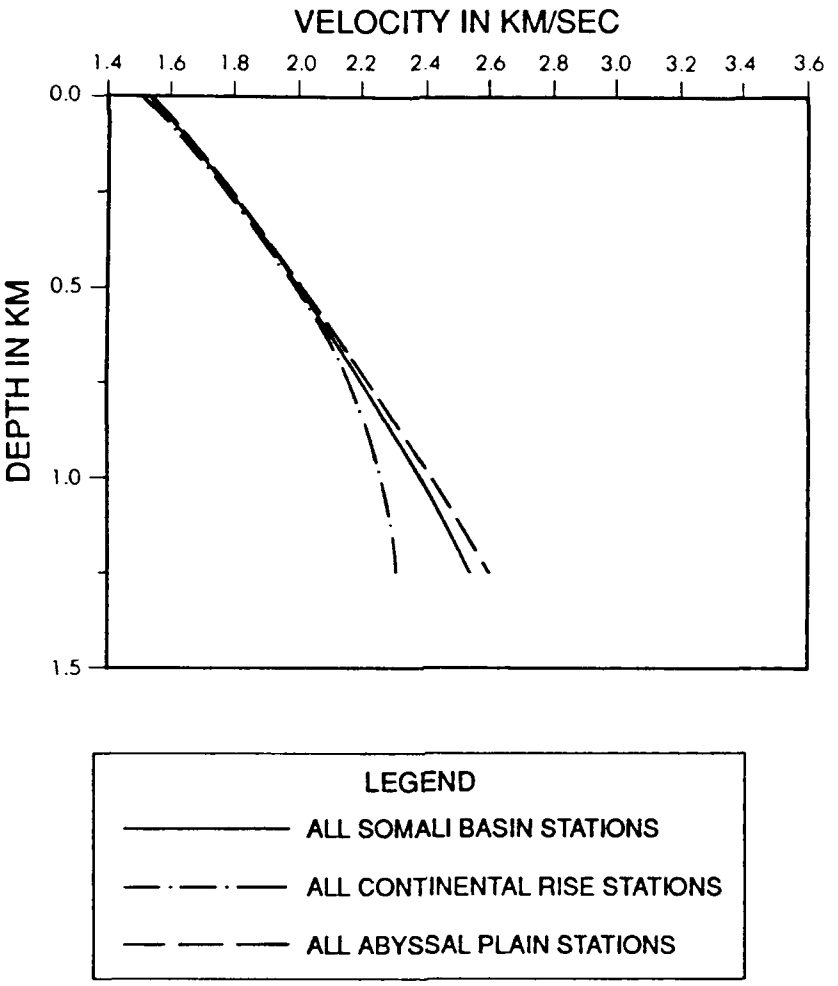

Figure 15. Velocity-Depth Curves for Abyssal Plain Versus Continental Rise in Somali Basin.

plain stations of the Somali Basin is a composite of these two curves. (See figure 16.) Given that the overall estimate of error in the velocity-depth curves is of the order of 200 m/s, the differences in the curves presented in figures 13 to 16 is not much greater than the statistical error. The differences in the curves are differences in velocity gradient, which depends on factors such as depth, particle size, sorting, sediment type, etc. The station group curve is derived from the data of a number of stations sampling different portions of the basin. Thus, each group curve is the result of an average sampling of different portions of the basin which results in variations in the gradient of the curves.

If a general velocity-depth function for the entire Somali Basin as an entity is desired, the parabolic function derived using all 70 stations would be appropriate; or the simpler linear function derived from the same data could also be used. A listing of the velocity-depth functions derived for this area is given in "section A" of table 1 and a similar listing of the instantaneous velocity-time functions is given in "section A" of table 2.

A fence diagram using the interval velocities and thicknesses obtained by WABR measurements in the Somali Basin is presented in figure 17. The diagram was plotted to ascertain the uniformity or nonuniformity of velocities and thicknesses in the two central abyssal plain areas of the Somali Basin. Obviously, the thickness of layers is not consistent between the two abyssal plains nor even within an individual abyssal plain itself. This may be due partially to the interpreter who picked the various reflectors. It was observed during the work, and may be verified by a study of table 3, that particular reflectors could not be traced for more than a station or two at a time. The diagram indicates a variability of velocity and thickness throughout each abyssal plain.

While processing the Somali Basin data, we calculated the ratio of the sediment surface sound velocity, as determined from cores, to the bottom-water sound velocity, as determined by SVSTD or CTD. During the calculations, we noted that the ratio was always less than 1.0 despite the fact that Hamilton (1980) indicates that in some cases it should be greater than 1.0. This situation led us to plot the bottom sediment surface velocity versus location of the measurement on a chart of the area. We also plotted the bottom-water sound velocity versus measurement location on another chart of the area. Both charts were contoured and one overlaid on the other. At those points where core velocity and bottom-water velocity measurements coincided, the ratio of core velocity to bottom-water velocity was taken and plotted in that position on a third chart. Intermediate ratio points for the third chart were obtained from the coincident contours of the previous two charts and by extrapolation guided by local sedimentology. We then contoured this ratio chart. It should be noted that in addition to the

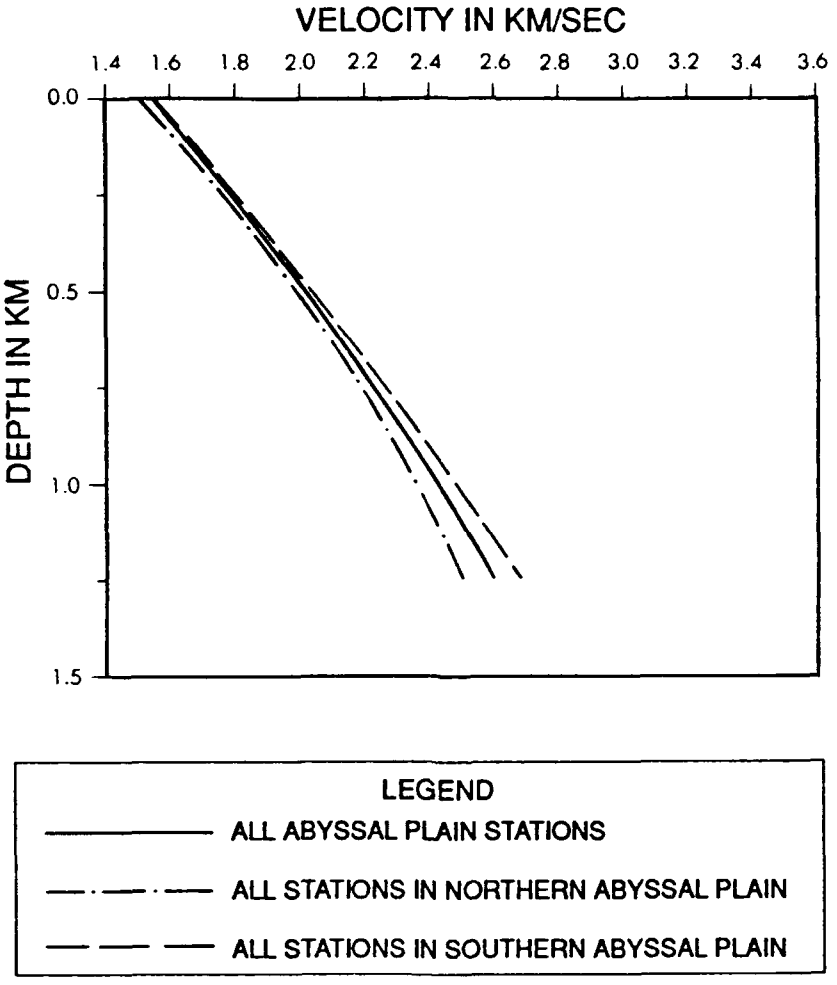

Figure 16. Velocity-Depth Curves for Northern Abyssal Plain Versus Southern Abyssal Plain.

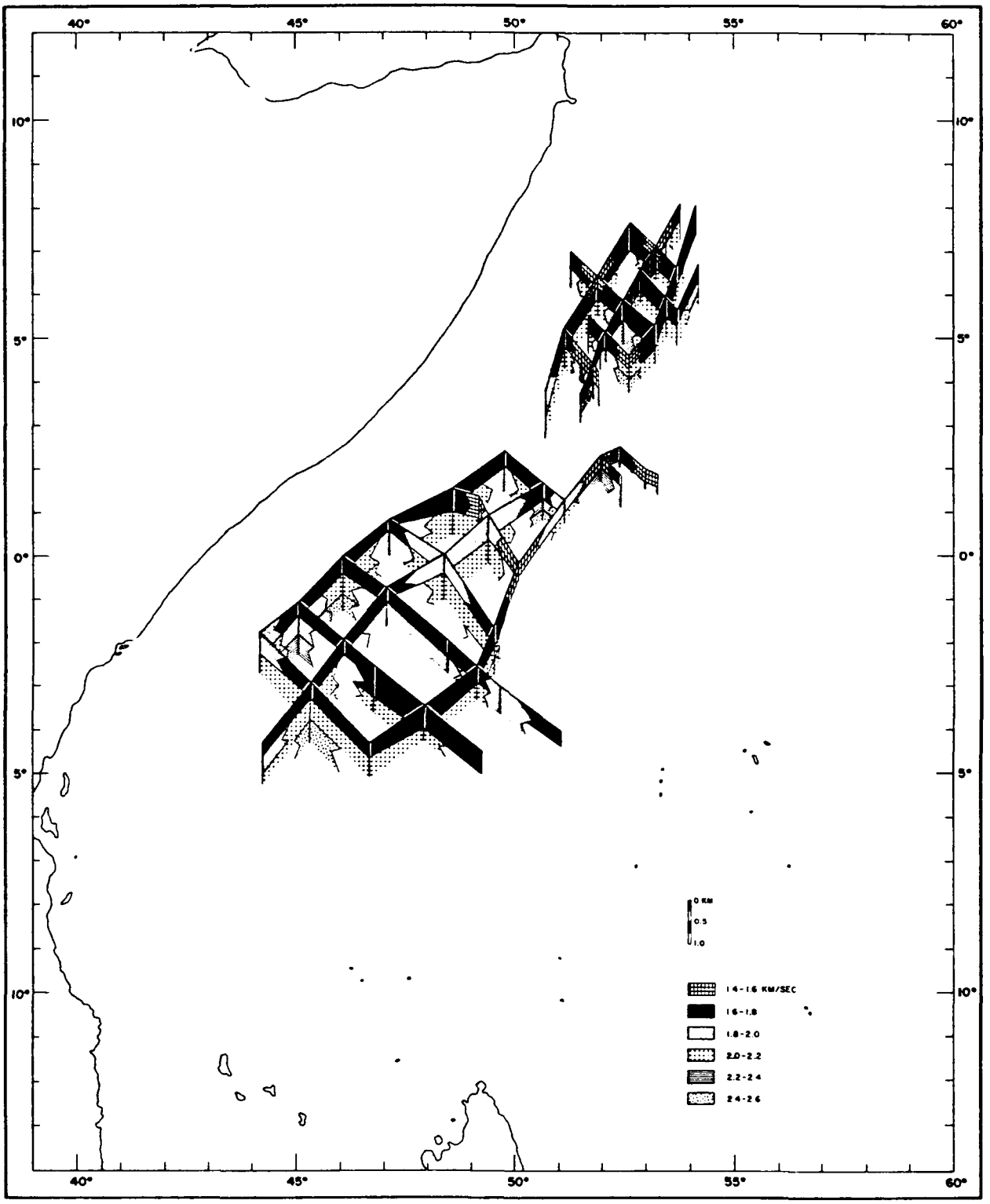

Figure 17. Fence Diagram of interval Veiocities and Thicknesses in Somali Basin.

velocities obtained by the USNS WILKES, all available sediment surface velocities from the National Oceanographic Data Center were included in the plot. The three plots are presented in figures 18, 19, and 20.

Consideration of figure 18, the contour plot of sediment surface velocities, indicates that the sediment surface velocities reflect the bathymetry or physiography to a considerable extent. Chain Ridge, though not well defined due to a lack of velocity measurements on the Ridge itself, is expressed by a high on either side. These highs delineate the abyssal plains on the east and west sides of the Ridge. The sediment surface velocities generally increase with ocean depth. Consideration of figure 19, the bottom-water velocity contour chart, shows as expected (Urick, 1983) that the bottom-water velocity is a function of depth and therefore controlled by physiography. In the northern and eastern portion of the Somali Basin, the bottom-water velocity reflects the physiography to a large degree. In the western and southern portion of the Basin, the bottom-water velocities are not as high, particularly in the African Continental Rise area and the southernmost portion of the abyssal plain area, as those in the northern portion of the Basin, due to the shallower depth. In the southern portion of the Basin both sediment surface velocity and bottom-water velocity do not reflect the physiography nearly as well. This situation results in a profound effect on the sediment surface velocity/bottom water velocity ratio plot in figure 20. Consideration of this figure indicates that the ratio reflects physiography quite well in the northern and east-southeast portion of the Basin but has little relationship in the south and west. The ratio contour chart shows a high in the southwest and a low in the south central portion of the basin. This central low is the obvious result of the nose of low sediment velocities indicated in that area in figure 18. The reason for the nose of high ratio in the southwest is not apparent when considering figures 18 and 19.

B. ARABIAN SEA

A list of the stations taken in this area, along with their interval velocities and thicknesses, is provided in table 4.

The general process used in this area was the same as that used in the Somali Basin. An instantaneous velocity-time curve was obtained for each station taken in the Oman Abyssal Plain. Individual stations were compared to each other to see if there were anomalous areas. In the Oman Abyssal Plain, it was thought that certain stations might be anomalous on the basis of their physiographic location. Stations 131 and 132 were two stations expected to be anomalous on the basis of their location in the northeast corner of the plain where the plain pinches down to somewhat of a trough. Stations 143, 144, and 145 were expected to be anomalous because of their positions at the extreme south end of the plain where the bottom rises to the Murray Ridge. In

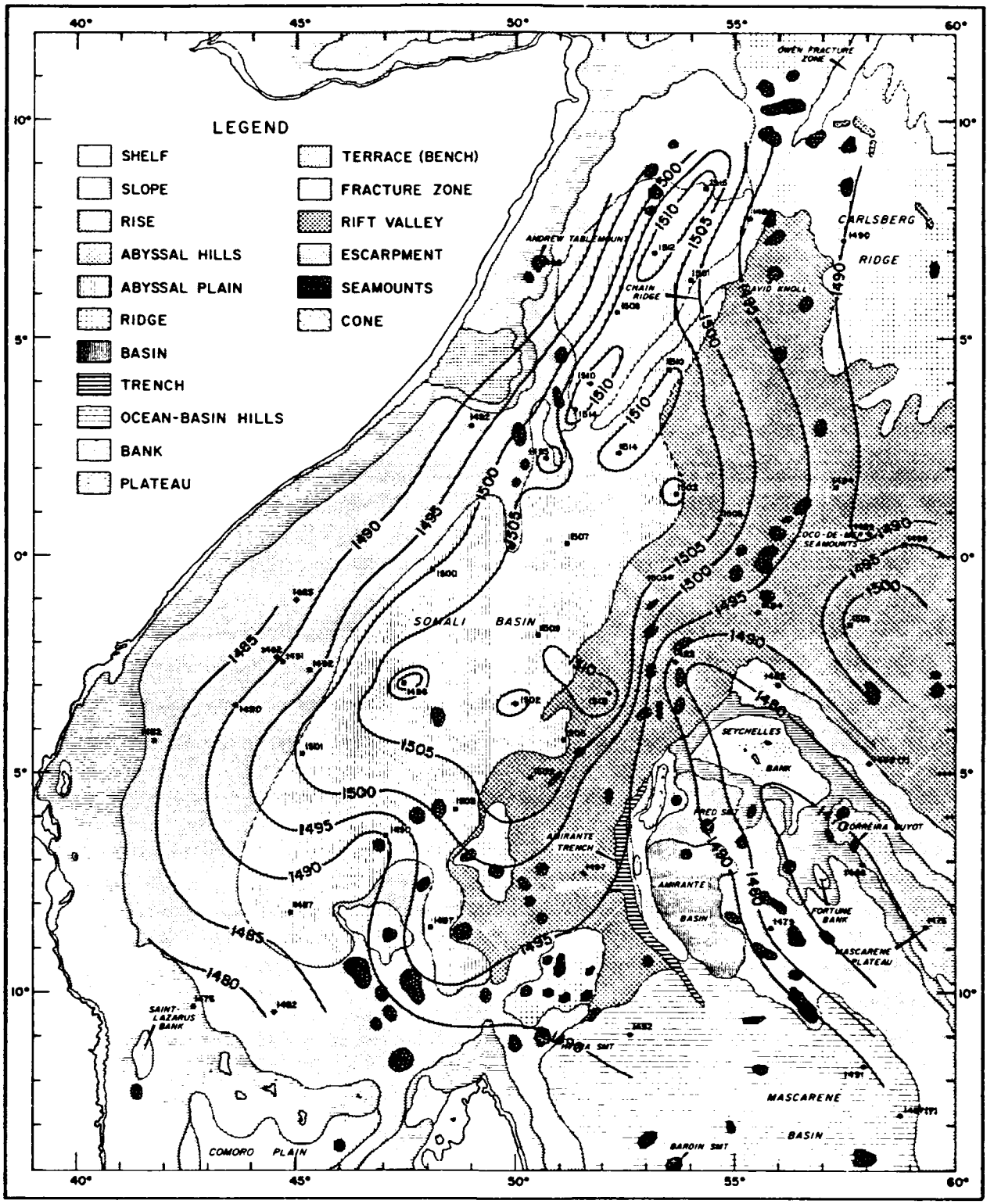

Figure 18. Somali Basin Sediment Surface Sound Velocity Contour Chart.

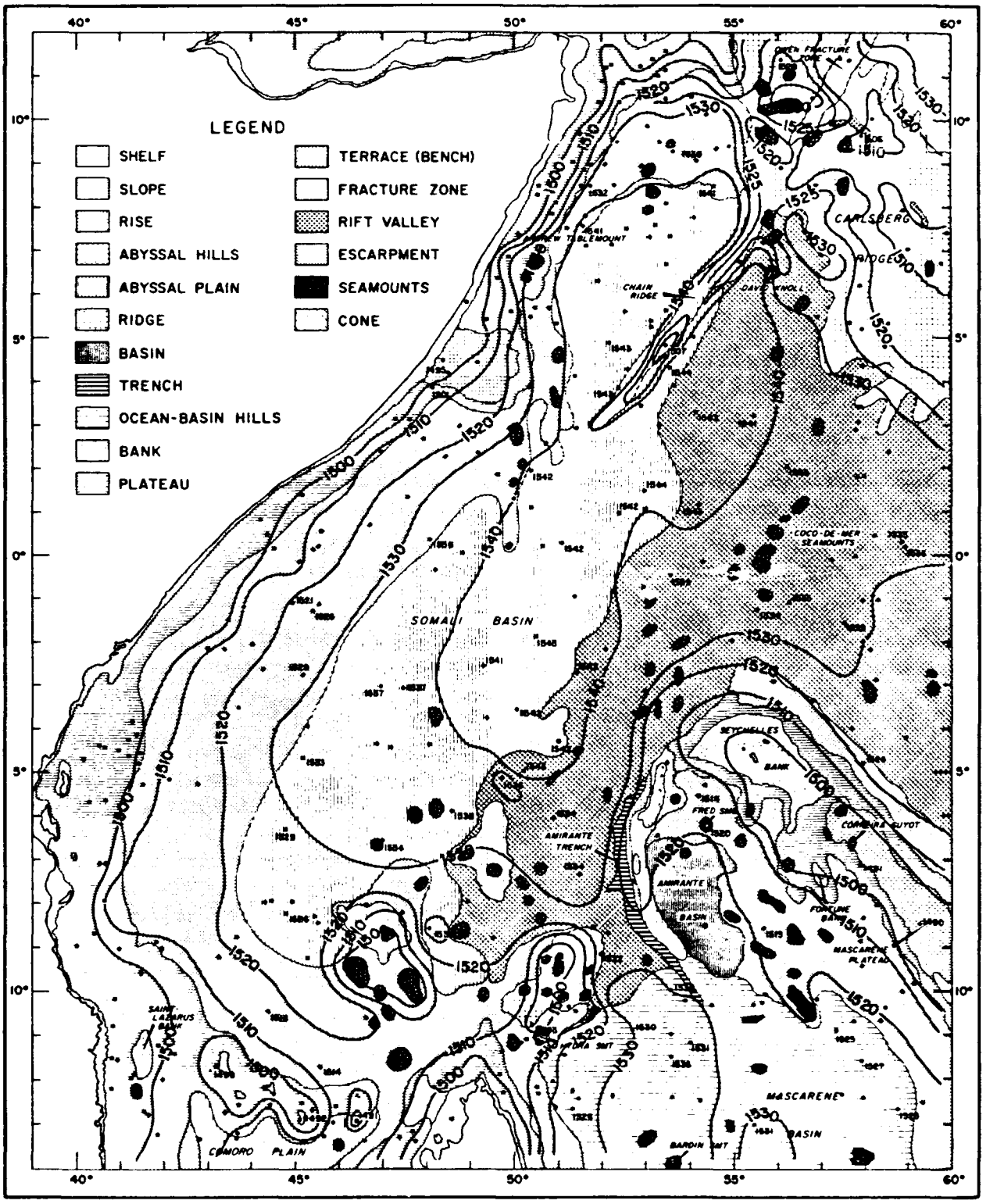

Figure 19. Somali Basin Bottom-Water Sound Velocity Contour Chart.

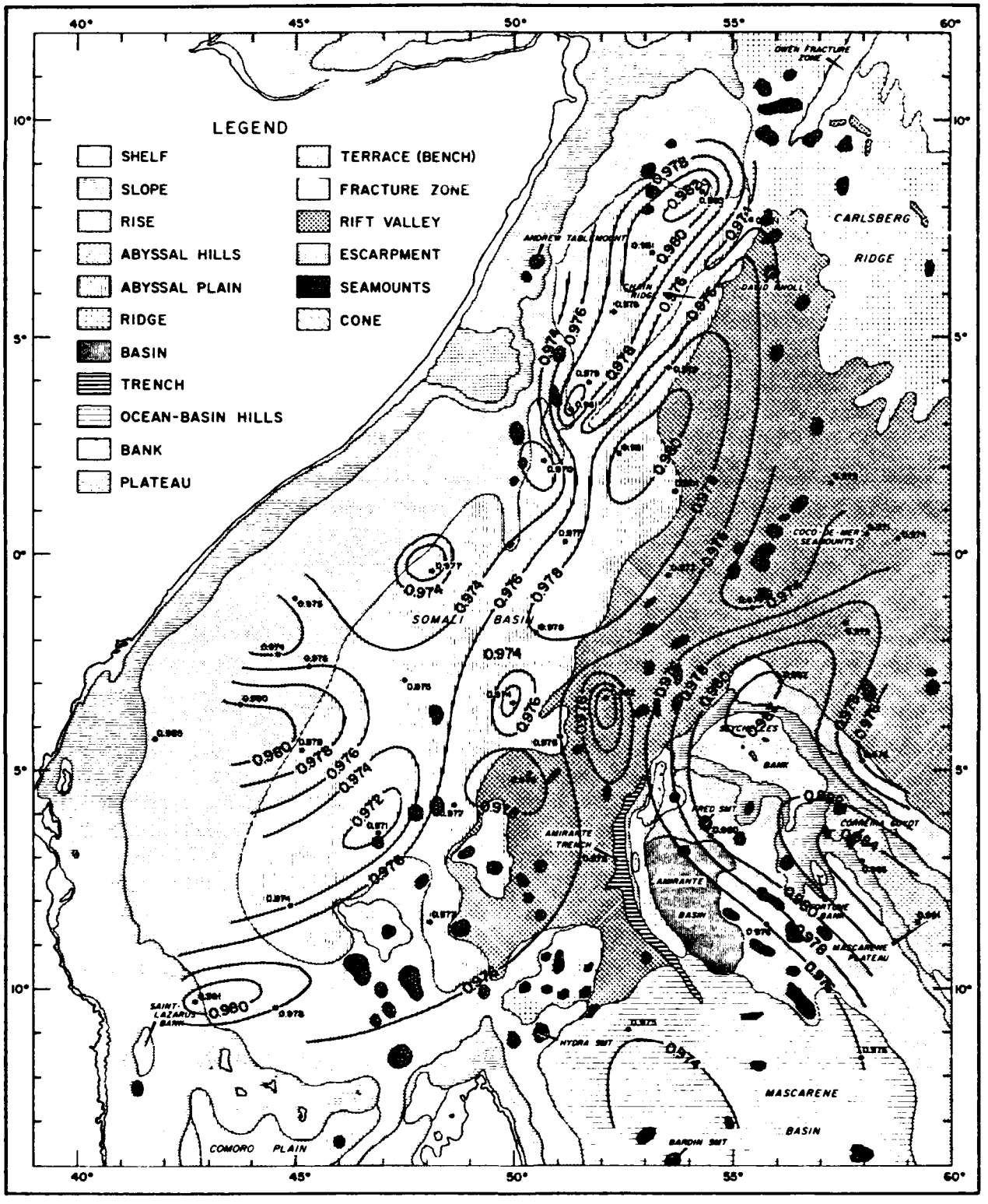

Figure 20. Sediment Surface to Bottom-Water Sound Velocity Ratio Contour Chart for the Somali Basin.

the analysis, station 124 was found to have a higher gradient than most of the remainder of the stations, and station 129 was found to have a lower gradient. However, both of these stations lacked velocities deeper in the sedimentary section; therefore, the observation may not be significant. Stations 131 and 132 are very similar to each other and somewhat similar to station 124. Stations 143, 144 and 145 were quite similar to each other and to the bulk of the stations.

In a comparison of the instantaneous velocity-time curves for each of the stations in the Oman Abyssal Plain, stations 124 and 129 were the only stations that seem to be somewhat anomalous in their gradients and they were suspect due to their lack of deeper velocities. Groupings of stations were used to look for any variations with direction but none were found. The end result of the analysis in the Oman Abyssal Plain was that two velocity-depth curves were derived for two separate conditions: (1) derived using all of the stations except 124 and 129, and (2) derived using all of the stations in the Abyssal Plain. There was no difference between the curves. Groups of stations were plotted together and a velocity-depth curve obtained for them. For example, the velocities from stations 124 through 130 and for stations 133 through 137 were plotted and curves obtained. The two curves were then compared for differences in gradient, etc. The velocities from a group of stations in a north-south line, stations 128, 134, 139, 141, and 145, were similarly plotted and a curve obtained. This curve could be compared to the curve obtained from stations in an east-west line. In fact, two north-south lines were run for comparison to each other and for comparison with an east-west line of stations. This was to detect possible N-S variation with longitude.

The group of stations 167 through 170 and 180 and 181 in the Owens Abyssal Plain which parallels the Arabian Coast was then analyzed. These stations are located along the longitudinal axis of the plain and were analyzed for variations in that direction by comparing individual station velocity-depth curves. No anomalies were detected and all of the station curves were similar as expected.

The third group of stations analyzed is that group taken on the Indus Cone and consisted of stations 146 through 166, 171 through 176, 182 through 186, 300 through 312, and 344 through 346. The wide grouping of station numbers is due to the fact that various legs were run in different years. The analysis of this group of stations was the most varied and also the most comprehensive due to the large number of stations and the geometric pattern of the stations allowing for great variety in the analysis. The instantaneous velocity-time curves were used to determine if there were any anomalous zones in the entire area. In this initial comparison, stations 146 and 149 are somewhat anomalous in that they have slightly higher velocity gradients than other stations. However, both of these stations

have only two velocities, a surface velocity and one layer velocity, and are not considered to be very reliable. In comparing all of the remaining stations, minor differences in initial velocity and minor differences in gradient are observed but all of the station curves are remarkably similar. Based on these results, the stations were arranged in various groupings. For example, all of the stations taken at the nose end of the Indus Cone in water less than 3,000 meters were put into one group, all of those in the mid-Cone area in water 3,000 to 4,000 meters were put in a second group and all of the stations on the distal end of the Cone in water 4,000 meters or more were put in a third group.

Another mode of analysis is to take each line of stations as a group, 146 through 148 or 149 through 153, and compare these composite curves to the curve for the adjacent line. Stations are plotted in a stepwise fashion with each line of the track down the entire Indus Cone. (See figure 21.) A number of stations whose positions form a line from north to south across the Cone are assembled into two groups and composite curves are derived for stations at different longitudes to evaluate possible variations between the two north-south lines. Two east-west lines of stations were also chosen and curves obtained to check for variations in curves between east-west lines at different latitudes. Comparisons were made between the north-south lines and east-west lines. Other lines of stations at various angles around the compass were also used to derive instantaneous velocity-time curves and check for any radial variations throughout the area.

After all the comparisons and evaluations had been carried out with all of the various possibilities for groupings, velocity-depth curves were derived for a dozen of the more significant groupings. These curves were used for the final evaluations. Three of the twelve pertained to the Oman Abyssal Plain area and the Owens Abyssal Plain area. Only one velocity-depth function is needed for each of the two abyssal plain areas. The remaining nine velocity-depth functions are derived for the Indus Cone area to verify observations from the instantaneous velocity-time functions. The gradient is sufficiently low on the first line of stations (146 through 148) to justify its own velocity-depth function. All of the remaining lines of stations are found to be similar enough to be modeled by only one velocity-depth function.

Thus, for the Arabian Sea, it is suggested that four separate velocity-depth functions apply: One for the Oman Abyssal Plain, one for the Owens Abyssal Plain, one for the upper reaches of the Indus Cone (within 160 miles of shore) and one for the remainder of the Cone. The functions for these four areas are tabulated in table 1B along with the variance and standard estimate of error for each function.

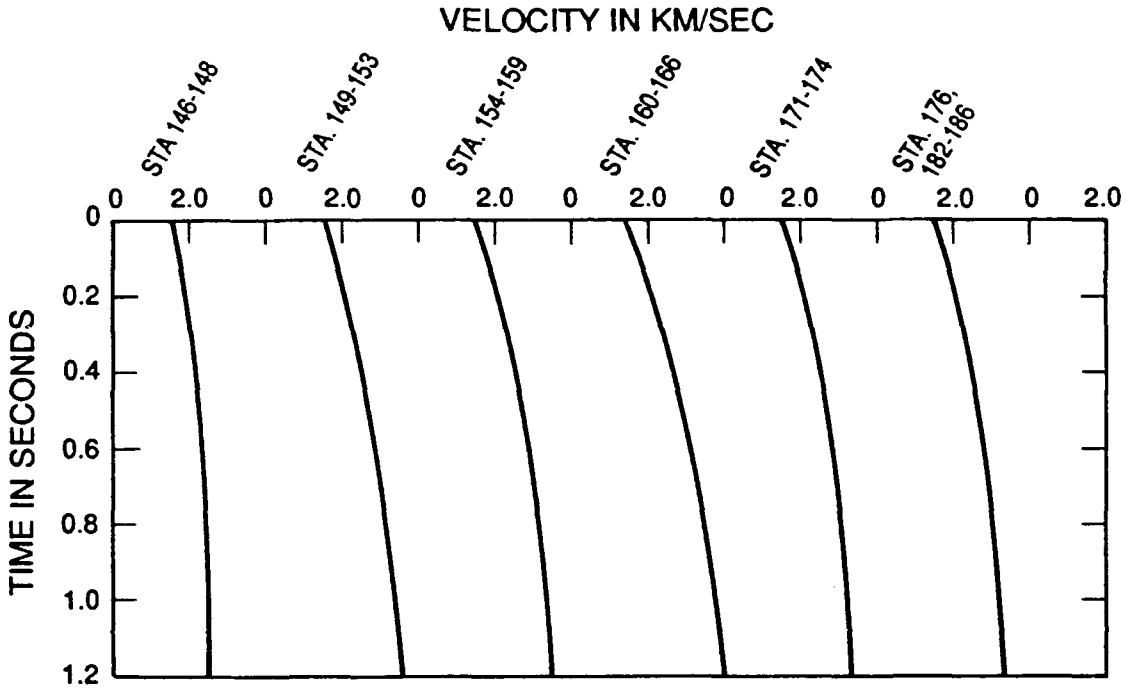

Figure 21. Instantaneous Velocity-Time Curves for the Indus Cone.

The velocity-depth function for the lower Indus Cone varies somewhat in gradient from that developed by Bachman and Hamilton (1980) from eight WABR stations taken in 1977 on the Indus Cone by the USNS WILKES. In this work we have the benefits of a considerably greater number of stations, well spaced across the Cone and with supporting core data for surface sediment velocity, to ensure that our quantification of regional velocity-depth parameters is valid. A presentation and comparison of the two curves is made in a later chapter.

Fence diagrams constructed for the interval velocities and thicknesses obtained for the Arabian Sea are presented in figure 22. These diagrams indicate even greater variability than those for the Somali Basin, at least for the Indus Cone. The Oman Abyssal Plain does seem to have a fairly uniform section in the upper few hundred meters throughout most of the Plain. Only in the southernmost portion of the Plain triangle does it differ. The Owens Abyssal Plain shows the same uniformity as the Oman Abyssal Plain. On the Indus Cone, the lowermost section velocity seems to be fairly consistent throughout the Cone but successive sections above this show a considerable amount of variation.

Charts of the sediment surface sound velocity, bottom-water sound velocity and the ratio of the sediment surface sound velocity to the bottom-water sound velocity are presented as figures 23, 24, and 25. Consideration of the sediment surface sound velocity chart in figure 23 shows a velocity increasing with distance from the source of deposition and in consequence with depth. A distortion of the smooth contour pattern of the upper section of the Indus Cone can be noted in the vicinity of the Lakshmi Ridge and is very likely due to a channeling of the sediments to the east of the Ridge as noted by Kolla and Coumes (1987). The bottom-water sound velocity contour chart shown in figure 24 exhibits a considerable uniformity with the velocity, again increasing with distance from the nose of the Cone as depth increases. The chart showing the ratio of the sediment surface velocity to bottom-water velocity is shown in figure 25. Considering the relative uniformity of the two previous charts, this chart is somewhat surprising. Aside from the ratio high in the upper portion of the Cone, the ratio generally decreases with distance from the source of the Cone. Obviously, the bottom-water velocity increases faster with distance from the nose of the Cone than does the sediment surface velocity. The implications of the fence diagrams and of the velocity contour diagrams of both the Somali Basin and the Arabian Sea are discussed in the following section.

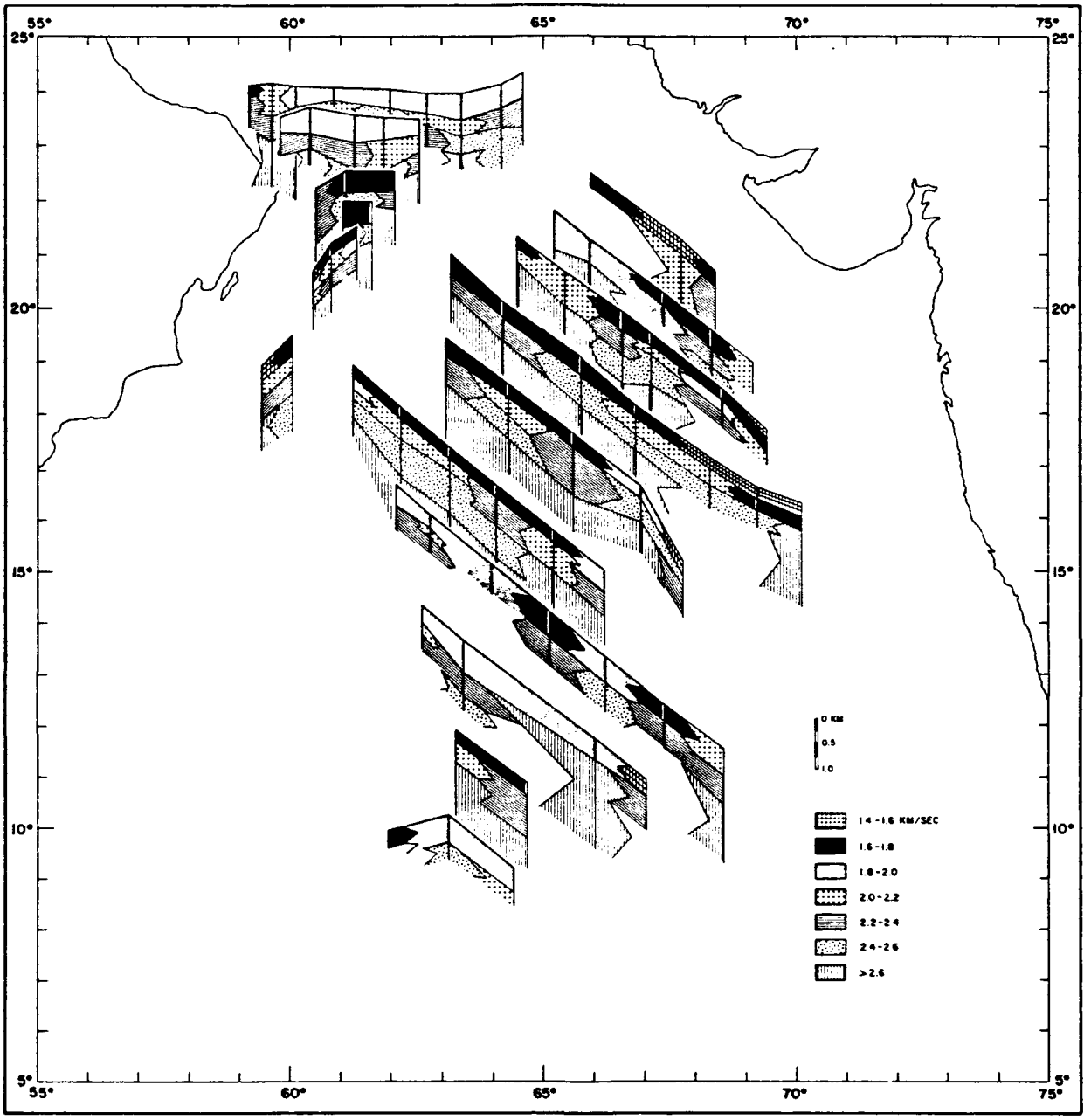

Figure 22. Fence Diagram of Interval Velocities and Thicknesses of the Arabian Sea.

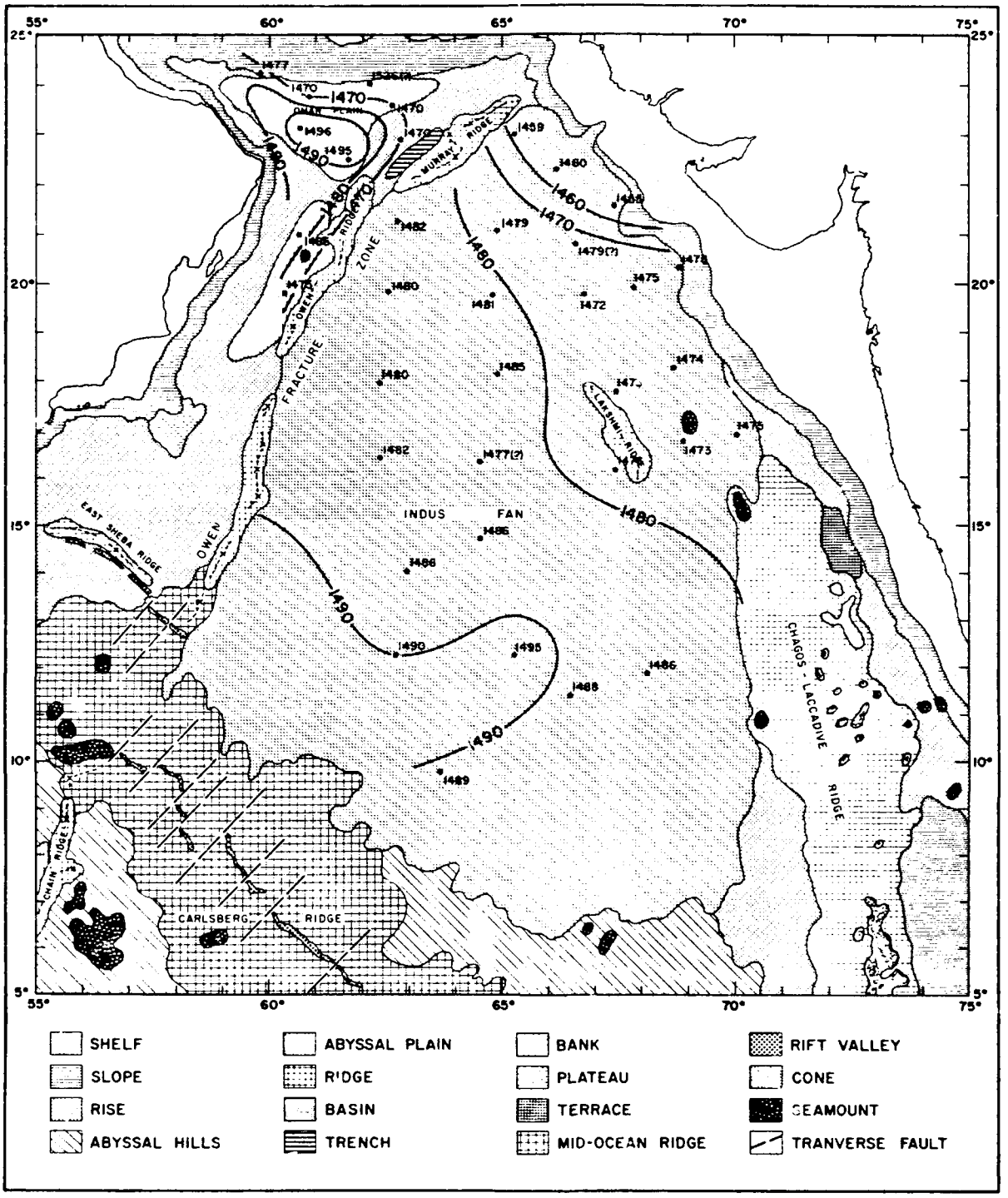

Figure 23. Arabian Sea Sediment Surface Sound Velocity Contour Chart.

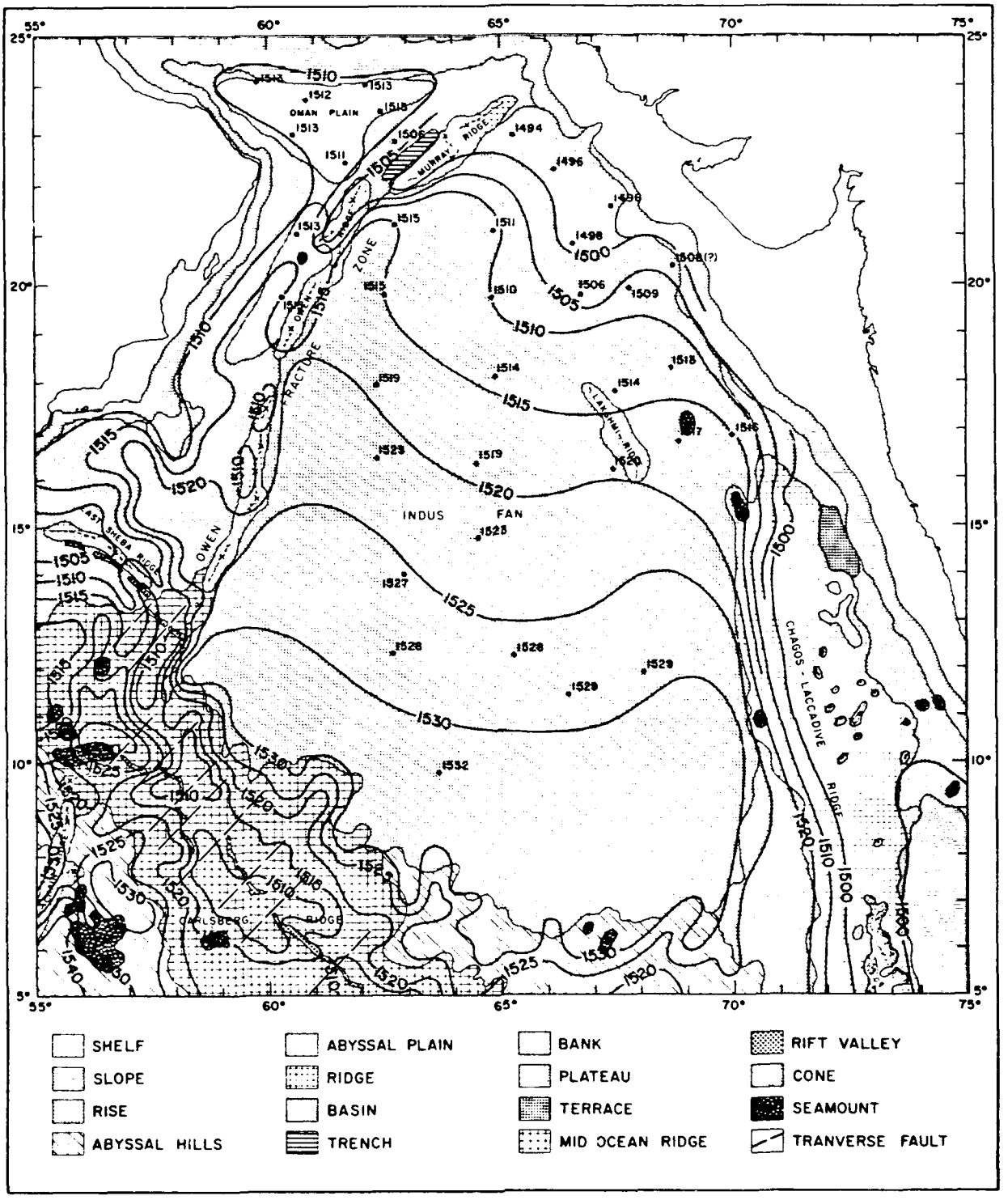

Figure 24. Arabian Sea Bottom-Water Sound Velocity Contour Chart.

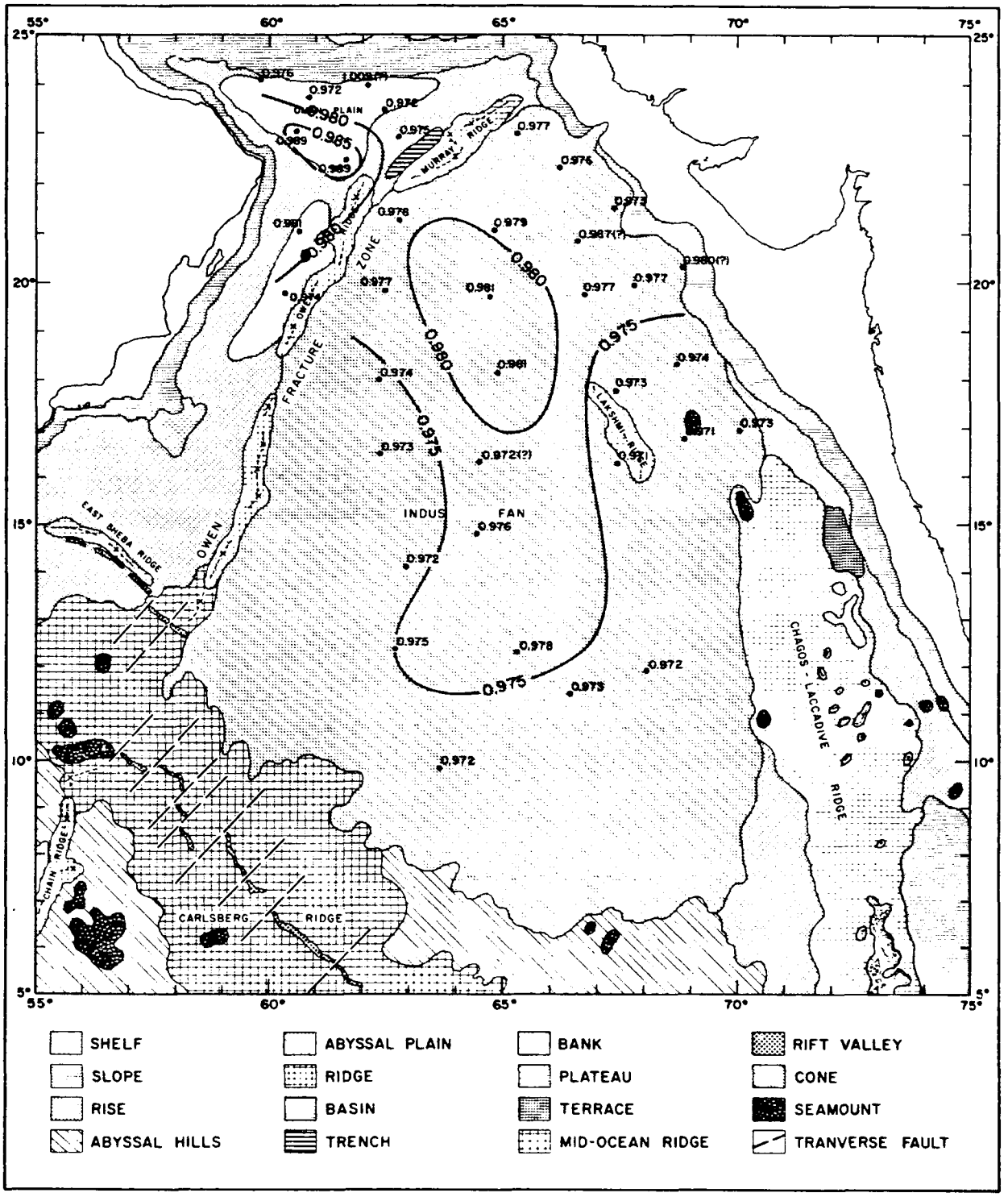

Figure 25. Sediment Surface to Bottom-Water Sound Velocity Ratio Contour Chart of the Arabian Sea.

IV. DISCUSSION

The construction of sound velocity contour charts for the sediment surface, the bottom water and the ratio of these two was detailed in the previous chapter. Some of the features noted in those charts are considered at this point. The most obvious feature in all of the contour charts is the relationship of the velocity to the physiography and depth. The relationship of the water sound velocity with depth is well known as noted by Urick (1983), and of interest to this discussion is the fact that the bottom-water velocity varies linearly with depth beyond the main thermocline. This relationship varies minimally with seasons but the particular linear relationship does vary from ocean area to ocean area.

The relationship of sediment surface velocity with depth suggested by the contour charts seems reasonable, when considering that the water content of the core samples in this study was determined by the NAVOCEANO Core Lab to be in the range of 40% to 50%, and the included water is the same bottom water. To test this observation, the sediment surface velocities were plotted versus water depth for both the Somali Basin and the Arabian Sea. A straight line was fit to the data by least squares for each case and a correlation coefficient determined to verify the relationship. The two plots are shown as figures 26 and 27. The particular bottom-water velocity versus depth relationship for each area was determined by plotting the bottom-water velocity measurements versus water depth and fitting with a straight line. These are included in the appropriate figures to facilitate comparison of the slopes of the linear fit. The correlation coefficient for the linear fit of the sediment surface velocities indicates a definite linear relationship in each area. The nearly identical slopes of the fit for sediment velocity and bottom-water velocity in each case indicate that the included water is a controlling factor.

Having noted the sediment surface velocity to water depth relationship, it was considered that this might be a factor in the differences noted in the velocity-depth functions of the subareas of the Somali Basin and the Arabian Sea. The weighting given to the sediment surface velocity influences the derived instantaneous velocity-time function, and in turn the velocity-depth function and might explain some of the differences in the functions of various subareas. To test this hypothesis, sediment surface velocities for a common water depth were obtained from figures 25 and 26. All of the sediment surface velocities for the Somali Basin were normalized to the same common depth of 4500 meters (1.490 Km/s) and all Arabian Sea velocities were normalized to the same common depth of 3220 meters (1.476 Km/s). Instantaneous velocity curves were recalculated using these normalized velocities for four of the eight cases in the Somali Basin and the four cases in the Arabian Sea. The resulting functions continue to show the minor variations between the

SOMALI BASIN

Sediment Surface Velocity versus Water Depth
Bottom Water Velocity versus Water Depth

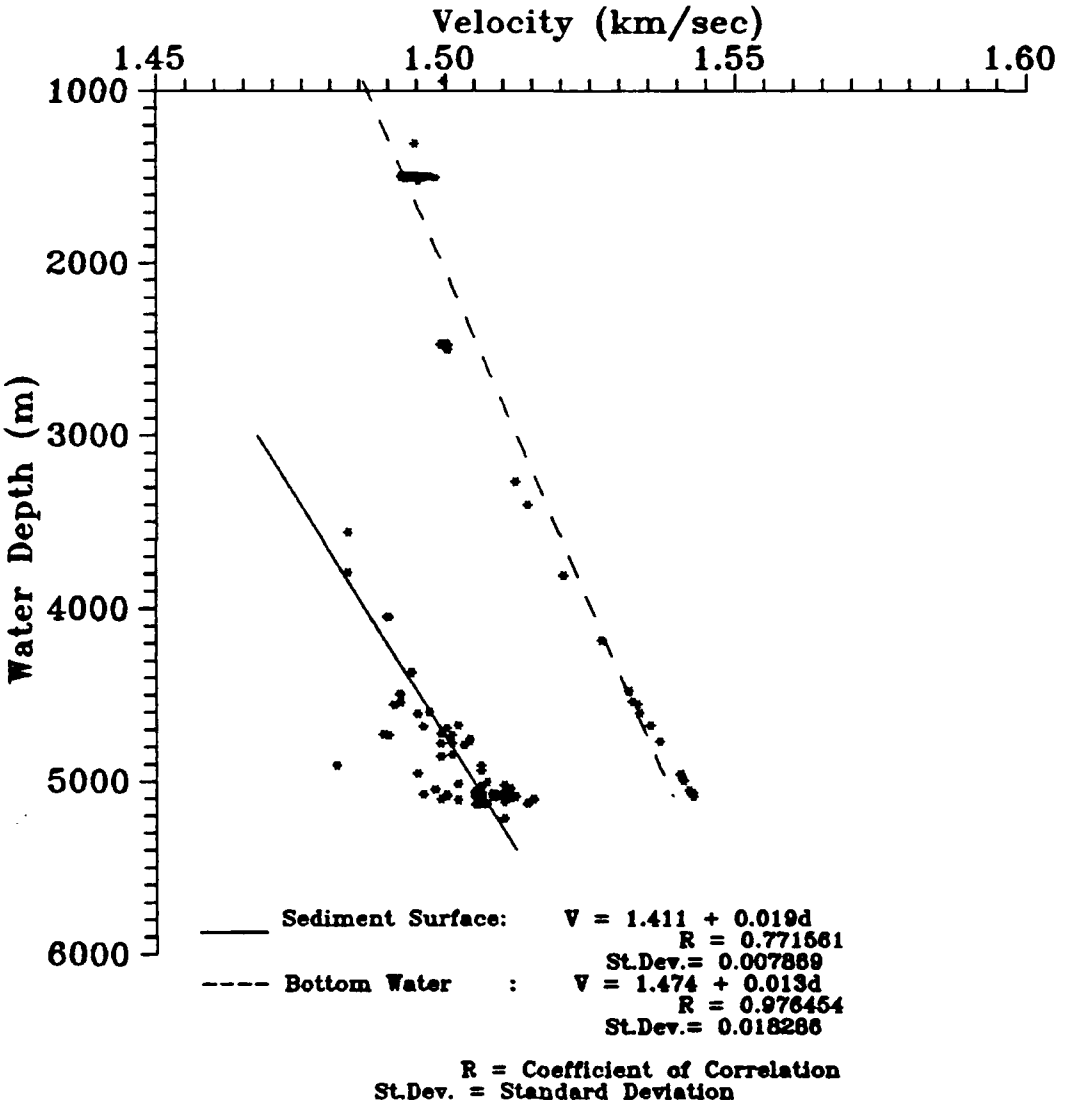

Figure 26. Sediment Surface Velocity Versus Water Depth in the Somali Basin.

ARABIAN SEA

Sediment Surface Velocity versus Water Depth
Bottom Water Velocity versus Water Depth

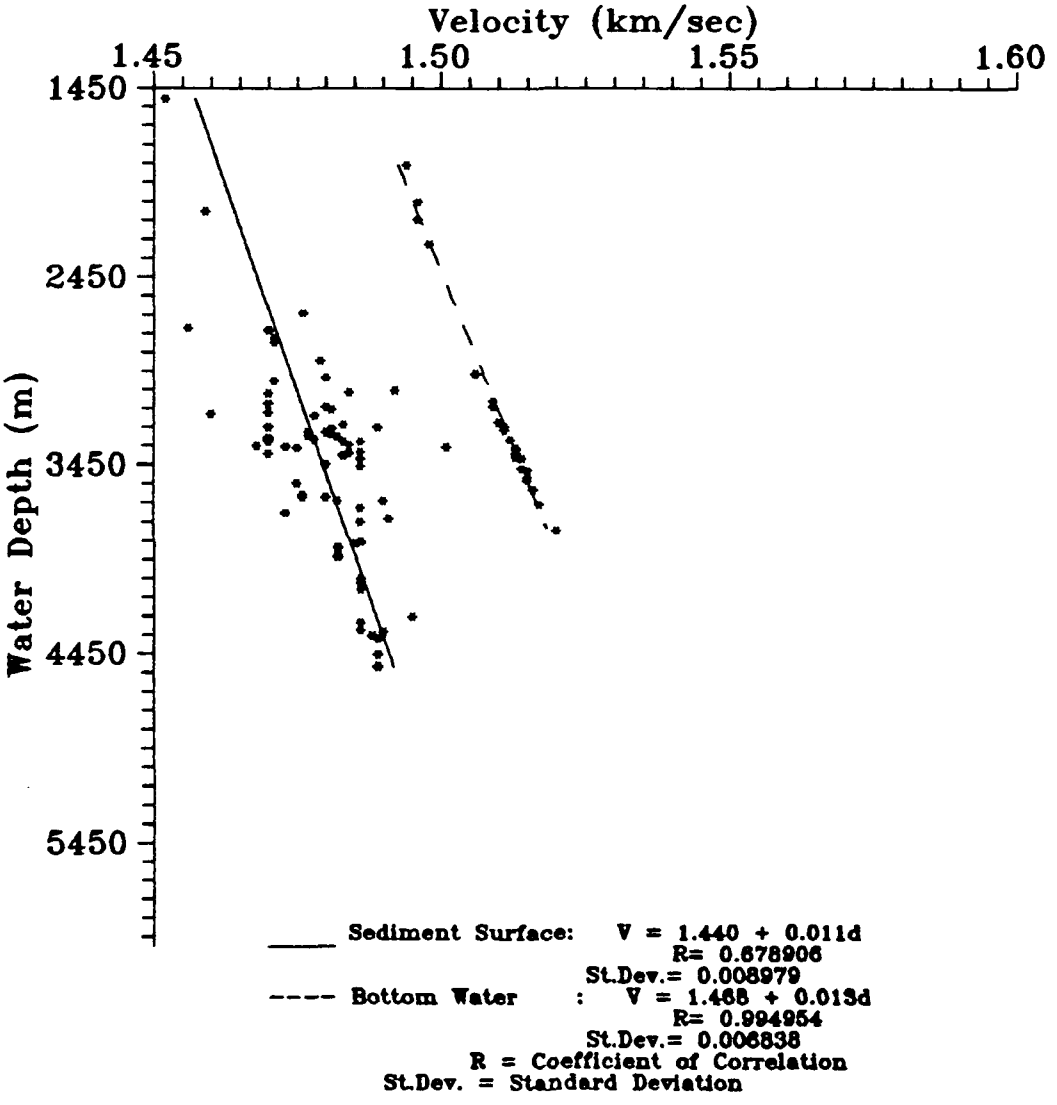

Figure 27. Sediment Surface Velocity Versus Water Depth in the Arabian Sea.

functions of different areas and were not significantly different from the original functions. A comparison of two normalized derived functions versus standard derived functions is presented in figures 28 and 29. As was the case in the original analysis, the curves obtained did not pass through the "normalized" origin point despite the heavy weighting of this point due to the normalization. This indicates that despite the control of water depth on sediment surface velocity, the velocity at depth in the sediments influences the initial velocity of the derived function to a considerable extent.

In the velocity contour charts of the Somali Basin, the high ratio in the southwest corner of the Basin is somewhat disconcerting given the smooth contours of the other two charts. The sediment surface velocity chart does not indicate a high at this point nor does the bottom-water contour chart indicate a low to explain the ratio high. Neither the descriptions of Deep Sea Drilling Project (DSDP) Site 241 nor the seismic cross section of Francis et al. (1966) gives any indication of an unusual sediment surface velocity high in this area which was not detected by our cores. The author concludes that it is a contouring artifact of the adjoining low just to the southeast.

In the velocity contour charts of the Arabian Sea, the ratio high in the upper portion of the Indus Cone in figure 25 is considered to be the result of the channeling effect of the Lakshmi Ridge on the sediment transport, as well as the decrease of the ratio further down the Cone. The observation was made earlier that the bottom-water velocity was increasing at a faster rate than the sediment surface velocity along the extent of the Cone. This is considered to be due to the transported sediments becoming finer with distance from the source at a higher rate than the increase of bottom-water velocity with depth. The result is a general decrease in the ratio with increasing depth.

The fence diagram of the Somali Basin indicates a considerable amount of consistency in the sediment section of the northern basin between Chain Ridge and the African coast. This is not surprising considering the limited nature of this portion of the Basin and its enclosure by coast and ridges. The southern portion of the Basin shows reasonable consistency considering its size. The major difference is in the very central portion of the southern fence diagram where slightly higher velocities occur nearer the surface. Despite the variation indicated by the fence diagrams, the individual station instantaneous velocity functions show little variation. This is presumed to be due to the smoothing effect of plotting curves through data points in which the layer velocity is assigned to the midpoint of the layer.

The fence diagrams of the Arabian Sea show quite a similar situation. The Oman Abyssal Plain and the Owens

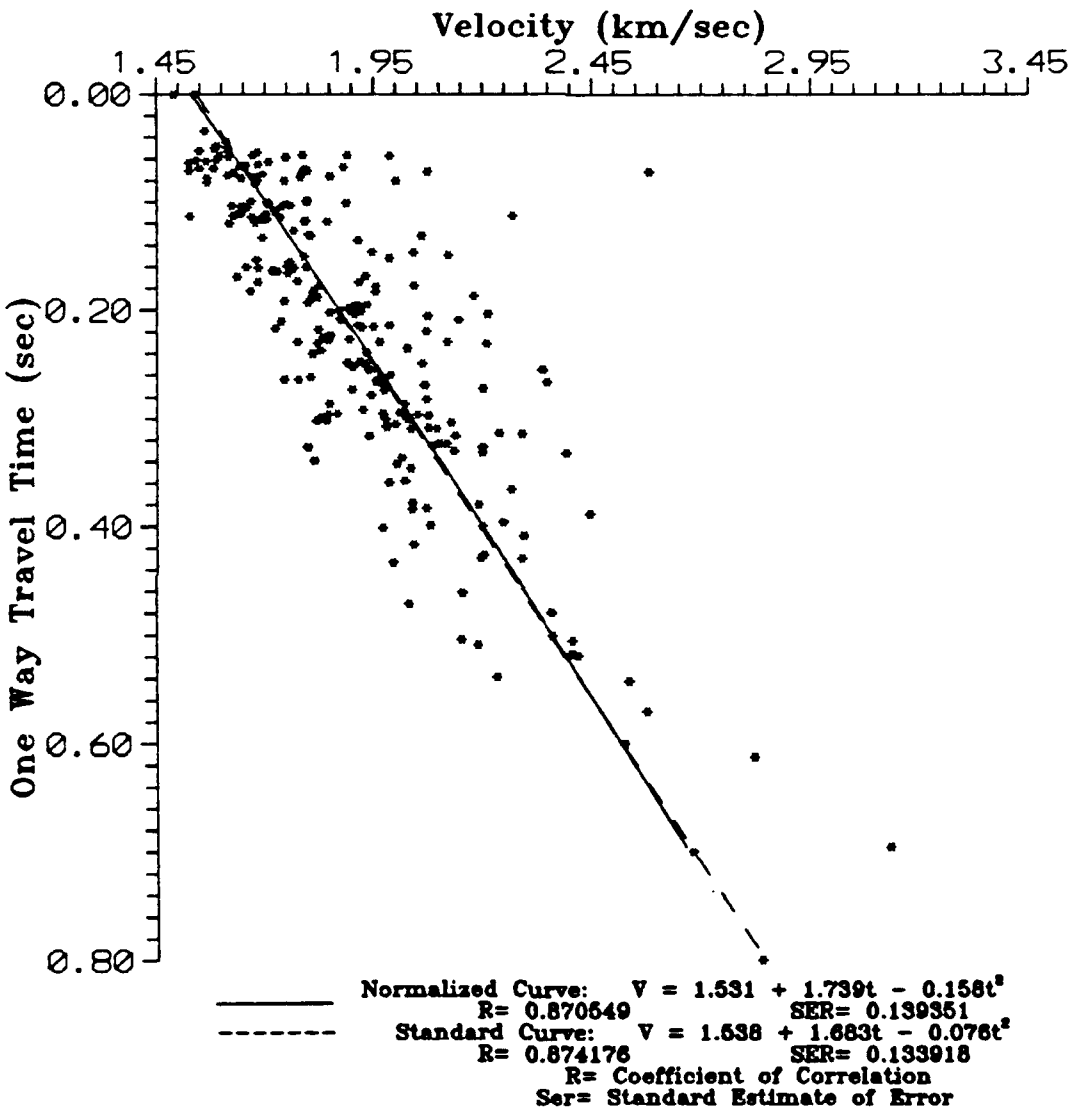

Figure 28. Instantaneous Velocity-Time Curves for Normalized Versus Standard Data in the Somali Basin.

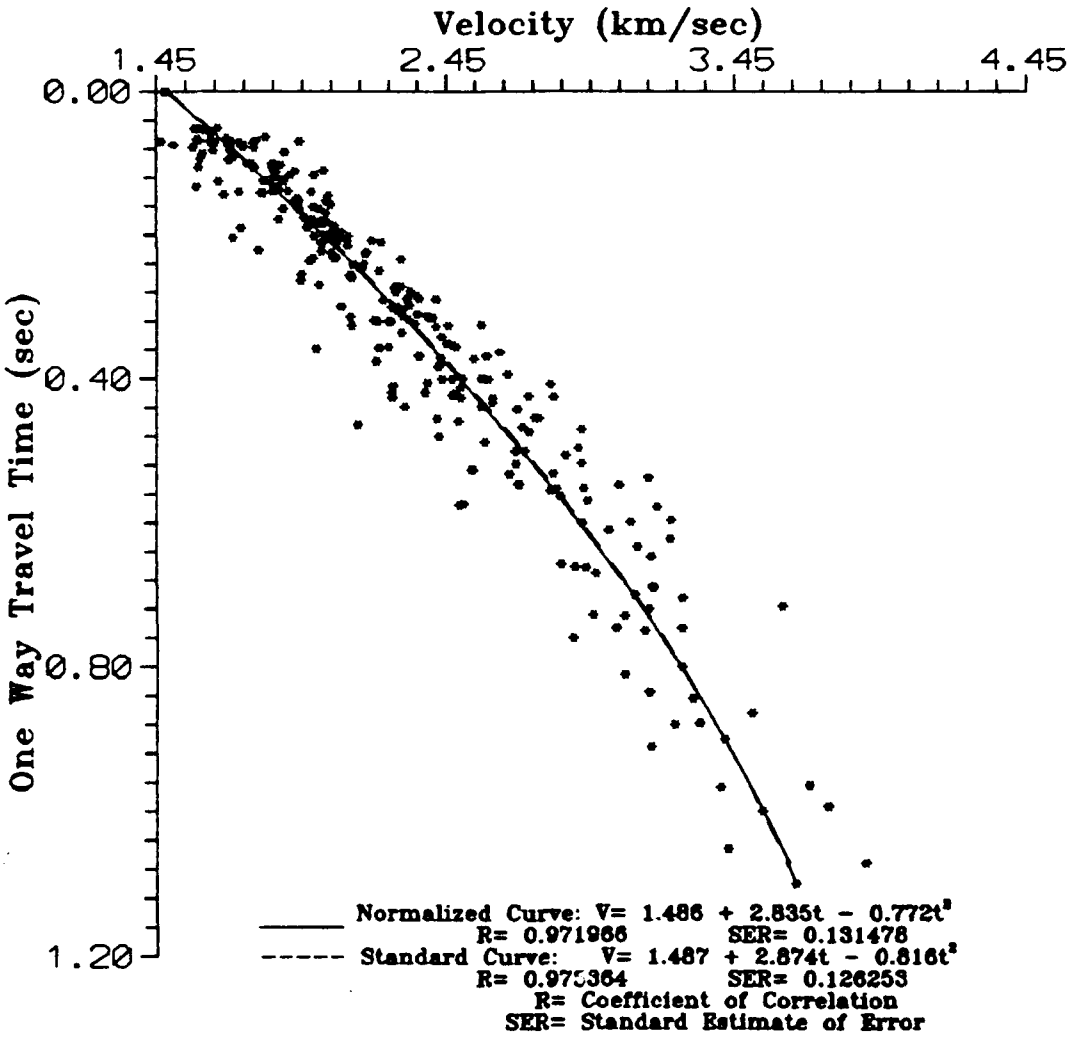

Figure 29. Instantaneous Velocity-Time Curves for Normalized Versus Standard Data in the Arabian Sea.

Abyssal Plain both show considerable consistency as did the northern Somali Basin, presumably for the same reason. The Indus Cone fence diagram exhibits extensive variation throughout. Unfortunately, all of the DSDP and Ocean Drilling Program (ODP) sites taken in the Arabian Sea have been on the fringes of the Indus Cone along the Chagos Laccadive Ridge or the Owens Ridge. Thus, the author relies on the work of the two authors who have conducted the bulk of the investigation of the Indus Cone, B.R. Naini and V. Kolla. A basal layer following the structural trends of the basement cited by Naini and Kolla (1981) would correspond to the >2.6 km/s layer, which seems to be fairly uniform throughout the fence diagram. The investigators believe the sediments in this basal layer were mainly influenced by pelagic sedimentation while the lower velocity sediments in the upper layers were mainly deposited by turbidite sedimentation. The considerable variation in the upper layers of the fence diagram is the result of the deposition by the three canyon complexes which migrated extensively across the fan as noted by Kolla and Coumes (1987).

The velocity ratio chart of figure 20 can be compared to a ratio chart whose ratios were obtained from the tables of Hamilton (1980) shown in figure 30. Core descriptions could be used to enter table IIB, under the heading of abyssal plain and obtain the appropriate ratio. Upon attempting this work, it was found that all of the cores for which velocity data were available had not yet been analyzed and description of sediment types were not available. Of the cores taken by NAVOCEANO in the Somali Basin, only 13 had sufficient core analysis beyond velocity measurements for this purpose. Another 16 cores with suitable analysis were found in Burroughs (1977) and 6 cores were obtained from the DSDP (Fisher et al., 1974; Simpson et al., 1974). Using the physiographic location and the percentages of sand, silt and clay to enter the tables, a velocity ratio for each of the 35 core locations was obtained and plotted. It is recognized that 35 data points is a limited number for contouring such a large area. However, this number of data points is sufficient to point out any obvious similarities or differences. It quickly became apparent that most of the sediments would fall into one table category (Hamilton, 1980 [Table IIB, Abyssal Hill, Calcareous Pelagic Sediment]); therefore, all have the same velocity ratio. The result is shown in figure 31.

Only two points can be made with any degree of confidence based on this comparison. First, the chart based on ratios from the table implies that the bulk of the area has a velocity ratio greater than one, while the measured ratio chart shows no ratio as great as one. Secondly, there is a general agreement between the two charts in that the velocity ratio in the southern portion of the basin is somewhat lower in general than that in the northern part of the basin. The explanation for the difference in the ratios obtained by NAVOCEANO and those presented in

TABLE IIB. Abyssal plain and abyssal hill environments; sediment densities, porosities, sound velocities, and velocity ratios.

Environment	Density [a] (g/cm³)		Porosity [a] (%)		Velocity [a] (m/s)		Velocity ratio [a]	
Sediment type	Av	SE	Av	SE	Av	SE	Av	SE
Abyssal plain [b]								
Clayey silt	1.454	0.022	74.2	1.58	1528	3	0.999	0.002
Silty clay	1.348	0.014	80.5	0.98	1515	2	0.991	0.001
Clay	1.352	0.037	80.0	2.20	1503	2	0.983	0.001
Bering Sea and Okhotsk Sea (siliceous-diatomaceous)								
Silt	1.447	...	70.8	...	1546	...	1.011	...
Clayey silt	1.228	0.019	85.8	0.86	1534	2	1.003	0.001
Silty clay	1.214	0.008	86.8	0.43	1525	2	0.997	0.001
Abyssal hill								
Deep-sea ("red") pelagic clay								
Clayey silt	1.347	0.020	81.3	0.95	1522	3	0.995	0.002
Silty clay	1.344	0.011	81.2	0.60	1508	2	0.986	0.001
Clay	1.414	0.012	77.7	0.64	1493	1	0.976	0.001
Calcareous pelagic sediment								
Sand-silt-clay	1.435	0.007	75.3	0.38	1556	2	1.017	0.001
Silt-clay	1.404	0.011	76.9	0.64	1536	1	1.004	0.001

[a] Laboratory values: 23 °C, 1 atm pressure; density: Saturated bulk density; porosity: Salt free; velocity ratio: Velocity in sediment/velocity in sea water at 23 °C, 1 atm, and salinity of sediment pore water; SE: Standard error of the mean.

[b] For approximate properties of thinner, coarser-grained layers in abyssal plain turbidities: See continental terrace Tables IA and IB in the fine sand to sand-silt-clay sizes (silt is most common).

Figure 30. Illustration of Hamilton's Table II B.

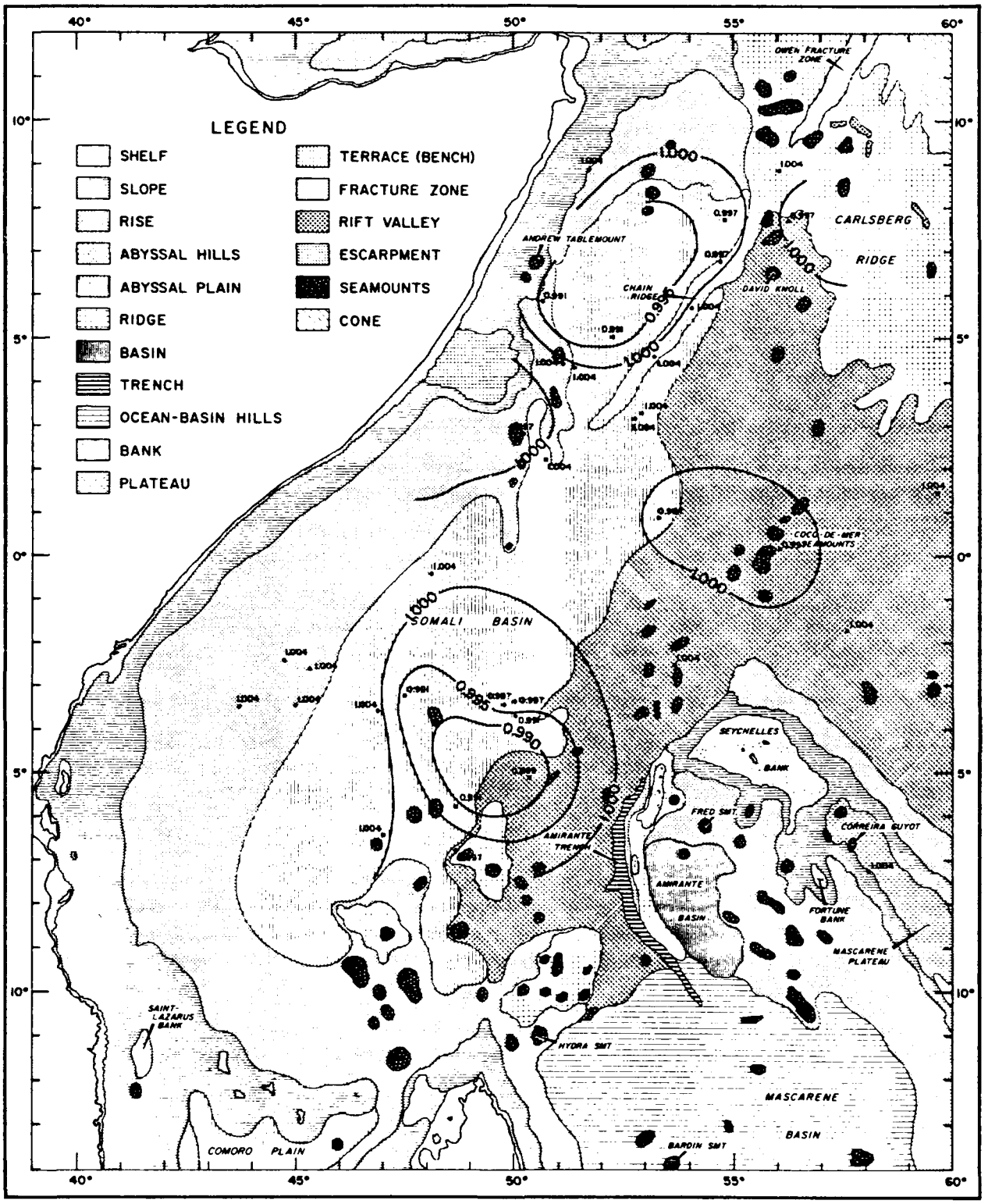

Figure 31. Velocity Ratio Contour Chart Using Hamilton's Tables.

the table is that those in the table are approximate values. In a phone discussion of this subject with Dr. Hamilton (pers.com. 1983), his comment was "always go with the measured quantity."

To see what effect a difference in velocity ratios might have on the Rayleigh reflection coefficient, two coefficients were calculated for a central location in the Somali Basin using a ratio derived from Hamilton's tables and a NAVOCEANO-derived ratio of 0.974. The bottom-water density was obtained from CTD data and the surface sediment density from core data. The expression for the reflection coefficient is that for a liquid-liquid interface, given as:

$$R = \frac{(D_S / D_W) \sin \theta - ((C_W / C_S)^2 - \cos^2 \theta)^{1/2}}{(D_S / D_W) \sin \theta + ((C_W / C_S)^2 - \cos^2 \theta)^{1/2}}$$

where:

Bottom-Water Density (D_W)	1.02782 g/cm
Surface Sediment Density (D_S)(Sta. 56)	1.33 g/cm
Bottom-Water Velocity (C_W)	taken from fig. 18
Surface Sediment Velocity (C_S)	taken from fig. 17
Grazing Angle (θ)	variable
Hamilton's Table Ratio (C_S / C_W)	1.004
NAVOCEANO Ratio (Sta. 56) (C_S / C_W)	0.974
Location	00° 30'N, 53° 30'E

The results are given in figure 32.

A velocity ratio greater than one indicates that the sediment surface velocity is greater than the bottom-water velocity. During this study, and in all other WABR work in deep water, no velocity ratios greater than or equal to one were encountered.

The numerical difference between NAVOCEANO-measured ratios and those derived from Hamilton's tables is small, but the significance of whether the ratio is less than or greater than 1 is important as can be noted in figure 32, particularly at small grazing angles.

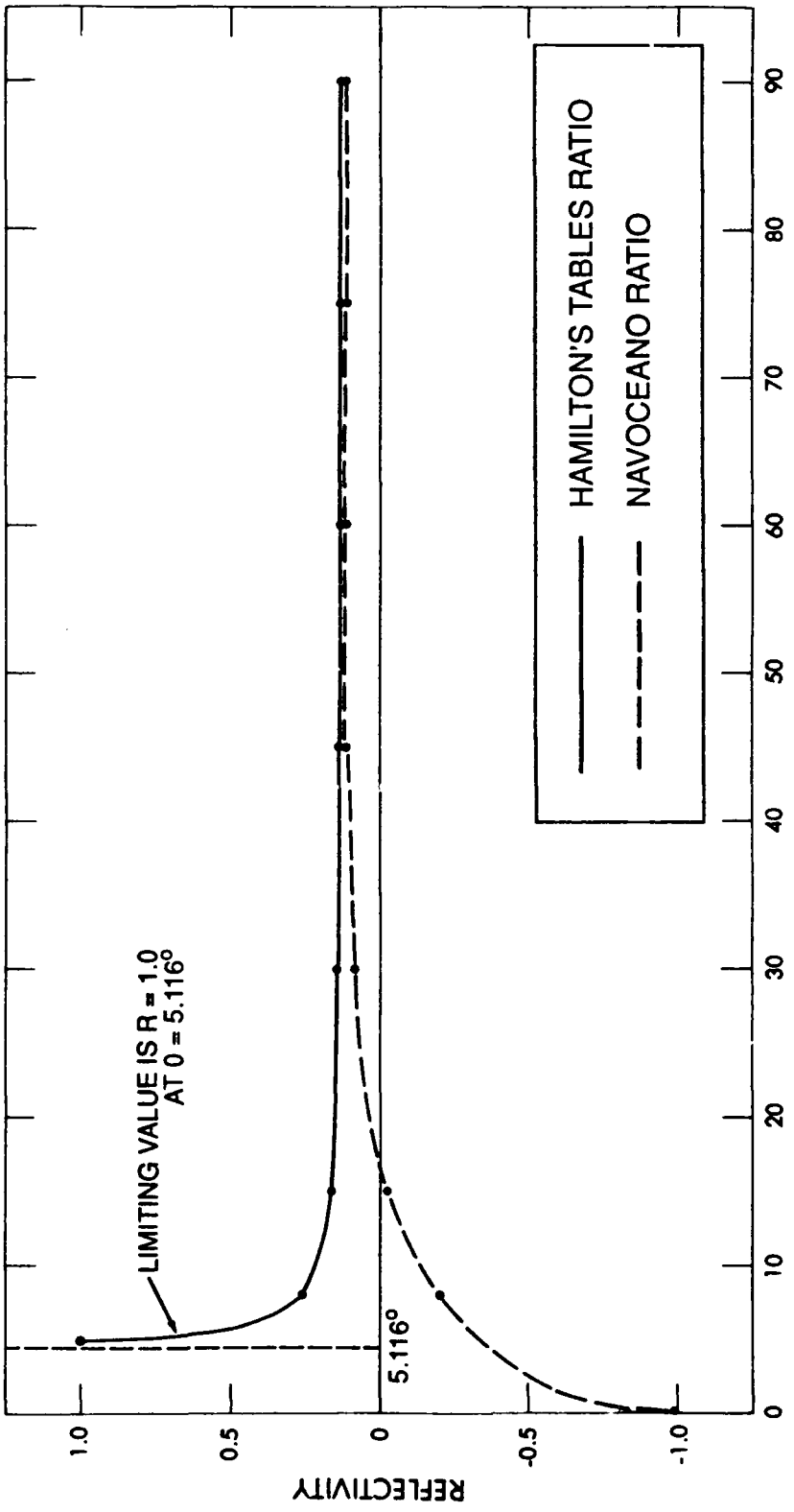

Figure 32. Plot of Reflection Coefficients Versus Grazing Angle.

V. CORRELATION WITH OTHER SEISMIC WORK

As mentioned earlier, considerable study of the Somali Basin has been carried on by various investigators such as Francis et al. (1966), Bunce et al. (1967), Davies and Francis (1964) and more recently by Coffin et al. (1986). Since Mombasa was a major port of operations during the International Indian Ocean Expedition, numerous tracks were made through the Basin. Unfortunately, many of the ships participating did not have seismic systems, and many of those with seismic systems took only seismic vertical reflection profiles. Aside from the refraction work by Francis et al. (1966), only a limited number of interval velocity measurements had been made until the measurements presented here and those recently published by Coffin et al. (1986).

The general velocity-depth structure as obtained by this study and the refraction work of Francis et al. (1966) can be compared. Both studies agree that the sediment velocity increases gradually and smoothly with depth to at least 1500 meters beneath the sea floor, the limit of our penetration. We also agree on the velocity range of 1.50 km/sec to 1.80 km/sec in the upper 1500 meters.

It is possible to correlate to the work of Coffin et al. (1986) only to a limited extent, since the bulk of our stations in the Somali Basin were to the east of the Coffin stations. Only 11 of our stations were in the Continental Rise area in the western portion of the Somali Basin, whereas all but 9 to 10 of their stations are on the Rise. Using only those stations taken on the Rise, we derived a linear instantaneous velocity function given by $V = 1.544+1.569t$. Their results are similar, $V = 1.577+1.655\ t$ (where t is one-way travel time).

In September of 1981, we received some preliminary global velocity data from Houtz at Lamont-Doherty Geological Observatory (pers. com. 1981). These velocity functions are given in the form $V= V'+ Kt$ where the sound velocity is expressed as a function of one-way travel time, t, V' is the sediment surface velocity and K is the vertical gradient of sound. For the Somali Basin, the Lamont function is $V = 1.58+1.74t$. An instantaneous velocity function from the data of all 70 Somali Basin stations in this study results in the function $V = 1.540+1.649t$. Our sediment surface velocity and velocity gradient are lower than that of Houtz, but in general the agreement is good (figure 33). For example, if one predicts the velocity of sound in the sediment at a depth equivalent to 0.3 seconds of one-way travel time, a velocity of 2.102 Km/sec would be obtained using the Houtz model and a velocity of 2.035 Km/sec according to the NAVOCEANO model. In the Somali Basin, near-surface velocities derived from the DSDP are 1.47, 1.48, 1.53, 1.51 and 1.58 km/sec from DSDP sites 234, 235, 236, 240 and 241, respectively (Fisher et al., 1974; Simpson et

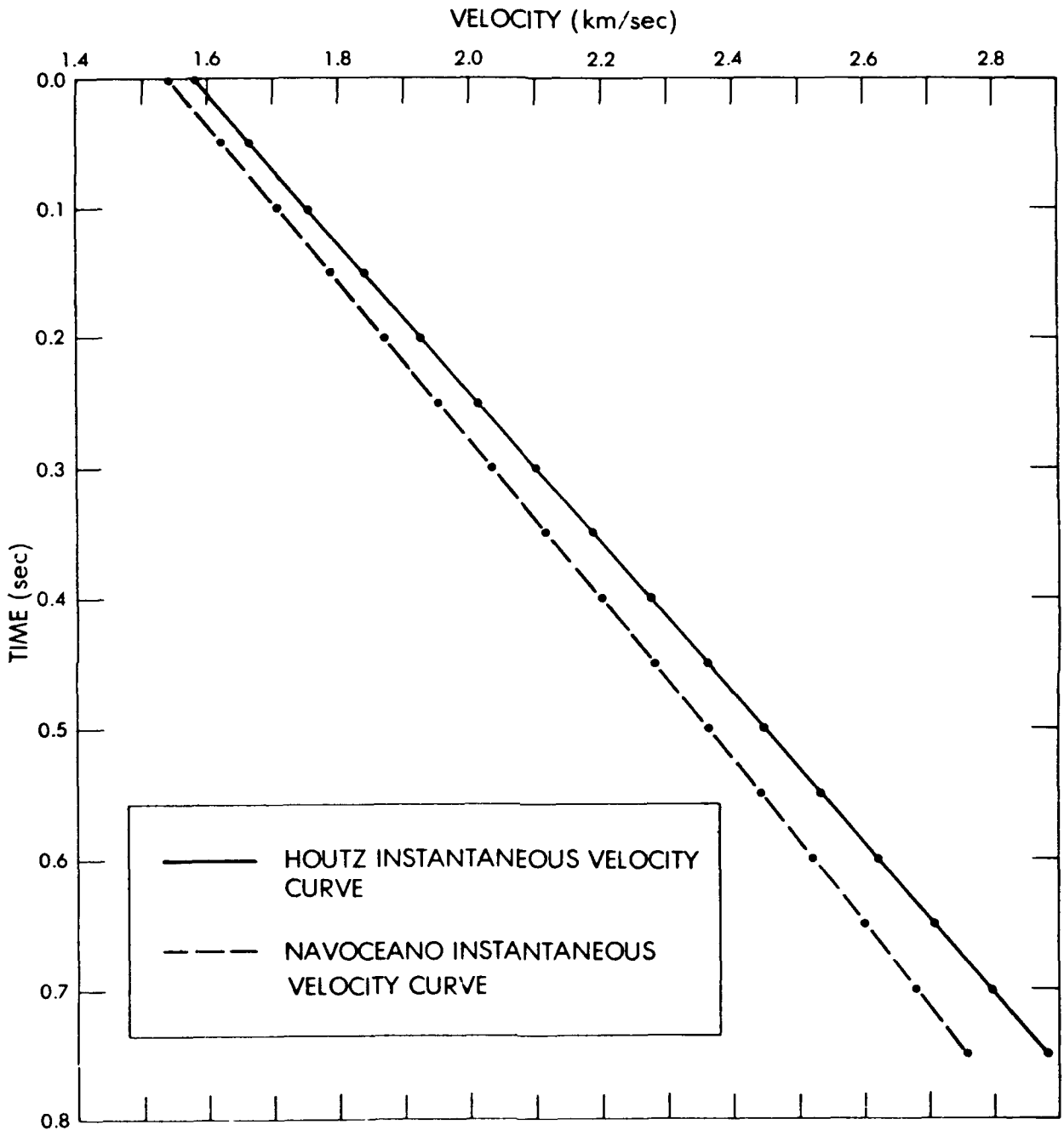

Figure 33. Instantaneous Velocity-Time Functions for the Somali Basin.

al., 1974). Our sediment surface velocity of 1.540 km/sec, obtained from our derived velocity function, falls within this range and is close to their mean value. The surface velocity of 1.58 km/sec reported by Houtz agrees well with the velocity from DSDP site 241, located on the edge of the African Continental Rise, and may be more typical of a rise velocity (Simpson et al., 1974).

In the Arabian Sea, correlation to other data is minimal due to the paucity of available seismic data. Considerable work was done by White and Ross (1979) in the Gulf of Oman; unfortunately, all but two of the lines were on the slope and shelf of Iran. The two lines extending into the Oman Abyssal Plain were taken with a single-channel seismic system, while most of the other lines were taken with a multichannel system. The two abyssal plain lines run essentially north-south, and indicate a thick sediment sequence at the northern end, gradually thinning toward the southern end. Our lines were east-west, but each successive line progressed to the south and they indicate a thinning sequence as well. In the Owens Abyssal Plain, only the DSDP site 223 could be reasonably considered for correlation. Other DSDP sites were located on the Owen Ridge and ODP sites were also located on the Ridge or on the Arabian Continental Slope or Rise. Site 223 was located just west of the Ridge on its slope, but velocities should be comparable. The velocities obtained by DSDP varied little from 1.55 km/sec in the upper 240 meters and from 1.60 to 1.75 km/sec in the next 220 meters (Whitmarsh et al., 1974). Below this, velocities increase to 1.8 to 2.0 km/sec and our results are in agreement with these.

In 1977, prior to the start of this study, a series of eight WABR stations was taken by NAVOCEANO on the Indus Cone. Six of these stations ran in a north-south direction on the Cone and were analyzed and reported by Bachman and Hamilton (1980). Their reported velocity-depth function is $V = 1.510+1.200D -0.253D^2+0.034D^3$. In this study, we characterized the Indus Cone by two velocity-depth functions, one for the upper portion of the Cone (within 160 miles of shore) and one for the remainder of the Cone. The function derived for the main portion of the Cone is $V = 1.488 + 1.754D - 0.622D^2$ and is representative of the area from which Bachman's function was derived. A plot of each is shown for comparison in figure 34. The two functions differ considerably in gradient, with theirs indicating a higher gradient at depth. Our function is derived from the data of all but three of the stations taken on the Cone and therefore is an averaging of the functions throughout the Cone.

The instantaneous velocity function obtained by Naini and Talwani (1977) $V = 1.534+1.965t$ is compared to the instantaneous velocity function obtained for the middle Cone area in this study ($V = 1.549+2.221t$), and the instantaneous velocity function derived by Bachman and Hamilton ($V = 1.510+1.863t$,

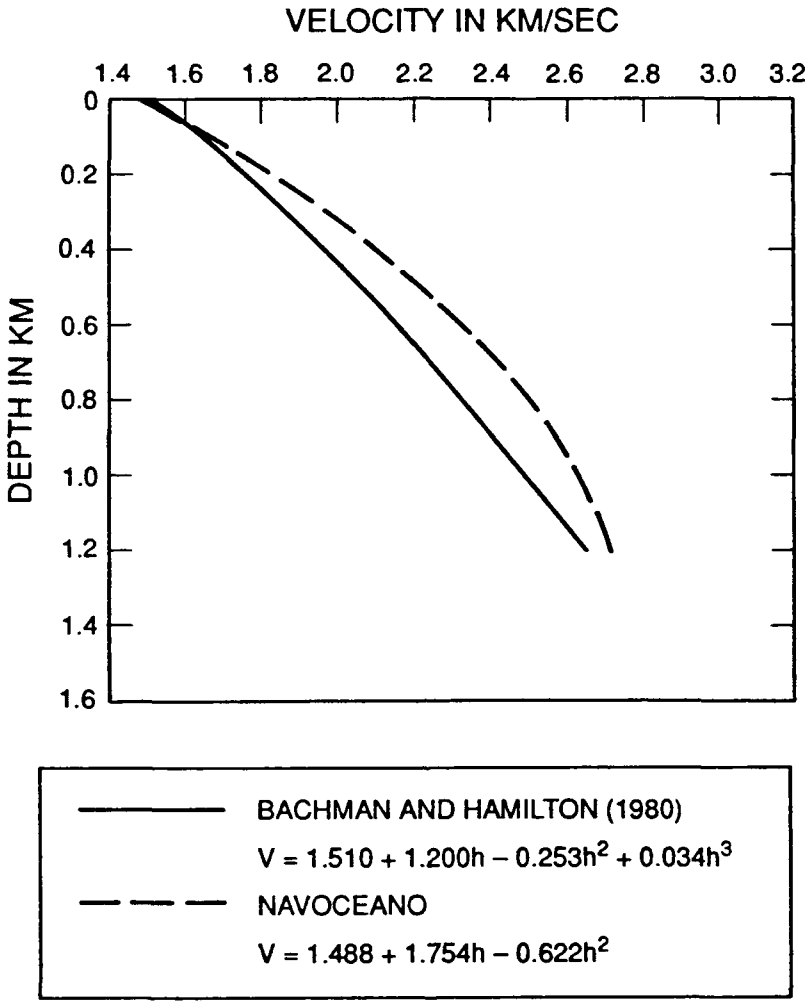

Figure 34. Velocity-Depth Functions for the Indus Cone.

1980) is included in this plot for comparison (figure 35). Again, it is noted that our function is a synthesis of data from numerous stations and thus reflects the effects of considerable variation in sediment sections throughout the Cone, while the other two functions reflect only a limited portion.

DSDP site 221 lies at the southeastern edge of the Cone and the uppermost velocity obtained from their coring was 1.41 km/sec, somewhat lower than the values we obtained in that area (Whitmarsh et al., 1974). The remainder of their cores had velocities from 1.45 to 1.74 km/sec and our values are in general agreement with these.

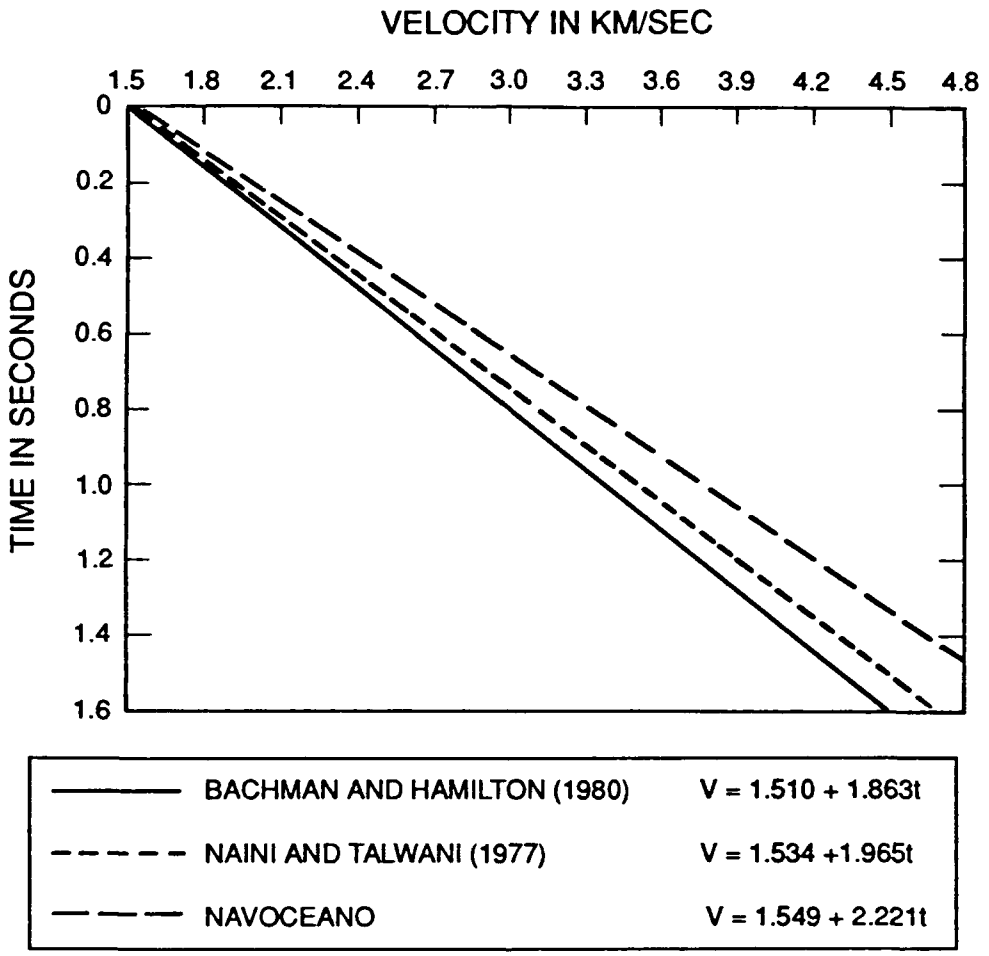

Figure 35. Instantaneous Velocity-Time Functions for the Indus Cone.

VI. SENSITIVITY ANALYSIS

There is an inherent factor in WABR affecting the sensitivity of all measurements. That factor is the drift of the sonobuoy after it has been deployed. There are some extremely strong currents in the Somali Basin about 5 to 50 miles offshore. These currents can be most disrupting, as was pointed out by Coffin et al. (1986) where a considerable amount of their work was in that area. On the inshore portions of some of our cruise legs in this area we experienced currents on the order of 12 to 15 knots. Fortunately, none of our WABR measurements were taken in this area but were taken some 300 miles or more out to sea where the drift of the sonobuoys was almost negligible over the period of the measurement. The same was true of the measurements made in the Arabian Sea.

As noted earlier, the WABR method is based on the Dix method developed for land reflection seismic exploration. In land exploration, the distance between source and receiver is small compared to the distances encountered in marine work, and ray parameters, or apparent velocity, are zero. Generally, in land work, the distance between the source and the furthest receiver is only a few thousand feet, whereas at sea this distance approaches 10 nautical miles. In the Dix method, the refraction or bending of rays between source and reflector is not considered, and simple straight line geometry is assumed for the reflections when plotted X^2-T^2. In land work the refraction effect is minimal, except where very strong velocity gradients are detected. In marine WABR work, this refraction effect shows up as a slight amount of curvature in the distal end of the X^2-T^2 plot giving rise to some problems in curve fitting. In this study, the limitations of the source level allowed a penetration of the sediments only on the order of 1200 to 1500 meters and the generally small gradual increase in velocity with depth caused little refraction at interfaces, and the assumption of straight line geometry is reasonable. This assumption is reflected in the lack of or the minimal amount of curvature in the distal ends of the X^2-T^2 plots.

Other investigators have developed a rule of thumb in that intervals between horizons chosen for study should not be less than 1/12 the depth of the water column. In general, this rule of thumb was followed in this study except in cases of unusually good reflecting horizons giving rise to intervals slightly less than 1/12 the water depth in thickness. Jim Matthews of the Naval Research Laboratory (NRL) studied the sensitivity of the factors involved in the wide-angle reflection method and concluded that the method was not particularly sensitive to the interval thickness as long as noise is not a major factor (pers. com. 1990).

A major point of sensitivity in the overall method arises in conversion of the interval velocity versus one-way travel time from the sediment surface to an instantaneous velocity-time

function. In water depths of 4000 to 5000 meters, using the rule of thumb, the first interval thickness is from 300 to 400 meters. When plotting the interval velocity at the midpoint of the interval, this point is from 150 to 200 meters from the sediment surface. After all of the interval velocities have been plotted at the midpoints of the intervals, a curve is fit to the data points. The point of sensitivity arises from the fact that without a data point at the sediment surface, there is no curve origin point to control the least squares fit, thus placing no limits on the initial velocity gradient. It is important, as pointed out by Hamilton (1974), to obtain a sediment surface velocity and force the curve through this point.

The methods used in this study to acquire and process the data have been used by investigators such as Houtz et al. (1968) and Bachman and Hamilton (1980) for some time and are sensitive primarily to attention to detail in the method of acquisition and to the detail and accuracy in reading travel times. Routine calibration of the acquisition components is necessary for the validity of the travel time data. The sensitivity of the analysis is predominantly in the comparison of instantaneous velocity functions and the detection of whether anomalous instantaneous velocity functions are true anomalies or reflecting problems in the acquisition and processing of that particular station. A check of the raw data and reflection profile will generally determine if there was a problem in the acquisition or processing of the data. If this is not the case, then other measurements must be taken in the same location to verify that the measurement was truly anomalous. A simultaneous vertical reflection profile during the WABR run is most helpful in assuring that the critical assumption of flat bottom and parallel layers is met.

VII. CONCLUSIONS

The primary conclusion of this study is that a velocity-depth function representative of the sediment velocity-depth relationship throughout a large ocean area can be derived from an adequate velocity-depth sampling in that area. The derived function will not describe the precise velocity-depth relationship in the sediments of any specific site, but is a reasonable representative of that relationship. In this study, the derived function describes the velocity-depth relationship in the upper 1200 to 1500 meters of the sediment section with a possible calculated error of 210 m/sec.

For the areas considered in this study, these functions are:

A. SOMALI BASIN

$V = 1.539 + 1.010d - 0.166d^2$

B. ARABIAN SEA

1. Oman Abyssal Plain

$V = 1.513 + 1.696d - 0.649d^2$

2. Owens Abyssal Plain

$V = 1.483 + 1.465d - 0.401d^2$

3. Upper Indus Cone

$V = 1.460 + 1.581d - 0.907d^2$

4. Lower Indus Cone

$V = 1.488 + 1.754d - 0.622d^2$

The area in which each of the above Arabian Sea functions applies is indicated in figure 36. These functions describe the velocity profiles of the upper 1200 to 1500 meters of the sediment section in the individual areas. In the Somali Basin, Oman Abyssal Plain and Owens Abyssal Plain, the velocity-depth functions describe a condition of terrigenous sedimentation and an upper sediment section consisting largely of turbidite flows. The Indus Cone velocity-depth functions describe a condition of voluminous terrigenous deposition primarily from one source with a mechanical segregation of material progressing away from the source and turbidite flows overall.

In other areas of the world's oceans of similar depositional environment where little or no data are available, the results obtained in this study may be used to derive generalized functions. Sediment surface velocity from core data can be used as the initial data point for a linear instantaneous velocity function of the Houtz type. The gradient for this function could be obtained from one of the functions derived for an area of similar depositional environment described in this study. The function so obtained could then be developed into a velocity-depth function in the manner described earlier.

A second conclusion reached in this study is that the sediment surface velocity of deep water sediments is linearly related to water depth. This appears to be due to the included bottom water of the surface sediments. This conclusion was

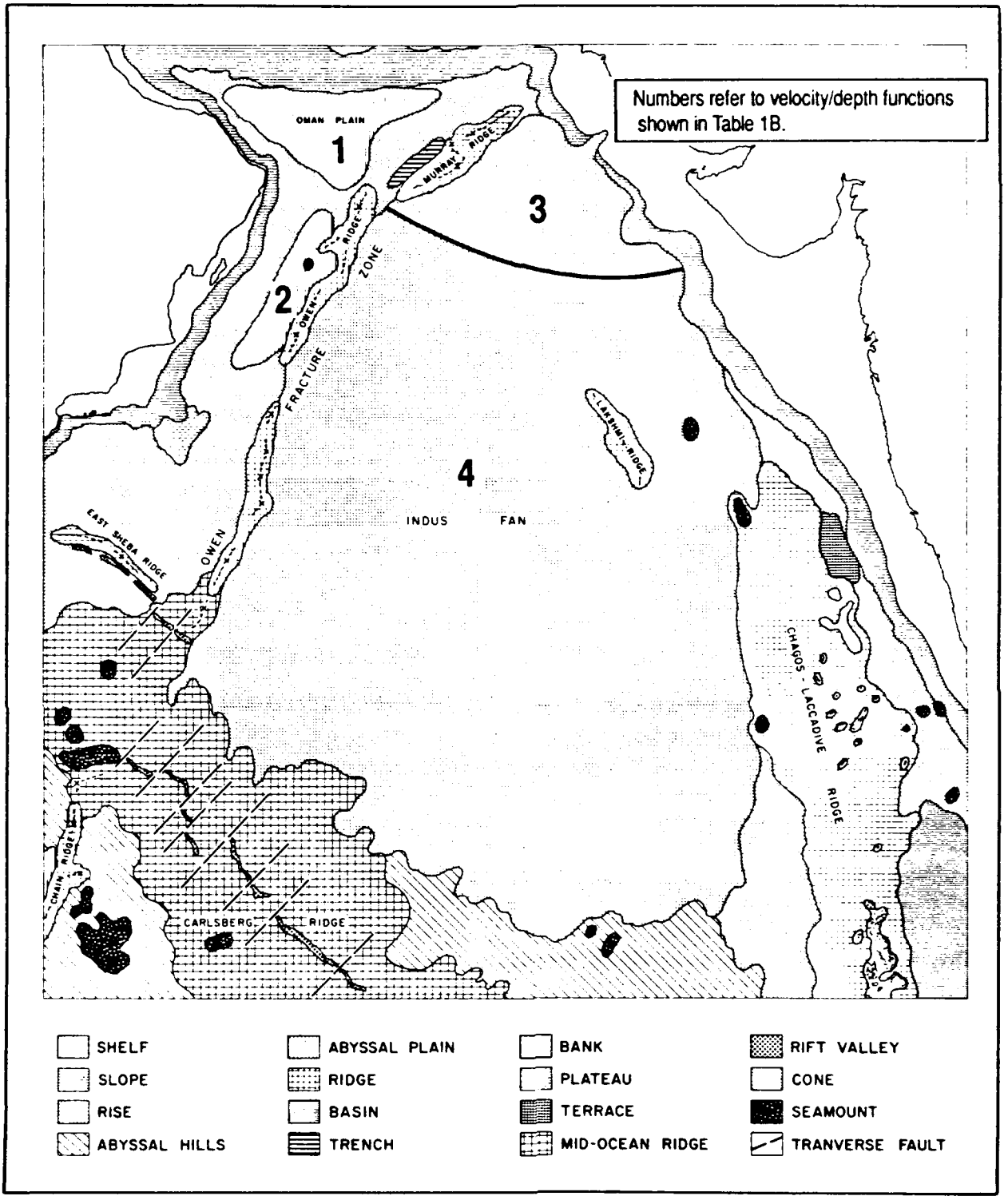

Figure 36. Illustration of Areas of Application for Various Velocity-Depth Functions in Arabian Sea.

reached in the course of an effort to chart the sediment surface sound velocity to bottom water sound velocity ratio for the areas under investigation. As a consequence of this effort, the author also reached the conclusion that this velocity ratio, in deep water, is generally less than 1.0. All of the velocity ratios determined in this study and in all subsequent work by the author have supported this conclusion. This conclusion is in line with the observation of Fry and Raitt (1961) that sediment surface velocities are generally 2% lower than the bottom-water velocities in the Pacific Ocean.

VIII. RECOMMENDATIONS FOR FUTURE WORK

Considering the primary conclusion reached in this study, it would only be consistent to recommend that other suitable large ocean areas be characterized in the same manner as the two areas in this study. In fact, work is underway to do just that in large areas of the South Atlantic Ocean.

One deficiency in the WABR method was cited earlier. The first data point, other than a surface sediment measurement from a core, occurs at depths of 150 to 200 meters or more because our source and receiver are far away from the boundary of interest. Those interested in modeling higher frequencies are interested in greater detail in the upper few hundred meters, which cannot be obtained using this method. If such detail is needed, it is recommended that a similar sampling arrangement to the one in this study be carried out with a system such as the "Deep Towed Array Geophysical System" (DTAGS). This system, developed by NRL, consists of a deep towed source and multichannel array. It collects multichannel data in the upper few hundred meters and has definition on the order of meters. These data could define the velocity structure of the upper few hundred meters in detail and could be used to adjust or modify the upper portion of the velocity-depth curve obtained by WABR methods.

The processing method used in this study for obtaining interval velocities and thicknesses is very labor intensive. At this time, WABR records are read by hand and the travel times recorded on tabulation sheets before being entered into the interval velocity computer program. The work is tedious and requires approximately 3 to 4 hours per record from initial setup to tabulation sheet by an experienced person. During this process, there are numerous opportunities for the introduction of errors such as those in the reading of travel times or those produced by the transposition of digits during the recording of the travel times.

I recommend that this process be modernized by acquiring the data digitally and processing it digitally for velocities and thicknesses, as is commonly done in the oil industry. Presently, work is underway at NAVOCEANO to accomplish this. A digital acquisition system was purchased and has been taken to sea to acquire data. The data are recorded on nine-track tape with three tapes being required for each WABR run. During a cruise in which 15 to 20 WABR runs are made, a considerable amount of tape is expended and results in additional storage and shipping problems. To alleviate this problem, a disc storage system for the recording of the data will be installed in the near future. It is planned to use a technique employing a velocity analysis module to compute the trace to trace coherence of events as a function of normal incidence travel time and obtain stacking velocities to derive interval velocities and thicknesses.

IX. REFERENCES

Bachman, R.T., and E.L. Hamilton; Sediment sound velocities from sonobuoys; Arabian Fan, J. Geophys. Res., 85, 849-852, 1980.

Bunce, E.T., M.G. Langseth, et al.; Structure of the Western Somali Basin, J. Geophys. Res., 72, 2547-2555, 1967.

Burroughs III, R.H.; Structural and sedimentological evolution of the Somali Basin; Paleooceanographic interpretations, WHOI-77-34, 1977, Woods Hole Oceanographic Institution, Woods Hole, MA.

Clay, C.S., and P.A. Rona; Studies of seismic reflections from thin layers on the ocean bottom in the Western North Atlantic, J. Geophys. Res., 70, 855-869, 1965.

Cochran, J.R.; The Somali Basin, Chain Ridge and the origin of the northern Somali Basin gravity and geoid low, J. Geophys. Res., 93, N. B10, 11985-12008, 1988.

Coffin, M.F., P.D. Rabinowitz, and R.E. Houtz; Crustal structure in the Western Somali Basin, Geophys. J. R. Astr. Soc., 86, 331-369, 1986.

Davies, D., and T.J.G. Francis; The crustal structure of the Seychelles Bank, Deep Sea Research, Vol. II, 921-927, 1964.

Dix, H.C.; Seismic velocities from surface measurements, Geophysics, 20, 68-86, 1955.

DuToit, A.L.; Our wandering continents, Edinburgh, Scotland, Oliver and Boyd, 1937.

Ewing, M., S. Eittreim, et al.; Sediment distribution in the Indian Ocean, Deep Sea Research, Vol. 16, 231-248, 1969.

Fisher, R.L., E.T. Bunce, et al.; Initial Reports of the Deep Sea Drilling Projects, Vol. 24, 249-389, U.S. Government Printing Office, Washington, DC, 1974.

Francis, T.J.G., D. Davies, and M.N. Hill; Crustal structure between Kenya and the Seychelles, Phil. Trans. Roy. Soc., London, A, 259, 240-261, 1966.

Fry, J.C., and R.W. Raitt; Sound Velocities at the Surface of Deep Sea Sediments, J. Geophys. Res., 66, 589-597, 1961.

Hamilton, E.L.; Telephone conversation with author, August 1983.

Hamilton, E.L.; Geoacoustic modeling of the seafloor, J. Acoust. Soc. Am., 68(5), 1313-1340, 1980.

Hamilton, E.L., D.G. Moore, et al.; Sediment velocities from sonobuoys: Bay of Bengal, Bering Sea, Japan Sea, and North Pacific, J. Geophys. Res., 79, 2653-2667, 1974.

Houtz, R.; Letter to Allan Lowrie at NAVOCEANO, September 1981.

Houtz, R., J. Ewing, and X. LePichon; Velocity of deep sea sediments from sonobuoy data, J. Geophys. Res., 73, 2615-2641, 1968.

Houtz, R., J. Ewing, and P. Buhl; Seismic data from sonobuoy stations in Northern and Equatorial Pacific, J. Geophys. Res., 75, 5093-5111, 1970.

Kolla, V., P.K. Ray, and J.A. Kostecki; Surficial Sediments of the Arabian Sea, Marine Geology, 41, 183-204, 1981.

Kolla, V. and F. Coumes; Morphology, internal structure, seismic stratigraphy and sedimentation of Indus Fan, Am. Assoc. Petr. Geol., 71, 650-677, 1987.

LePichon, X., J. Ewing, and R. Houtz; Deep-sea sediment velocity determination made while reflection profiling, J. Geophys. Res., 73, 2597-2614, 1968.

Matthews, James E.; Conversation with author, April 1990.

Menard, H.W., and T.E. Chase; Fracture zones, in THE SEA, Vol. IV, Part 1, ed. A. E. Maxwell, 421-444, New York, NY, Wiley Interscience, 1970.

Naini, B.R. and V. Kolla; Acoustic character and thickness of sediments of the Indus Fan and the continental margin of Western India, Mar. Geol., 47, 181-195, 1981.

Naini, B.R. and M. Talwani; Sediment distribution and structures in the Indus Cone and western continental margin of India (Arabian Sea), E.O.S., Trans. Am. Geophys. Union, 58, p. 405 (abstract), 1977.

Simpson, E.S.W., Schlick, R., et al.; Initial Reports of the Deep Sea Drilling Project, Vol. 25, 65-138, U.S. Government Printing Office, Washington, DC, 1974.

Urick, R.J.; Principles of Underwater Sound, 3rd edition, New York, NY, McGraw-Hill, Inc., 1983.

White, R.S., and K. Klitgord; Sediment deformation and plate tectonics in the Gulf of Oman, Earth and Planetary Science Letters, Vol. 32, 199-209, 1976.

White, R.S., and D.A. Ross; Tectonics of the western Gulf of Oman, J. Geophys. Res., 64, 3479-3489, 1979.

Whitmarsh, R.B., C.E. Weser, D.A. Ross, et al.; Initial Reports of the Deep Sea Drilling Project, Vol. 23, U.S. Government Printing Office, Washington, DC, 1974.

Windsor, Sara; Conversations with author, Summer 1982.

APPENDIX A

TABLES OF VELOCITIES AND VELOCITY FUNCTIONS

Table 1. Velocity-Depth Functions for the Somali Basin and the Arabian Sea.

A. SOMALI BASIN

1. All Somali Basin Stations:

$V=1.539 + 1.010d - 0.166d^2$

var.=0.000016 $S_{x,y}=0.0052$

2. All Abyssal Plain Stations:

$V=1.545 + 0.991d - 0.199d^2$

var.=0.000012 $S_{x,y}=0.0037$

3. All Continental Rise Stations:

$V=1.517 + 1.200d - 0.451d^2$

var.=0.00016 $S_{x,y}=0.0124$

4. Northern Abyssal Plain Stations:

$V=1.501 + 1.078d - 0.220d^2$

var.=0.000052 $S_{x,y}=0.0073$

5. Southern Abyssal Plain Stations:

$V=1.541 + 1.025d - 0.088d^2$

var.=0.0000042 $S_{x,y}=0.0021$

B. ARABIAN SEA

1. Oman Abyssal Plain:

$V=1.513 + 1.696d - 0.649d^2$

var.=0.00004 $S_{x,y}=0.0064$

2. Owens Abyssal Plain:

$V=1.483 + 1.465d - 0.401d^2$

var.=0.00001 $S_{x,y}=0.0033$

3. Upper Cone:

$V=1.460 + 1.581d - 0.907d^2$

var.=0.00004 $S_{x,y}=0.0063$

4. Main Portion of Cone:

$V=1.488 + 1.754d - 0.622d^2$

var.=0.000039 $S_{x,y}=0.0062$

var.= Variance
$S_{x,y}$= Standard Estimate of Error

Table 2. Instantaneous Velocity Functions for the Somali Basin and the Arabian Sea

A. SOMALI BASIN:

1.	Linear for Somali Basin	$V=1.540 + 1.649t$
2.	All Basin Stations $S_{x,y}=0.1339$	$V=1.538 + 1.683t - 0.076t^2$ var.=0.01792
3.	All Abyssal Plain $S_{x,y}=0.1181$	$V=1.545 + 1.612t + 0.199t^2$ var.=0.0202
4.	All Continental Rise $S_{x,y}=0.1072$	$V=1.514 + 2.180t - 1.450t^2$ var.=0.0125
5.	North Abyssal Plain $S_{x,y}=0.0925$	$V=1.500 + 1.799t - 0.291t^2$ var.=0.0186
7.	South Abyssal Plain $S_{x,y}=0.1387$	$V=1.540 + 1.622t + 0.469t^2$ var.=0.01799

B. ARABIAN SEA:

1.	Oman Abyssal Plain $S_{x,y}=0.1761$	$V=1.505 + 2.857t - 1.128t^2$ var.=0.01975
2.	Owens Abyssal Plain $S_{x,y}=0.1172$	$V=1.483 + 2.303t - 0.144t^2$ var.=0.01376
3.	Upper Cone $S_{x,y}=0.0702$	$V=1.458 + 2.962t - 0.986t^2$ var.=0.00462
4.	Main Portion of Cone $S_{x,y}=0.1262$	$V=1.487 + 2.874t - 0.816t^2$ var.=0.01592

$S_{x,y}$= Standard Estimate of Error
var.= Variance

Table 3. Tabulation of Interval Velocities and Layer Thicknesses in the Somali Basin

STATION	LAYER	VELOCITY (m/sec)	LAYER THICKNESS (m)	WATER DEPTH (m)	LOCATION LAT.	LONG.
53		1492	000	4543	01°35'S	54°42'E
	A	1562	105			
	B	2269	210			
	A&B	2001	320			
54		1501	000	4778	00°30'S	53°59'E
	A	1851	282			
55		1506	000	4938	00°21'N	53°31'E
	A	1792	249			
56		1510	000	5072	01°51'N	52°26'E
	A	1750	206			
	B	1988	566			
	A&B	1921	773			
57		1511	000	5079	02°17'N	51°59'E
	A	1582	219			
	B	2212	291			
	A&B	1915	517			
58		1499	000	4858	03°44'N	50°40'E
	A	1894	858			
	B	2152	219			
	A&B	1944	1079			
59		1495	000	4953	05°08'N	51°08'E
	A	1616	189			
	B	2043	244			
	C	2075	299			
	A&B	1844	436			
	B&C	2061	543			
60		1502	000	5015	04°44'N	51°27'E
	A	1542	189			
	B	1969	556			
	A&B	1850	749			
61		1512	000	5089	04°17'N	51°53'E
	A	1527	344			
	B	1867	261			
	A&B	1666	608			

Table 3. Tabulation of Interval Velocities and Layer Thicknesses in the Somali Basin (con.)

STATION	LAYER	VELOCITY (m/sec)	LAYER THICKNESS (m)	WATER DEPTH (m)	LOCATION LAT.	LOCATION LONG.
62		1510	000	5124	03°24'N	52°50'E
	A	1736	397			
63		1506	000	5085	05°16'N	53°11'E
	A	1683	181			
	B	1762	191			
	C	2035	379			
	A&B	1723	372			
	B&C	1939	572			
64		1508	000	5073	05°50'N	52°30'E
	A	1701	378			
	B	2391	518			
	A&B	2071	908			
65		1496	000	5079	06°24'N	51°53'E
	A	1584	158			
	B	1685	206			
	C	2117	429			
	A&B	1640	365			
	B&C	1965	639			
66		1481	000	4910	06°58'N	51°16'E
	A	1786	263			
	B	1973	481			
	A&B	1905	745			
67		1499	000	5104	07°39'N	52°39'E
	A	1739	363			
	B	1777	195			
	A&B	1752	558			
68		1511	000	5097	07°06'N	53°12'E
	A	1525	217			
	B	1745	170			
	C	2075	239			
	A&B	1618	388			
	B&C	1930	410			
69		1506	000	5095	06°35'N	53°41'E
	A	1683	269			
	B	2050	557			
	A&B	1922	830			

Table 3. Tabulation of Interval Velocities and Layer Thicknesses in the Somali Basin (con.)

STATION	LAYER	VELOCITY (m/sec)	LAYER THICKNESS (m)	WATER DEPTH (m)	LOCATION LAT.	LOCATION LONG.
70		1500	000	5079	06°41'N	54°10'E
	A	1672	186			
	B	1684	212			
	C	1901	135			
	D	2265	262			
	A&B	1678	399			
	B&C	1738	342			
	C&D	2134	398			
71		1505	000	5086	07°23'N	54°22'E
	A	1595	181			
	B	1776	212			
	C	1979	294			
	D	1993	207			
	A&B	1691	394			
	B&C	1891	507			
	C&D	1985	501			
72		1512	000	5090	08°05'N	54°09'E
	A	1708	348			
	B	1745	211			
	A&B	1722	560			
73		1511	000	5044	08°06'N	53°45'E
	A	1624	334			
	B	2094	431			
	A&B	1874	771			
74		1511	000	5092	07°31'N	53°28'E
	A	1567	243			
	B	1934	324			
	C	2037	249			
	A&B	1767	570			
	B&C	1978	574			
75		1512	000	5091	06°52'N	53°06'E
	A	1799	256			
	B	2021	582			
	A&B	1950	839			
76		1510	000	5092	06°31'N	52°50'E
	A	1704	394			
	B	2137	361			
	A&B	1898	760			

Table 3. Tabulation of Interval Velocities and Layer Thicknesses in the Somali Basin (con.)

STATION	LAYER	VELOCITY (m/sec)	LAYER THICKNESS (m)	WATER DEPTH (m)	LOCATION LAT.	LOCATION LONG.
77		1509	000	5091	06°09'N	52°37'E
	A	1550	160			
	B	1717	206			
	C	2085	424			
	A&B	1642	366			
	B&C	1956	633			
78		1508	000	5095	05°56'N	52°31'E
	A	1627	366			
	B	2200	445			
	A&B	1915	819			
79		1500	000	5088	05°22'N	52°04'E
	A	1659	347			
	B	2127	399			
	A&B	1892	750			
80		1505	000	5091	04°57'N	51°55'E
	A	1759	364			
	B	1846	329			
	A&B	1800	693			
81		1508	000	5077	04°36'N	51°49'E
	A	1565	193			
	B	1753	149			
	C	1971	340			
	A&B	1644	343			
	B&C	1902	490			
82		1512	000	5094	04°12'N	51°43'E
	A	1795	354			
	B	1849	328			
	A&B	1821	683			
83		1515	000	5107	03°44'N	51°30'E
	A	1643	220			
	B	1932	133			
	C	2347	296			
	A&B	1747	355			
	B&C	2209	431			

Table 3. Tabulation of Interval Velocities and Layer Thicknesses in the Somali Basin (con.)

STATION	LAYER	VELOCITY (m/sec)	LAYER THICKNESS (m)	WATER DEPTH (m)	LOCATION LAT.	LOCATION LONG.
84		1501	000	4733	01°50'N	49°48'E
	A	1549	215			
	B	1964	354			
	A&B	1795	574			
85		1499	000	4722	01°22'N	49°06'E
	A	1525	194			
	B	1846	371			
	C	2041	362			
	A&B	1729	568			
	B&C	1940	734			
86		1496	000	4681	01°00'N	48°31'E
	A	1657	530			
87		1494	000	4371	04°20'S	44°11'E
	A	1656	217			
	B	1954	203			
	C	2034	453			
	A&B	1794	421			
	B&C	2009	656			
88		1502	000	4678	04°21'S	45°29'E
	A	1616	170			
	B	1986	184			
	C	2337	269			
	A&B	1799	355			
	B&C	2145	445			
89		1504	000	4769	04°20'S	46°37'E
	A	1745	280			
	B	2021	543			
	A&B	1922	825			
90		1494	000	4368	02°56'S	45°15'E
	A	1694	250			
	B	2067	501			
	C	2405	613			
	A&B	1934	754			
	B&C	2247	1118			

Table 3. Tabulation of Interval Velocities and Layer Thicknesses in the Somali Basin (con.)

STATION	LAYER	VELOCITY (m/sec)	LAYER THICKNESS (m)	WATER DEPTH (m)	LOCATION LAT.	LOCATION LONG.
91		1483	000	3560	01°44'S	44°05'E
	A	1806	473			
	B	2038	473			
	A&B	1919	948			
92		1483	000	3792	01°03'S	44°56'E
	A	1645	255			
	B	1955	388			
	C	2358	593			
	A&B	1826	645			
	B&C	2190	985			
93		1503	000	4788	02°33'S	46°41'E
	A	1647	360			
	B	1799	387			
	C	2190	330			
	A&B	1724	747			
	B&C	1970	720			
94		1504	000	4753	02°36'S	46°45'E
	A	2119	972			
	B	2534	424			
	C	3131	434			
	A&B	2238	1401			
	B&C	2820	863			
95		1507	000	5006	04°30'S	49°10'E
	A	1757	546			
96		1505	000	5060	04°06'S	51°00'E
	A	1678	277			
97		1506	000	5027	03°00'S	49°32'E
	A	1812	658			
98		1506	000	4908	01°58'S	48°23'E
	A	1627	238			
	B	1842	573			
	A&B	1776	812			
99		1497	000	4601	00°43'S	47°01'E
	A	1748	202			
	B	1830	666			
	A&B	1810	868			

Table 3. Tabulation of Interval Velocities and Layer Thicknesses in the Somali Basin (con.)

STATION	LAYER	VELOCITY (m/sec)	LAYER THICKNESS (m)	WATER DEPTH (m)	LOCATION LAT.	LOCATION LONG.
100		1490	000	4051	00°00'N	46°00'E
	A	1791	421			
	B	2199	423			
	C	2406	373			
	A&B	1986	849			
	B&C	2294	797			
101		1490	000	4047	00°52'N	47°03'E
	A	1708	216			
	B	2079	1135			
	A&B	2014	1355			
102		1499	000	4778	00°12'S	48°22'E
	A	1882	256			
	B	2003	824			
	A&B	1974	1081			
103		1501	000	4846	00°59'N	49°22'E
	A	1946	569			
	B	2195	598			
	A&B	2070	1169			
104		1495	000	4608	01°35'N	48°32'E
	A	1636	554			
	B	2031	539			
	A&B	1820	1099			
105		1500	000	4692	02°25'N	49°44'E
	A	1782	276			
	B	1814	667			
	A&B	1805	943			
106		1502	000	5110	01°44'N	50°39'E
	A	1668	329			
	B	2201	330			
	C	2445	202			
	A&B	1916	666			
	B&C	2290	533			
107		1506	000	5134	01°17'N	51°07'E
	A	1890	212			
	B	2180	326			
	A&B	2060	539			
108		1491	000	4560	01°45'N	54°44'E
	A	2580	374			

Table 3. Tabulation of Interval Velocities and Layer Thicknesses in the Somali Basin (con.)

STATION	LAYER	VELOCITY (m/sec)	LAYER THICKNESS (m)	WATER DEPTH (m)	LOCATION LAT.	LOCATION LONG.
109		1510	000	5216	04°05'N	53°12'E
	A	1987	228			
	B	2074	373			
	A&B	2041	602			
110		1509	000	5080	04°34'N	52°35'E
	A	1566	258			
	B	2000	560			
	C	2574	643			
	A&B	1851	824			
	B&C	2289	1213			
111		1498	000	5049	05°28'N	51°38'E
	A	1681	513			
	B	2070	321			
	C	2233	352			
	A&B	1822	838			
	B&C	2154	673			
112		1505	000	5134	05°36'N	53°41'E
	A	1670	380			
	B	2100	399			
	A&B	1878	784			
113		1490	000	4733	00°34'N	58°23'E
	A	1612	145			
114		1489	000	4728	00°31'N	58°04'E
	A	1674	259			
	B	1905	186			
	A&B	1767	446			
115		1510	000	5093	04°12'N	53°44'E
	A	1614	242			
	B	1926	549			
	A&B	1824	794			
116		1510	000	5023	03°09'N	52°41'E
	A	2073	297			
117		1514	000	5132	02°31'N	52°25'E
	A	1614	161			
	B	1791	179			
	C	1830	137			
	A&B	1705	341			
	B&C	1808	316			

Table 3. Tabulation of Interval Velocities and Layer Thicknesses in the Somali Basin (con.)

STATION	LAYER	VELOCITY (m/sec)	LAYER THICKNESS (m)	WATER DEPTH (m)	LOCATION LAT.	LOCATION LONG.
118	Deleted					
119		1507	000	5135	01°49'N	53°08'E
	A	1684	219			
	B	1913	249			
	A&B	1802	469			
120		1492	000	4498	00°41'S	55°32'E
	A	1591	153			
	B	2121	225			
	A&B	1888	381			
121		1506	000	5036	02°45'S	49°05'E
	A	1788	202			
	B	2027	494			
	A&B	1955	697			
122		1506	000	5067	01°40'S	49°28'E
	A	1694	451			
	B	2021	370			
	C	2419	337			
	A&B	1834	824			
	B&C	2202	710			
123		1505	000	5068	00°08'S	50°01'E
	A	1588	195			

Table 4. Tabulation of Interval Velocities and Layer Thicknesses in the Arabian Sea.
(Oman Abyssal Plain, Stations 124-145)

STATION	LAYER	VELOCITY (m/sec)	LAYER THICKNESS (m)	WATER DEPTH (m)	LOCATION LAT.	LOCATION LONG.
124		1473	000	3351	24°04'N	59°08'E
	A	1667	183			
	B	2235	251			
	C	2361	395			
	A&B	1975	439			
	B&C	2311	647			
125		1477	000	3293	24°08'N	59°40'E
	A	2079	706			
	B	2388	449			
	C	3117	840			
	A&B	2194	1157			
	B&C	2840	1299			
126		1470	000	3392	24°02'N	60°06'E
	A	1925	407			
	B	2335	378			
	C	2549	599			
	D	3446	836			
	A&B	2113	789			
	B&C	2464	978			
	C&D	3038	1451			
127		1470	000	3323	24°03'N	60°50'E
	A	1836	277			
	B	2085	234			
	C	2530	539			
	D	2944	468			
	A&B	1946	512			
	B&C	2386	776			
	C&D	2715	1010			
128		1470	000	3304	24°02'N	61°53'E
	A	1815	402			
	B	2400	288			
	C	2940	1742			
	A&B	2040	697			
	B&C	2856	2035			

Table 4. Tabulation of Interval Velocities and Layer Thicknesses in the Arabian Sea (con.)

STATION	LAYER	VELOCITY (m/sec)	LAYER THICKNESS (m)	WATER DEPTH (m)	LOCATION LAT.	LONG.
129		1470	000	3248	23°58'N	62°37'E
	A	1836	250			
	B	1969	162			
	C	2021	176			
	D	2334	431			
	A&B	1887	412			
	B&C	1996	338			
	C&D	2238	608			
130		1470	000	3169	23°56'N	63°21'E
	A	1941	538			
	B	2180	379			
	C	2412	292			
	D	2804	296			
	A&B	2037	919			
	B&C	2278	672			
	C&D	2602	589			
131		1470	000	3123	24°07'N	64°08'E
	A	1907	454			
	B	2201	325			
	C	2506	356			
	D	2575	520			
	A&B	2025	781			
	B&C	2355	682			
	C&D	2547	876			
132		1470	000	3066	24°19'N	64°34'E
	A	1972	422			
	B	2307	555			
	C	2438	447			
	A&B	2156	980			
	B&C	2364	1003			
133		1477	000	3275	23°29'N	62°36'E
	A	1813	300			
	B	2140	296			
	C	2387	461			
	D	2680	592			
	A&B	1969	598			
	B&C	2287	758			
	C&D	2548	1055			

Table 4. Tabulation of Interval Velocities and Layer Thicknesses in the Arabian Sea (con.)

STATION	LAYER	VELOCITY (m/sec)	LAYER THICKNESS (m)	WATER DEPTH (m)	LOCATION LAT.	LOCATION LONG.
134		1484	000	3345	23°30'N	61°50'E
	A	1896	479			
	B	2184	613			
	C	2934	1276			
	A&B	2053	1094			
	B&C	2665	1907			
135		1483	000	3325	23°33'N	61°15'E
	A	1931	565			
	B	2316	549			
	C	2524	487			
	D	3119	778			
	A&B	2112	1118			
	B&C	2411	1037			
	C&D	2875	1272			
136		1480	000	3280	23°42'N	60°22'E
	A	1914	550			
	B	2363	313			
	C	2618	353			
	A&B	2066	868			
	B&C	2495	667			
137		1478	000	3317	23°31'N	59°44'E
	A	1852	352			
	B	2205	452			
	A&B	2043	807			
138	Deleted					
139		1501	000	3353	23°02'N	61°48'E
	A	2014	634			
140	Deleted					
141		1492	000	3052	22°31'N	62°01'E
	A	1636	352			
	B	2390	368			
	C	3072	733			
	A&B	1986	733			
	B&C	2824	1109			
142		1489	000	3249	22°29'N	61°06'E
	A	1716	412			
	B	2468	605			
	A&B	2129	1033			

Table 4. Tabulation of Interval Velocities and Layer Thicknesses in the Arabian Sea (con.)

STATION	LAYER	VELOCITY (m/sec)	LAYER THICKNESS (m)	WATER DEPTH (m)	LOCATION LAT.	LONG.
143		1470	000	2732	22°12'N	60°30'E
	A	2284	1142			
	B	3106	598			
	A&B	2540	1759			
144		1484	000	3063	21°57'N	61°01'E
	A	1788	510			
	B	2488	504			
	C	2818	613			
	A&B	2107	1027			
	B&C	2664	1119			
145		1481	000	3158	21°56'N	61°38'E
	A	1771	399			
	B	2187	330			
	C	2632	450			
	D	3144	575			
	A&B	1949	733			
	B&C	2434	784			
	C&D	2908	1030			

Table 4. Tabulation of Interval Velocities and Layer Thicknesses in the Arabian Sea (con.)
(OWENS Abyssal Plain, Stations 167, 168, 169, 170, 180, 181)

STATION	LAYER	VELOCITY (m/sec)	LAYER THICKNESS (m)	WATER DEPTH (m)	LOCATION LAT.	LOCATION LONG.
167		1481	000	3258	21°29'N	61°17'E
	A	1690	181			
	B	1877	246			
	C	2288	332			
	D	2623	289			
	E	3363	2044			
	A&B	1795	427			
	B&C	2103	580			
	C&D	2438	622			
	D&E	3260	2341			
168		1481	000	3289	21°12'N	60°47'E
	A	1602	235			
	B	2137	401			
	C	2318	287			
	D	2737	475			
	E	3467	1774			
	A&B	1921	641			
	B&C	2211	689			
	C&D	2570	765			
	D&E	3298	2259			
169		1483	000	3398	20°41'N	60°29'E
	A	1562	255			
	B	1995	315			
	C	2513	285			
	D	2737	374			
	A&B	1788	575			
	B&C	2227	605			
	C&D	2637	659			
170		1480	000	3446	20°17'N	60°30'E
	A	1665	311			
	B	2108	318			
	C	2512	392			
	A&B	1876	634			
	B&C	2322	713			

Table 4. Tabulation of Interval Velocities and Layer Thicknesses in the Arabian Sea (con.)

STATION	LAYER	VELOCITY	LAYER THICKNESS	WATER DEPTH	LOCATION	
					LAT.	LONG.
		(m/sec)	(m)	(m)		
180		1486	000	3382	18°51'N	59°25'E
	A	1546	292			
	B	2095	392			
	C	2392	383			
	D	2891	580			
	A&B	1840	692			
	B&C	2266	786			
	C&D	2681	967			
181		1486	000	3326	19°26'N	59°58'E
	A	1786	412			
	B	2079	305			
	C	2271	311			
	D	2526	802			
	A&B	1905	718			
	B&C	2174	616			
	C&D	2452	1114			

Table 4. Tabulation of Interval Velocities and Layer Thicknesses in the Arabian Sea (con.)
(Indus Cone, Stations 146-166, 171-176, 182-186, 300-312 and 344-346)

STATION	LAYER	VELOCITY (m/sec)	LAYER THICKNESS (m)	WATER DEPTH (m)	LOCATION LAT.	LOCATION LONG.
146		1459	000	2102	22°30'N	65°58'E
	A	1753	245			
147		1452	000	1507	21°19'N	67°43'E
	A	1596	335			
	B	2143	1088			
	A&B	1998	1434			
148		1456	000	2721	20°43'N	68°18'E
	A	1715	315			
	B	2260	1063			
	A&B	2121	1387			
149		1460	000	3180	18°59'N	69°07'E
	A	2033	620			
150		1480	000	3142	19°36'N	68°17'E
	A	1784	383			
	B	2354	350			
	C	2583	637			
	A&B	2036	740			
	B&C	2499	987			
151		1480	000	2982	20°19'N	67°20'E
	A	1637	190			
	B	1975	474			
	A&B	1871	666			
152		1471	000	2771	21°19'N	65°52'E
	A	1882	463			
	B	2609	978			
	A&B	2348	1458			
153		1471	000	2796	21°52'N	65°11'E
	A	1993	804			
	B	3087	1230			
	C	3327	567			
	D	3472	608			
	A&B	2595	2081			
	B&C	3161	1799			
	C&D	3401	1175			

Table 4. Tabulation of Interval Velocities and Layer Thicknesses in the Arabian Sea (con.)

STATION	LAYER	VELOCITY (m/sec)	LAYER THICKNESS (m)	WATER DEPTH (m)	LOCATION LAT.	LOCATION LONG.
154		1482	000	3300	21°24'N	64°27'E
	A	1635	229			
	B	2080	260			
	C	2820	903			
	D	3064	881			
	A&B	1858	492			
	B&C	2634	1172			
	C&D	2938	1785			
155		1479	000	2893	20°43'N	65°23'E
	A	2022	743			
	B	2769	487			
	A&B	2291	1245			
156		1476	000	2639	19°56'N	66°29'E
	A	1787	380			
	B	2392	493			
	C	2542	544			
	D	3151	1276			
	A&B	2107	882			
	B&C	2470	1037			
	C&D	2955	1829			
157		1471	000	3003	19°34'N	67°06'E
	A	1660	168			
	B	2008	252			
	C	2451	611			
	D	3224	941			
	A&B	1861	421			
	B&C	2312	867			
	C&D	2905	1567			
158		1470	000	3311	18°31'N	68°29'E
	A	1606	168			
	B	1957	281			
	C	2298	299			
	A&B	1818	451			
	B&C	2126	581			
159		1468	000	3347	17°44'N	69°22'E
	A	1469	207			
	B	1714	216			
	C	2199	227			
	A&B	1589	424			
	B&C	1947	446			

Table 4. Tabulation of Interval Velocities and Layer Thicknesses in the Arabian Sea (con.)

STATION	LAYER	VELOCITY (m/sec)	LAYER THICKNESS (m)	WATER DEPTH (m)	LOCATION LAT.	LOCATION LONG.
160		1476	000	3622	16°19'N	70°04'E
	A	1577	244			
	B	1799	238			
	C	3148	1569			
	A&B	1683	484			
	B&C	2917	1841			
161		1476	000	3605	16°37'N	69°12'E
	A	1590	209			
	B	1741	206			
	C	2402	312			
	A&B	1664	416			
	C&B	2113	525			
162		1475	000	3544	17°12'N	68°15'E
	A	1597	221			
	B	2074	288			
	C	2589	472			
	A&B	1851	514			
	B&C	2380	765			
163		1475	000	3360	18°12'N	66°47'E
	A	1704	277			
	B	2145	354			
	C	2422	270			
	D	2808	653			
	A&B	1939	635			
	B&C	2261	625			
	C&D	2689	925			
164		1478	000	3187	19°07'N	65°44'E
	A	1764	357			
	B	2456	606			
	C	3047	599			
	D	3264	653			
	E	3705	874			
	A&B	2172	975			
	B&C	2734	1211			
	C&D	3158	1252			
	D&E	3509	1530			

Table 4. Tabulation of Interval Velocities and Layer Thicknesses in the Arabian Sea (con.)

STATION	LAYER	VELOCITY (m/sec)	LAYER THICKNESS (m)	WATER DEPTH (m)	LOCATION LAT.	LOCATION LONG.
165		1483	000	3235	20°07'N	64°11'E
	A	1746	268			
	B	2274	540			
	C	2735	449			
	D	3110	485			
	E	3899	2808			
	A&B	2083	814			
	B&C	2473	993			
	C&D	2924	936			
	D&E	3771	3303			
166		1470	000	3317	21°02'N	63°10'E
	A	1699	323			
	B	2269	374			
	C	2754	547			
	A&B	1985	705			
	B&C	2545	925			
171		1486	000	3416	19°26'N	63°03'E
	A	1699	257			
	B	2323	588			
	C	2831	842			
	D	3066	667			
	A&B	2111	853			
	B&C	2610	1437			
	C&D	2932	1510			
172		1486	000	3457	18°37'N	64°16'E
	A	1785	280			
	B	2163	359			
	C	2469	388			
	D	3011	780			
	E	3241	911			
	A&B	1988	642			
	B&C	2317	748			
	C&D	2818	1172			
	D&E	3133	1692			
173		1484	000	3388	17°40'N	65°34'E
	A	1707	239			
	B	2223	311			
	C	2262	662			
	D	3161	751			
	A&B	1982	555			
	B&C	2249	973			
	C&D	2702	1432			

Table 4. Tabulation of Interval Velocities and Layer Thicknesses in the Arabian Sea (con.)

STATION	LAYER	VELOCITY (m/sec)	LAYER THICKNESS (m)	WATER DEPTH (m)	LOCATION LAT.	LOCATION LONG.
174		1480	000	3622	16°40'N	66°54'E
	A	1824	228			
	B	2191	362			
	C	2808	660			
	A&B	2041	592			
	B&C	2571	1029			
175		1482	000	3930	15°09'N	67°40'E
	A	1584	162			
	B	2032	274			
	C	2084	263			
	D	2305	349			
	A&B	1852	440			
	B&C	2057	537			
	C&D	2207	613			
176		1485	000	3866	15°01'N	66°09'E
	A	1909	441			
	B	2250	402			
	C	2690	576			
	A&B	2064	845			
	B&C	2500	981			
182		1473	000	3702	18°58'N	61°13'E
	A	1616	174			
	B	1870	107			
	C	2066	200			
	D	2413	322			
	E	2711	384			
	A&B	1708	282			
	B&C	1996	307			
	C&D	2273	524			
	D&E	2571	707			
183		1482	000	3638	18°10'N	62°08'E
	A	1782	258			
	B	2049	328			
	C	2431	321			
	D	2537	445			
	E	3035	809			
	A&B	1927	588			
	B&C	2230	651			
	C&D	2492	766			
	D&E	2848	1259			

Table 4. Tabulation of Interval Velocities and Layer Thicknesses in the Arabian Sea (con.)

STATION	LAYER	VELOCITY (m/sec)	LAYER THICKNESS (m)	WATER DEPTH (m)	LOCATION LAT.	LOCATION LONG.
184		1491	000	3733	17°26'N	63°03'E
	A	1645	269			
	B	2015	241			
	C	2571	798			
	D	3147	787			
	A&B	1810	512			
	B&C	2429	1045			
	C&D	2843	1593			
185		1490	000	3638	16°43'N	64°01'E
	A	1603	299			
	B	2296	539			
	C	2509	759			
	D	3157	1184			
	A&B	2019	851			
	B&C	2418	1300			
	C&D	2886	1955			
186		1486	000	3678	15°50'N	65°08'E
	A	1790	246			
	B	2153	475			
	C	2668	925			
	D	3302	918			
	A&B	2021	724			
	B&C	2481	1407			
	C&D	2967	1853			
300		1482	000	3884	16°44'N	062°04'E
	A	1926	428			
	B	2211	434			
	A&B	2065	864			
301		1482	000	3936	16°06'N	062°44'E
	A	1941	270			
	B	2061	196			
	C	2323	296			
	A&B	1991	466			
	B&C	2215	493			
302		1486	000	3753	15°09'N	064°00'E
	A	1890	319			
	B	1986	255			
	A&B	1932	575			

Table 4. Tabulation of Interval Velocities and Layer Thicknesses in the Arabian Sea (con.)

STATION	LAYER	VELOCITY (m/sec)	LAYER THICKNESS (m)	WATER DEPTH (m)	LOCATION LAT.	LOCATION LONG.
303		1486	000	4287	11°33'N	068°33'E
	A	2025	447			
	B	2295	530			
	C	2895	1210			
	A&B	2167	979			
	B&C	2697	1750			
304		1488	000	4353	10°58'N	066°59'E
	A	1510	223			
	B	2278	722			
	A&B	2065	959			
305		1495	000	4253	11°48'N	066°01'E
	A	1876	385			
	B	2661	997			
	C	3265	811			
	A&B	2412	1399			
	B&C	2917	1817			
306		1486	000	4072	13°45'N	063°22'E
	A	1850	375			
	B	1944	237			
	C	2376	449			
	D	2495	306			
	A&B	1886	613			
	B&C	2217	689			
	C&D	2424	755			
307		1486	000	4109	14°24'N	062°34'E
	A	1848	389			
	B	2118	199			
	C	2355	298			
	A&B	1936	589			
	B&C	2257	498			
308		1490	000	4332	11°58'N	063°13'E
	A	1692	219			
	B	2106	366			
	C	2094	750			
	D	3612	970			
	A&B	1940	589			
	B&C	2484	1124			
	C&D	3178	1738			

Table 4. Tabulation of Interval Velocities and Layer Thicknesses in the Arabian Sea (con.)

STATION	LAYER	VELOCITY (m/sec)	LAYER THICKNESS (m)	WATER DEPTH (m)	LOCATION LAT.	LOCATION LONG.
309		1489	000	4372	10°55'N	064°38'E
	A	1748	266			
	B	2291	377			
	C	2385	427			
	D	3228	644			
	A&B	2048	648			
	B&C	2341	804			
	C&D	2861	1083			
310		1489	000	4514	C9°16'N	064°22'E
	A	1887	471			
	B	2116	273			
	A&B	1968	745			
311		1489	000	4455	10°18'N	063°06'E
	A	1902	530			
	B	2433	307			
	A&B	2082	842			
312		1489	000	4518	10°00'N	061°54'E
	A	1651	236			
344		1486	000	3856	14°14'N	065°08'E
	A	1735	487			
	B	2265	587			
	A&B	2007	1083			
345		1486	000	4052	13°21'N	066°12'E
	A	1817	514			
	B	2435	576			
	A&B	2121	1102			
346		1486	000	4323	12°25'N	067°22'E
	A	1609	281			
	B	2344	517			
	A&B	2052	810			

APPENDIX B
CORE VELOCITY CORRECTION PROCEDURES

FIELD DETERMINATION OF APPROXIMATE IN SITU SOUND VELOCITY

Information Supplied:

(1) Core Interval Depth (cm.)
(2) Laboratory Temperature (Reference/Sediment) (=°C)
(3) Time Delay Through the Reference Water Sample (Tw)
(4) Time Delay Through the Sediment (Ts)

To calculate the laboratory sediment sound velocity (in meters per second), use the formula:

$$Cs = Cw \quad 1 \;/\; 1-Cw*(t/d)$$

Where:

Cs is the sound velocity through the sediment;

Cw is the sound velocity through the reference water sample. This value is extrapolated from Wilson's Tables for the speed of sound in distilled water;

t is the difference in time arrival for the pulse through the sediment as compared to the reference water sample. [(Tw-Ts) 20x10-6];

d is the inside diameter of the core liner USE:0.059m

To correct the laboratory sediment sound velocity to approximate in situ velocity, the following information is needed:

(1) The uncorrected laboratory sediment sound velocity value (in meters per second)
(2) The in situ environmental data, which include:
    (a) Bottom depth
    (b) Bottom temperature (°C)
    (c) Bottom salinity (o/oo)
(3) Wilson's Sound Speed Tables: #12B, 12E, and 12F (From SP-68, Handbook of Oceanographic Tables)

Steps:

(1) Find the correction factor for changes in depth (Table 12B).
    (a) Obtain the sound velocity at the given depth (extrapolate).
    (b) Subtract the sound velocity 1449.1 m/sec from the sound velocity at the given depth.
    (c) The result is the positive correction factor for changes in depth.

FIELD DETERMINATION OF APPROXIMATE IN SITU SOUND VELOCITY (CON.)

(2) Find the correction factor for changes in temperature (Table 12E).
   (a) Obtain the factor for laboratory temperature.
   (b) Subtract the factor for in situ temperature from the factor for laboratory temperature.
   (c) The result is the negative correction factor for temperature.

(3) Find the correction factor for simultaneous changes in salinity, temperature and pressure, VSTP (Table 12F) using the in situ temperature, salinity and depth.
   (a) The result of the above search is the negative correction factor for VSTP.

(4) Add algebraically the three correction factors which are:
   (a) The negative temperature correction factor.
   (b) The positive depth correction factor.
   (c) The negative VSTP correction factor.

(5) The above result, when added or subtracted, whichever the case, to the laboratory sediment sound velocity will yield an approximate in situ sound velocity.

Example:

Required information

1. Depth = 4250 meters
2. Salinity = 34.75 o/oo
3. In situ Temp. = 1.39 °C
4. Laboratory Temp. = 26.42 °C
5. Measured Sound velocity = 1489.58 m/sec

Correction Factor (Depth)
4250 meters = 1522.2 m/sec
VO = 1449.1 m/sec
VP = + 73.1 m/sec
Correction Factor (Temperature)
Lab = 26.42= = 88.8
In situ = 1.39 = 6.3
-82.5 m/sec
Correction Factor VSTp = -.1

VT + VP + VSTP = Total Correction Factor
-82.5 + 73.1 + (-.1) = -9.5.m/sec

Measured Sound Velocity = 1489.58 + (-9.5)
= 1480.08 in situ Sound Velocity

LABORATORY DETERMINATION OF IN SITU SOUND VELOCITY

COMPRESSIONAL WAVE VELOCITY

Descriptions which delineate sediment boundary layers are observed from X-radiographs of the core. Each core is analyzed for compressional wave velocity (sound velocity) at the sediment boundary layers.

An underwater sediment velocimeter measures the time required for a 400-Hz signal to travel through the core liner thickness at the transiting crystal, travel through the sediment thickness, and travel through the core liner at the receiving crystal. Another time delay measurement (90° to the axis of the first time delay measurement) is taken so that sound velocity changes caused by grain orientation will be detected. Similar time delay measurements are noted for a distilled water reference standard.

The time delay difference between the reference standard and the sediment is calculated for each sub-sampling interval within the core. This difference is needed to calculate the sound velocity using Wilson's equations for computing the speed of sound in seawater.

In situ salinity (in parts per thousand), in situ temperature (in °C), and water column depth (in meters) values are either directly measured by field surveys or obtained from historical database records. Salinity, temperature, and pressure correction factors are calculated using a modified version of Wilson's equations.

The sound velocity of the bottom water is calculated from the relationship:

CWB=1449.1+VP2+VS2+VT2+VSTP2)*3.28083

Equation terms are identical to those used by Wilson with the exception of CWB. This term combines Wilson's use of the letter "C" to denote sound velocity with the letter "W" to denote "water", and the letter "B" to denote "bottom".

Sediment sound velocity is calculated from an enhanced version of the Mandex, Incorporated velocity calculation formula:

Cs = Cw * 1/1-Cw *(T/D)

Where:

- Cs = Sound velocity through sediment (M/Sec.)
- Cw = Sound velocity through distilled water (M/Sec.)
- T = Difference in arrival time for the pulse through sediment as compared to the reference standard.
- D = Inside diameter of the core tube (M.)

The enhanced version adjusts the sound velocity for temperature, pressure, and salinity conditions. Sediment interstitial salinity is assumed to be identical to the water in situ salinity. The sediment core and distilled water reference standards are allowed to reach ambient temperature conditions (usually an 8-hour equilibrium period) prior to time delay measurements. The pressure correction factor is reflected in Wilson's equations.

A graphical representation of the average sound velocity variations within the core is generated with a tabular listing which shows each plane's sediment sound velocity and the average of the two planes.

A discrete average and a weighted average tabular listing which also indicates the sediment/water velocity ratio is included when it is requested by the user community.

APPENDIX C

INTERVAL VELOCITY COMPUTER PROGRAM WABR

```
      CHARACTER*6 SHIP,IAR*1(5),HORIZ*16
      CHARACTER*5 AREA1,AREA2,AREA3,AREA4,CHK
      DIMENSION A(30,30),S(30,30),B(15),COC(8),ISTAT(30)
      DATA IAR/'A','B','C','D','E'/
C     WABR MADE BY MICHAEL A. MCGLAUGHLIN, AUG. 79,
C     THIS PROGRAM MODIFIED BY STEVEN G. CARRUBBA O/A DEC 1983
C     CONVERTED TO DISSPLA9-0 6/12/84 MARTIN H. BOODA
C     IT WILL NOW ALLOW ONE TO OMIT CERTAIN HORIZONS AND
C     CALCULATE SO DESIGNATED SEDIMENT THICKNESSES
      CALL COMPRS
C     STATION CARD FORMAT:COL.1-3 STA.#,COL.4-23 OCEAN AREA,
C     COL.24-29 SHIP NAME, COL.30-35 CRUISE#, COL.36-38
C     JD, COL.39-40 YEAR, COL.41-46 LATITUDE (DD.MM)N OR S,
C     COL.47-53  LONGITUDE (DDD.MM)E OR W,COL.54-56 # OF
C     DATA CARDS, COL.57-58 LEG #, COL.59-63 SURFACE WATER
C     VELOCITY (X.XXX)KM/SEC.
  100 READ(5,1)ISTANM,AREA1,AREA2,AREA3,AREA4,SHIP,ICRUZ,JD,
     * IYR, ALAT,MLAT,DLT,ALON,MLON,DLN,NCDS,LEG,SWV,ICOU  1
     *FORMAT(I3,4A5,A6,I6,I3,I2,A2,1X,A2,A1,A3,1X,A2,A1,I3,
     *I2,F5.3,I1)
C     USE 999 FOR STA. # AT END OF DATA CARDS TO GET
C     OUT OF LOOP
      IF(ISTANM.EQ.999) GO TO 101  NUM=0
C     THE NEXT TWO DO LOOPS FILL THE ARRAY "A" WITH 30 VALUES
C     IN BOTH DIRECTIONS
      DO 77 L=1,30
      DO 77 M=1,30
      77 A(L,M)=0.
C     THESE ARE MATRICES TO STORE STA. ARRIVAL TIMES A(30,30)
C     INTERMEDIATE LEAST SQUARES QUOTIENT (B(15)) AND
C     COEFFICIENT DATA CARD FORMAT:COL.1-5 DIRECT WAVE TRAVEL
C     TIME(X.XXX)KM/SEC. COL.11-31 TWO WAY REFLECTION TIME TO
C     EACH HORIZON IN LOGICAL ORDER(X.XXX)KM/SEC.,NO SPACING.
      READ(5,3)(A(I,J),J=1,7)
    3 FORMAT(F6.3,4X,6F6.3)
    2 CONTINUE
      DO 88 I=1,30
      DO 88 J=1,30
   88 S(I,J)=A(I,J)
   85 READ(5,82)CHK
   82 FORMAT(A5)
      DO 83 K=1,NCDS
      DO 81 I=1,5
   81 ISTAT(I)=INDEX(CHK,IAR(I))
   83 J=1,5
      IF (ISTAT(J).EQ.0)GO TO 84
      A(K,ISTAT(J)+2)=A(K,J+2)
   84 IF(J.GT.ISTAT(J))A(K,J+2)=0.
   83 CONTINUE
```

```
      NUM=NUM+1
C     AN APPROPRIATE SWV MUST BE INPUT ON THE STATION
C     HEADER CARD.
      DO 4 I=1,NCDS
      DO 5 J=1,7
      A(I,7+J)=A(I,J)**2.
      A(I,15)=A(I,1)*SWV
      A(I,16)=A(I,15)**2.
    5 CONTINUE
    4 CONTINUE
C     CONSTRUCT TABLE
C     THIS SERIES OF STATEMENTS SIMPLY ESTABLISHES THE TABLE
C     FORMAT WHICH IS PRINTED BY THE COMPUTER AS PART
C     OF THE OUTPUT.
      WRITE(6,14)ISTANM,AREA1,AREA2,AREA3,AREA4,SWV
   14 FORMAT(1H1,'SONOBUOY STATION NO.',I3,23X,' AREA ',4A5,
     *10X,'SURFACE WATER VELOCITY  ',F5.3//)
      WRITE(6,15)SHIP,ICRUZ,LEG,JD,IYR,ALAT,MLAT,DLT,ALON,
     *MLON,DLN
   15 FORMAT(' SHIP ',A6,1X,I6,3X,'LEG',1X,I2,18X,'DATE ',I3,
     *'/',I2,6X,'LATITUDE ',A2,1X,A2,1X,A1,12X,'LONGITUDE ',
     *A3,1X,A2,1X,A1//)
      WRITE(6,16)
   16 FORMAT(2X,' DIRECT WAVE',7X,'DISTANCE',22X,'2-WAY
     *REFLECTION TIME ( SECONDS)')
      WRITE(6,17)
   17 FORMAT(2X,' TRAVEL TIME',7X,'SHIP TO')
      WRITE(6,18)
   18 FORMAT(2X,' (ONE WAY) IN',6X,'SONOBUOY',6X,'SEA FLOOR',
     *6X,'HORIZON A',6X,'HORIZON B',6X,'HORIZON C',6X,'
     *HORIZON D',6X,'HORIZON E')
      WRITE(6,19)
   19 FORMAT(2X,' SECONDS',11X,'IN KM.',12X,'1',14X,'2',14X,
     *'3',14X,'4',14X,'5',14X,'6')
      WRITE(6,20)
   20 FORMAT(5X,'T',4X,'T^2',8X,'X',5X,'X^2',6(6X,'T',5X,
     *'T^2'))
      DO 5000 I=1,NCDS
      WRITE(6,21)A(I,1),A(I,8),A(I,15),A(I,16),A(I,2),A(I,9),
     *A(I,3),A(I,10),A(I,4),A(I,11),A(I,5),A(I,12),A(I,6),
     *A(I,13),A(I,7),A(I,14)
   21 FORMAT(1X,F6.3,1X,F7.3,1X,F7.3,1X,F8.3,1X,6(F6.3,1X,
     *F7.3,1X))
 5000 CONTINUE
      THIS ROUTINE ESTABLISHES THE GRAPH ITSELF AND THE TITLE
C     AND LEGEND ETC.
      CALL NOBRDR
      CALL PAGE(16.,14.)
      CALL AREA2D(12.,12.)
      CALL HEIGHT(.21)
      CALL MX1ALF('STANDA','/')
      CALL MX2ALF('INSTRU','+')
      *X/)',57)
      CALL YNAME('REFL TIME SQUARED, SEC+E0.9H.5/2+EXHX/
```

```
      *(T+E0.9H.5/2+EXHX/)',58)
       CALL XREVTK
       CALL YREVTK
       CALL INTAXS
       CALL GRAF(0.,10.,200.,0.,10.,200.)
       CALL INTNO(ISTANM,7.,2.)
       CALL INTNO(ICRUZ,9.,2.)
       ENCODE(2002,HORIZ)CHK
  2002 FORMAT('HORIZONS:  ',A5)
       CALL MESSAG(HORIZ,16,11.,2.)
C      LEAST-SQUARES ROUTINE
C      THIS SERIES OF STATEMENTS DOES A LEAST-SQUARES LINEAR
C      FIT TO THE PLOT OF THE SQUARES OF THE DATA POINTS. THE
C      LEAST-SQUARES FIT IS DONE MATHEMATICALLY BY USING THE
C      SUM OF THE X'S AND Y'S AND XY ETC. LINES 81 THRU 100
C      CALCULATE ALL OF THESE PRODUCTS. LINES 109 THRU 116
C      ACTUALLY DETERMINE THE CONSTANTS A & B FOR THE BEST FIT
C      LINE Y=A+BX. LINES 105 THRU 108 SCALE THE DIRECT AND
C      CORRESPONDING HORIZON ARRIVALS TO THE GRAPH SCALE AND
C      PLOTS THEM ON THE GRAPH. LINES 117 THRU 120 ARE COMMENT
C      CARDS FOR THIS PROCESS.
       DO 1000 J=1,7
       SQX=0.
       SQY=0
       YPX=0.
       XBAR=0.
       YBAR=0.
       DO1001 I=1,NCDS
       IF(A(I,J).EQ.0..AND.I.NE.1)GO TO 1003
       XBAR=XBAR+A(I,16)
       YBAR=YBAR+A(I,J+7)
       SQX=A(I,16)**2.+SQX
       SQY=A(I,J+7)**2.+SQY
       GO TO 1001
  1003 PXY=XBAR*YBAR/(I-1)
       XBAR=(XBAR**2.)/(I-1)
       XNCDS=(I-1)
       GO TO 1002
  1001 YPX=A(I,16)*A(I,J+7)+YPX
       PXY=XBAR*YBAR/NCDS
       XBAR=(XBAR**2.)/NCDS
       XNCDS=NCDS
  1002 SSXY=0.
       SSX=0.
       DO 1004 I=1,NCDS
       IF(A(I,J+7).EQ.0..AND.I.NE.1)GO TO 3000
C      PLOT SYMBOL ON GRAPH
       CALL MARKER(J)
       CALL HEIGHT(.1)
       CALL CURVE(A(I,16),A(I,J+7),1,-1)
       SSX=SQX-XBAR
       SSXY=YPX-PXY
  1004 CONTINUE
  3000 BETA=SSXY/SSX
```

```
      COC(J)=BETA*((SQRT(SQX/XNCDS-XBAR/XNCDS))/(SQRT(SQY/
      *XNCDS-((YBAR/XNCDS)**2.))))
      ALPHA=YBAR-BETA*XBAR
      B(J)=BETA
C     Y=12.*ALPHA/200.+1.
C     CALL PLOT(2.,Y,3)
C     Y=ALPHA+BETA*200.+1.
C     CALL PLOT(14.,Y,2)
 1000 CONTINUE
C     CALCULATE AND PRINT VEL. AND THK.
C     CALCULATES THK. AND VEL. FOR EACH LAYER AND PRINTS THEM
C     OUT UNDER THE TABLE OF ARRIVALS.
      DO 1005 I=2,7
      IF(A(1,I).LE.A(1,I-1))GO TO 6000
      AVEL=SQRT(((1/B(I))*A(1,I)-(1/B(I-1))*A(1,I-1))/(A(1,I)
      *-A(1,I-1)))
      THK=AVEL*(A(1,I)-A(1,I-1))/2.
      IB=I-2
      IT=IB+1
      WRITE(6,22)IB,IT,AVEL,COC(I)
   22 FORMAT(' VELOCITY (',I1,' TO ',I1,' )',20X,F5.3,
      *' KM./SEC.',7X,' COC = ',3X,F6.4)
      WRITE(6,23)IB,IT,THK
   23 FORMAT(' THICKNESS (',I1,' TO ',I1,')',19X,F5.3,' KM.')
 1005 CONTINUE
 6000 WRITE(6,87)CHK
   87 FORMAT(1H0,'COMPUTED HORIZONS:',2X,A5)
      IF (NUM.NE.ICOU)GO TO 92
      CALL ENDPL(0)
      GO TO 100
   92 DO 91 I=1,30
      DO 91 J=1,30
   91 A (I,J)=S(I,J)
      CALL ENDPL(0)
      GO TO 85
  101 CALL DONEPL
      END
EOF:193
```

APPENDIX D

INSTANTANEOUS VELOCITY PROGRAM FOR INDIVIDUAL STATIONS

PROGRAM TIMVEL WITH SUBPROGRAMS LEAST,PARA AND EXPO

```
C     PROGRAM TIMVEL4 SETS UP A TIME/VELOCITY PLOT FOR A LAYER
C     AND LAYERS.  (STANDARD NAVOCEANO WABR DATA)  AN OPTION
C     "1" IN COLUMN  64 SETS UP A PLOT FOR CDP VALUES, I.E.,
C     ONE WAY TRAVEL TIME FROM  THE SEDIMENT SURFACE TO A
C     DEPTH AT WHICH A VELOCITY APPLIES. (USE PROGRAM TIMVEL6
C     IF USING LAMONT DATA.) SETS UP MATRICES FOR THE STORAGE
C     OF THICKNESS, VELOCITY, AND TIME DATA.
      IMPLICIT DOUBLE PRECISION (S)
      DIMENSION THICK(100),
     *          VELOC(100),
     *          TIME(100)
      CHARACTER XTITLE*36,ICRUZ*6
      CALL COMPRS
C     INDICATES THAT UP TO 70 INDIVIDUAL STATIONS CAN BE
C     PROCESSED IN ONE RUN.
      DO 5000 II=1,70
C     READS IN STATIONS DATA SUCH AS NUMBER, AREA, LOCATION,
C     SHIP CRUISE DATA AND NUMBER OF DATA CARDS IE ONE FOR
C     EACH LAYER. NOTE: THE FIRST DATA CARD IS THE SEDIMENT
C     SURFACE VELOCITY AND THEREFORE HAS A THICKNESS OF ZERO.
      READ(5,50)ISTANM,AREA1,AREA2,AREA3,AREA4,SHIP,ICRUZ,JD,
     *IYR,ALAT,DLT,ALON,DLN,NCDS,LEG,ITHTIM
   50 FORMAT(I3,4A5,A6,A6,I3,I2,F5.2,A1,F6.2,A1,I3,A2,6X,I1)

C     INDICATES THE USE OF A 999 CARD TO GET OUT OF THE LOOP
      AND END THE RUN.
      IF (ISTANM.EQ.999) GO TO 9999
      IF(ITHTIM.LT.1)GO TO 51
      DO 52 JJ=1,NCDS
   52 READ(5,60)TIME(JJ),VELOC(JJ)
      GO TO 2500
C     READ IN SEDIMENT SURFACE DATA
C     READS IN THE SEDIMENT SURFACE VELOCITY AND THICKNESS.
   51 READ(5,55) THICK(1),VELOC(1)
   55 FORMAT(F5.3,1X,F5.3)
      TIME(1)=0.0
C     ESTABLISHES THE NUMBER OF INDIVIDUAL LAYERS TO BE USED
C     NCDS INCLUDES THOSE DATA CARDS FOR COMBINATION LAYERS
C     THUS NCRS/2 + 1 WILL ALWAYS GIVE ONLY THE NUMBER OF
C     INDIVIDUAL LAYERS INCLUDING THE SEDIMENT SURFACE LAYER.
      LAYER=NCDS/2+1
      CTIME=0.0
C     SINGLE SEDIMENT LAYER DATA IS STORED IN ARRAYS
```

```
C     TIME, VELOC, AND THICK FROM SUBSCRIPT (2) TO
C     SUBSCRIPT (LAYER)
C     READS IN THE INDIVIDUAL LAYER THICKNESS AND VELOCITIES
C     ON EACH DATA CARD IN TURN (NOT INCLUDING SEDIMENT
C     SURFACE) UP TO THE NUMBER SPECIFIED BY LAYER
C     (SEE LINE 35).  IT THEN CALCULATES THE ONE WAY TRAVEL
C     TIME FROM THE SEDIMENT SURFACE  TO THE MIDPOINT OF THE
C     LAYER AND THIS TIME IS STORED IN A MATRIX.
      DO 1000 JJ=2,LAYER
      READ(5,60) THICK(JJ),VELOC(JJ)
   60 FORMAT(F5.3,1X,F5.3)
      TIME(JJ)=CTIME+((THICK(JJ)*0.5)/VELOC(JJ))
      CTIME=CTIME+(THICK(JJ)/VELOC(JJ))
 1000 CONTINUE
C     CALCULATES THE ONE WAY TRAVEL TIME TO THE MIDPOINT OF
C     THE LAYER FOR EACH OF THE COMBINATIONS OF LAYERS AND
C     STORES THESE TIMES.  LINE 60 TAKES IT OUT OF THE LOOP
C     IF THESE ARE TWO LAYERS OR LESS (IE. SURFACE LAYERS AND
C     ONE LAYER) SINCE A COMBINATION CANNOT BE MADE OF THESE.
C     CALCULATE ONE WAY TRAVEL TIME FOR COMBINED LAYERS
C     SKIP THIS LOOP IF THERE IS ONLY SURFACE SEDIMENT DATA OR
C     IF THERE IS ONLY SURFACE SEDIMENT DATA AND ONE LAYER
C     IN THAT STATION
      IF(NCDS.LE.2) GO TO 2500
      CTIME=0.0
      ITALLY=2
C     COMBINED LAYER DATA IS STORED IN ARRAYS FROM
C     SUBSCRIPT (ICOMB) TO SUBSCRIPT (NCDS)
      ICOMB=LAYER+1
      DO 2000 KK=ICOMB,NCDS
      READ(5,70) THICK(KK),VELOC(KK)
   70 FORMAT(F5.3,1X,F5.3)
      TIME(KK)=CTIME+((THICK(KK)*0.5)/VELOC(KK))
      CTIME=CTIME+(THICK(ITALLY)/VELOC(ITALLY))
      ITALLY=ITALLY+1
 2000 CONTINUE
C     ESTABLISHES THE TITLE AND FORMAT FOR PRINTING OUT
C     THE INDIVIDUAL STATION THICKNESS, VELOCITIES AND ONE
C     WAY TRAVEL TIMES.
 2500 ENCODE(80,XTITLE) ICRUZ,LEG,ISTANM
   80 FORMAT(' CRUISE ',A6,2X,'LEG ',A2,2X,
     *       'STATION ',I3,'$')
      WRITE(6,72) ISTANM
   72 FORMAT(' DATA FOR STATION ',I3)
      DO 3000 LL=1,NCDS
      IF(ITHTIM.LT.1)WRITE(6,75) LL,THICK(LL),VELOC(LL),TIME(LL)
   75 FORMAT(' POINT NUMBER ',I2,3X,'THICKNESS= '
     *   F5.3,3X,'VELOCITY= ',F5.3,3X,'TIME= ',F5.3)
      IF(ITHTIM.GE.1)WRITE(6,76) LL,VELOC(LL),TIME(LL)
   76 FORMAT(' POINT NUMBER ',I2,3X,'VELOCITY= ',F5.3,3X,'TIME= '
     *,F5.3)
```

```
 3000 CONTINUE
      CALL TITLE(' ',1,0,0,'ONE WAY TRAVEL TIME IN SECS.$',
      *100,6.0,8.0)
      CALL XTICKS(1)
      CALL YTICKS(2)
      CALL GRAF(1.4,0.2,5.0,4.0,-0.5,0.0)
      CALL XGRAXS(1.4,0.2,5.0,6.0,'VELOCITY-KM/SEC$',
      *-100,0.,8.)
      CALL MARKER(8)
      CALL CURVE(VELOC,TIME,NCDS,-1)
C     SETS UP THE GRAPH OF THE INDIVIDUAL STATION VELOCITIES
C     VERSUS ONE WAY TRAVEL TIME, ESTABLISHES THE GRAPH SCALE,
C     AXES AND AXES TITLES.
      CALL MESSAG(XTITLE,100,0.5,9.0)
      CALL LEAST(VELOC,TIME,NCDS,XTITLE)
      CALL PARA(VELOC,TIME,NCDS,XTITLE)
      CALL EXPO(VELOC,TIME,NCDS,XTITLE)
 5000 CONTINUE
 9999 CALL DONEPL
      STOP
      END
 EOF:111
 0:END ED. NO CORRECTIONS APPLIED
```

```
C     SUBPROGRAM FOR LINEAR FIT OF VEL/TIME DATA
C     SUMX=SUM OF THE XS (VELOC)
C     SUMY=SUM OF THE YS (TIME)
C     SUMW=SUM OF THE WS
C     SUMXW=SUM OF THE X * W
C     SUMYW=SUM OF THE Y * W
C     SUMXYW=SUM OF THE X*Y*W'S
C     SUMYSW=SUM OF Y SQ * W
C     YAVE=AVERAGE OF THE YS
      SUBROUTINE LEAST(VELOC,TIME,NCDS,XTITLE)
C     THIS ESTABLISHES MATRICES FOR STORING VARIOUS QUANTITIES
C     TO BE MANIPULATED IN THE PROGRAM.
      DIMENSION VELOC(12),
     *          XEST(12),
     *          TIME(12)
      CHARACTER XTITLE*36,YTITLE*37,ZTITLE*31
      DIMENSION X(80),
     *          Y(80),
     *          W(12)
C     THIS SEQUENCE SETS ALL OF THE QUANTITIES TO BE
C     CALCULATED TO INITIAL ZERC VALUE.
      SUMW=0
      SUMX=0
      SUMXW=0
      SUMY=0
      SUMYW=0
      SUMXYW=0
      SUMYSW=0
      SUMYS=0
C     WEIGHT FIRST POINT BY GIVING W(1) A HIGH VALUE
C     IN ORDER TO GIVE MORE WEIGHT TO THE SEDIMENT SURFACE
C     VELOCITY AND FORCE THE CURVE THROUGH THIS POINT, A
C     WEIGHTING FACTOR IS USED IN THE CALCULATIONS AND THE
C     SEDIMENT SURFACE VELOCITY IS GIVEN A WEIGHT OF 5 AND
C     ALL OTHER VELOCITY POINTS A WEIGHT OF ONE.
      W(1)=5
      DO 500 LL=2,NCDS
  500 W(LL)=1.
C     READ THROUGH VELOC AND TIME TO OBTAIN
C     VARIABLES FOR LEAST SQUARES EQUATION
C     THIS SERIES OF STATEMENTS CALCULATES THE VARIOUS
C     QUANTITIES (SUMS) NEEDED TO PERFORM A MATHEMATICAL
C     LEAST SQUARES FIT TO THE DATA. THE DATA ARE PULLED FROM
C     THE MAIN PROGRAM AND NEED NOT BE READ IN AGAIN.
      DO 1000 JJ=1,NCDS
      SUMX=SUMX+VELOC(JJ)
      SUMY=SUMY+TIME(JJ)
      SUMW=SUMW+W(JJ)
      SUMXW=SUMXW+(VELOC(JJ)*W(JJ))
      SUMYW=SUMYW+(TIME(JJ)*W(JJ))
      SUMXYW=SUMXYW+(VELOC(JJ)*TIME(JJ)*W(JJ))
      SUMYS=SUMYS+TIME(JJ)**2
```

```
 1000 SUMYSW=SUMYSW+(TIME(JJ)**2*W(JJ))
      XAVE=SUMX/NCDS
C     CREATE A0 VARIABLE FOR LEAST SQ EQUATION
C     CALCULATES THE CONSTANTS A IN THE LINE Y=A+BX
      B0=((SUMXW*SUMYSW)-(SUMYW*SUMXYW))/
      * ((SUMW*SUMYSW)-SUMYW**2)
C     CREATE A1 VARIABLE FOR LEAST SQ EQUATION
C     CALCULATES THE CONSTANT B IN THE LINE Y=A+BX
      B1=((SUMW*SUMXYW)-(SUMXW*SUMYW))/
      * ((SUMW*SUMYSW)-SUMYW**2)
C     THIS SERIES OF STATEMENTS USES THE EQUATION DETERMINED
C     ABOVE, Y=A+BX OR ACTUALLY X=A+BY TO DERIVE THE LINE
C     WHICH BEST FITS THE DATA.  INCREMENTAL VALUES OF Y ARE
C     USED ALONG WITH THE DETERMINED CONSTANTS A AND B. DERIVE
C     X AND Y POINTS FOR LINE BY USING EQUATION FOR EVERY TICK
C     MARK ON THE X AXIS
      YORIG=0.0
      DO 2000 II=1,50
      Y(II)=YORIG
      YORIG=YORIG+0.05
      X(II)=B0+B1*Y(II)
 2000 CONTINUE
C     DETERMINES THE COEFFICIENT OF CORRELATION FOR THE LEAST
C     SQUARES FIT LINE AND PRINTS IT OUT.
C     FIND ESTIMATED YS BY USING FORMULA ON EACH
C     ACTUAL X VALUE
      SSR=0
      SST=0
      DO 1500 LL=1,NCDS
      XEST(LL)=B0+(B1*TIME(LL))
      SSR=SSR+(VELOC(LL)-XEST(LL))**2
      SST=SST+(VELOC(LL)-XAVE)**2
 1500 CONTINUE
      COC=SQRT(1-(SSR/SST))
      ENCODE(70,ZTITLE) COC
   70 FORMAT(' CORRELATION COEFFICIENT= ',F5.3)
C     POINTS OUT THE COEFFICIENTS A AND B.
      ENCODE(80,YTITLE) B1,B0
   80 FORMAT(' B1=',F6.3,2X,'B0=',F6.3,5X,'X=B0 + B1*Y')
C     THESE PLOT THE DATA AND THE BEST FIT LINE WITH HEADINGS
C     AND AXIS NOTATION.
      CALL CURVE(X,Y,50,0)
      CALL MESSAG(YTITLE,37,0.5,-0.5)
      CALL MESSAG(ZTITLE,31,0.5,0.0)
      RETURN
      END
```

```
C     SUBROUTINE FOR PARABOLIC CURVE ON VELOCITY/TIME DATA
      SUBROUTINE PARA(VELOC,TIME,NCDS,XTITLE)
C     SUMX=SUM OF THE XS (VELOC)
C     SUMY=SUM OF THE YS (TIME)
C     SUMXSQ=SUM OF THE X SQUAREDS
C     SUMXCU=SUM OF THE X CUBEDS
C     SUMXFO=SUM OF THE X TO THE FOURTHS
C     SUMXY=SUM OF THE X*YS
C     SUMXSY=SUM OF THE X SQ. * YS
C     YAVE= AVERAGE OF YS (WITHOUT WEIGHTED PTS.)
C     THESE ESTABLISH MATRICES FOR STORING DATA TO BE
C     MANIPULATED.
      DIMENSION VELOC(60),
     *          TIME(60)
      DIMENSION X(80),
     *          Y(80)
      CHARACTER XTITLE*36,YTITLE*32,ZTITLE*36
      DIMENSION A(3,3),
     *          B(3),
     *          XEST(12)
C     THESE INITIALLY SET ALL QUANTITIES TO BE CALCULATED
C     AT ZERO.
      SUMX=0
      SUMY=0
      SUMYSQ=0
      SUMYCU=0
      SUMYFO=0
      SUMXY=0
      SUMYSX=0
      ZERO=1.0E-06
C     WEIGHTING FOR SEDIMENT SURFACE VALUES
C     IWT IS THE WEIGHTING FACTOR FOR THE POINT
C     THE VALUES FOR THAT POINT ARE ADDED ONTO
C     THE EXISTING DATA ARRAYS
C     NUM=FINAL NUMBER OF POINTS USED
C     NOTE: AN IWT VALUE OF 1 MEANS THE VALUE IS WEIGHTED BY
C     2 SINCE THE VALUE HAS ALREADY BEEN READ INTO
C     THE VELOC AND TIME ARRAYS IN THE INITIAL READ
C     GIVES THE SURFACE SEDIMENT VELOCITY A WEIGHTING OF 5.
      IWT=4
      ITALLY=NCDS+1
      NUM=NCDS+IWT
      DO 500 MM=ITALLY,NUM
      VELOC(MM)=VELOC(1)
      TIME(MM)=TIME(1)
  500 CONTINUE
C     READ THROUGH VELOC AND TIME TO OBTAIN SUMS
C     CALCULATES THE QUANTITIES NEEDED TO DETERMINE THE
C     COEFFICIENTS OF THE BEST FIT CURVE  X=A+BY+CY**2.
      DO 1000 JJ=1,NUM
      SUMX=SUMX+VELOC(JJ)
      SUMY=SUMY+TIME(JJ)
      SUMYSQ=SUMYSQ+(TIME(JJ)**2)
```

```
      SUMYCU=SUMYCU+(TIME(JJ)**3)
      SUMYFO=SUMYFO+(TIME(JJ)**4)
      SUMXY=SUMXY+(VELOC(JJ)*TIME(JJ))
      SUMYSX=SUMYSX+((TIME(JJ)**2)*VELOC(JJ))
 1000 CONTINUE
C     PRINTS THE CALCULATED VALUES DETERMINED ABOVE.
      PRINT 90,SUMX,SUMY,SUMYSQ,SUMYCU,SUMYFO,SUMXY,SUMYSX
C     SUM THE YS WITHOUT THE WEIGHTED VALUES
C     FOR USE IN THE COC EQUATION
C     DETERMINES THE SUM OF THE VELOCITIES AND THE AVERAGES
C     OF THE VELOCITIES FOR DETERMINING THE COEFFICIENT OF
C     CORRELATION. THIS IS THEN PRINTED OUT.
      XSUM=0
      DO 1200 KK=1,NCDS
 1200 XSUM=XSUM+VELOC(KK)
      XAVE=XSUM/NCDS
      PRINT 90,XAVE
C     THIS DETERMINES THE COEFFICIENT A,B,AND C BY THE MATRIX
C     METHOD OF SOLVING 3 EQUATIONS SIMULTANEOUSLY AND PRINTS
C     OUT THE COEFFICIENTS. SOLVE SIMULTANEOUS EQUATIONS TO
C     GET COEFFICIENTS FOR EQUATION.
      A(1,1)=NUM
      A(1,2)=SUMY
      A(1,3)=SUMYSQ
      A(2,1)=SUMY
      A(2,2)=SUMYSQ
      A(2,3)=SUMYCU
      A(3,1)=SUMYSQ
      A(3,2)=SUMYCU
      A(3,3)=SUMYFO
      B(1)=SUMX
      B(2)=SUMXY
      B(3)=SUMYSX
      DO 100 I=1,3
      DIV=A(I,I)
      IF(ABS(DIV)-ZERO) 99,99,1
    1 DO 101 J=1,3
      A(I,J)=A(I,J)/DIV
  101 CONTINUE
      B(I)=B(I)/DIV
      DO 102 J=1,3
      IF(I-J) 2,102,2
    2 RATIO=A(J,I)
      DO 103 K=1,3
      A(J,K)=A(J,K)-RATIO*A(I,K)
  103 CONTINUE
      B(J)=B(J)-RATIO*B(I)
  102 CONTINUE
  100 CONTINUE
      PRINT 90,B(1),B(2),B(3)
C     USES THE COEFFICIENTS DETERMINED, IN THE EQUATION
C     X=A+BY+CY2 TO DERIVE THE BEST FIT PARABOLIC CURVE
C     TO THE DATA.
   99 YORIG=0.0
```

```
C     DERIVE X AND Y POINTS FOR LINE BY USING
C     EQUATION FOR EVERY TICK MARK ON THE X AXIS
      DO 2000 II=1,50
      Y(II)=YORIG
      YORIG=YORIG+0.05
      X(II)=B(1)+(B(2)*Y(II))+(B(3)*Y(II)**2)
 2000 CONTINUE
C     CALCULATES THE COEFFICIENT OF CORRELATION FOR THE BEST
C     FIT CURVE AND PRINTS THIS VALUE.
C     FIND ESTIMATED XS BY USING FORMULA
C     ON EACH Y VALUE
      SSR=0.
      SST=0.
      DO 1500 LL=1,NCDS
      XEST(LL)=B(1)+(B(2)*TIME(LL))+(B(3)*TIME(LL)**2)
      SSR=SSR+(VELOC(LL)-XEST(LL))**2
      SST=SST+(VELOC(LL)-XAVE)**2
 1500 CONTINUE
      COC=SQRT(1-(SSR/SST))
      PRINT 90,COC
      ENCODE(70,ZTITLE) COC
   70 FORMAT(' CORRELATION COEFFICIENT PARA= ',F5.3)
C     PRINTS OUT THE DETERMINED COEFFFICIENTS.
      ENCODE(80,YTITLE) B(1),B(2),B(3)
   80 FORMAT(' A0=',F6.3,2X,'A1=',F6.3,2X,'A2=',F6.3)
C     PRODUCES THE GRAPH OF THE DATA POINTS AND THE CURVE AND
C     ALL LEGEND INFORMATION
      CALL CURVE(X,Y,50,0)
      CALL MESSAG(YTITLE,32,0.5,1.0)
      CALL MESSAG(ZTITLE,36,0.5,1.5)
      CALL MESSAG('  X= A0 + A1*Y + A2*Y**2',24,0.5,0.5)
   90 FORMAT( )
      RETURN
      END
```

```
C     SUBPROGRAM FOR EXPONENTIAL CURVE
C     (IF PROBLEMS OCCUR WITH NEGATIVE NUMBERS USE
C     PROGRAM EXPO5. IT SOLVES EQUATION WITH ABSOLUTE VALUES.)
C     SUMX=SUM OF THE XS (VELOC)
C     SUMY=SUM OF THE YS (TIME)
C     SUMW=SUM OF THE WS
C     SUMXW=SUM OF THE X * W
C     SUMYW=SUM OF THE Y * W
C     SUMXYW=SUM OF THE X*Y*W'S
C     SUMXSW=SUM OF X SQ * W
C     YAVE=AVERAGE OF THE YS
      SUBROUTINE EXPO(VELOC,TIME,NCDS,XTITLE)
C     PROVIDES MATRICES FOR THE STORAGE OF QUANTITIES TO BE
C     MANIPULATED.
      DIMENSION VELOC(12),
     *          LOGVEL(12),
     *          TIME(12)
      CHARACTER*36 XTITLE,YTITLE,ZTITLE
      DIMENSION X(80),
     *          Y(80),
     *          W(12),
     *          XEST(12)
      REAL LOGVEL
C     INITIALIZE ALL OF THE QUANTITIES AT ZERO.
      SUMY=0
      SUMW=0
      SUMX=0
      SUMXW=0
      SUMYW=0
      SUMXYW=0
      SUMYSW=0
C     TAKES THE NATURAL LOG OF THE VELOCITIES FROM THE MAIN
C     PROGRAM AND STORES THESE VALUES FOR FURTHER USE.  ALSO
C     PRINTS OUT THESE QUANTITIES.
C     LOG X AND Y VALUES
      DO 300 KK=1,NCDS
      LOGVEL(KK)=ALOG(VELOC(KK))
      PRINT 90,VELOC(KK),TIME(KK),LOGVEL(KK)
  300 CONTINUE
C     WEIGHTS THE SEDIMENT SURFACE VELOCITY WITH A WEIGHT OF
C     5 TO FORCE THE BEST FIT CURVE  THROUGH THIS POINT.
C     WEIGHT FIRST POINT BY GIVING W(1) A HIGH VALUE
      W(1)=5
      DO 500 LL=2,NCDS
  500 W(LL)=1.
C     CALCULATES THE VARIOUS SUMS NEEDED TO MAKE A LEAST
C     SQUARE FIT AND PRINTS OUT THE SUMS.
C     READ THROUGH VELOC AND LOGTIM TO OBTAIN
C     VARIABLES FOR LEAST SQUARES EQUATION
      DO 1000 JJ=1,NCDS
      SUMX=SUMX+VELOC(JJ)
      SUMY=SUMY+TIME(JJ)
      SUMW=SUMW+W(JJ)
      SUMXW=SUMXW+(LOGVEL(JJ)*W(JJ))
```

```
      SUMYW=SUMYW+(TIME(JJ)*W(JJ))
      SUMXYW=SUMXYW+(LOGVEL(JJ)*TIME(JJ)*W(JJ))
 1000 SUMYSW=SUMYSW+(TIME(JJ)**2*W(JJ))
      PRINT 90,SUMX,SUMY,SUMW,SUMXW,SUMYW,SUMXYW,SUMYSW
      XAVE=SUMX/NCDS
C     THE EXPONENTIAL EQUATION X=AB**Y HAS BEEN PUT IN THE
C     FORM LOGX=LOGA+YLOGB (STRAIGHT LINE FORM).  THIS
C     SEQUENCE DETERMINES THE CONSTANT B0 = LOGA.
C     CREATE A1 VARIABLE FOR LEAST SQ EQUATION
      B1=((SUMW*SUMXYW)-(SUMXW*SUMYW))/
      * ((SUMW*SUMYSW)-SUMYW**2)
C     THIS SEQUENCE DETERMINES THE CONSTANT B1=LOG B.
C     CREATE A0 VARIABLE FOR LEAST SQ EQUATION
      B0=((SUMXW*SUMYSW)-(SUMYW*SUMXYW))/
      * ((SUMW*SUMYSW)-SUMYW**2)
C     TAKES THE ANTILOG OF B0 AND B1 AND PRINTS THESE VALUES.
      A0=EXP(B0)
      A1=EXP(B1)
      PRINT 90,A0,A1
C     PRODUCES THE BEST FIT CURVE BY CALCULATING VALUES OF X
C     FOR INCREMENTAL VALUES OF Y USING THE CONSTANTS
C     DETERMINED ABOVE.
C     DERIVE X AND Y POINTS FOR LINE BY USING
C     EQUATION FOR EVERY TICK MARK ON THE X AXIS
      YORIG=0.0
      DO 2000 II=1,50
      Y(II)=YORIG
      YORIG=YORIG+0.05
      X(II)=A0*(A1**Y(II))
 2000 CONTINUE
C     CALCULATES THE CORRELATION COEFFICIENT FOR THE BEST FIT
C     CURVE TO THE DATA POINTS AND PRINTS THIS VALUE.
C     CORRELATION COEFFICIENT
C     FIND ESTIMATED YS BY USING FORMULA ON EACH
C     ACTUAL X VALUE
      SSR=0.
      SST=0.
      DO 1500 LL=1,NCDS
      XEST(LL)=A0*(A1**TIME(LL))
      SSR=SSR+(VELOC(LL)-XEST(LL))**2
      SST=SST+(VELOC(LL)-XAVE)**2
 1500 CONTINUE
      COC=SQRT(1-(SSR/SST))
      PRINT 90,COC
C     PLOTS THE DATA POINTS ON A GRAPH, DRAWS THE BEST FIT
C     CURVE, LABELS THE AXIS AND PRINTS THE STATION NUMBERS,
C     CURVE EQUATION AND CONSTANTS,
      ENCODE(70,ZTITLE) COC
   70 FORMAT(' CORRELATION COEFFICIENT EXPO= ',F5.3)
      ENCODE(80,YTITLE) A1,A0
   80 FORMAT(' A1=',F6.3,2X,'A0=',F6.3,5X,'X=A0*A1**Y')
      CALL CURVE(X,Y,50,0)
      CALL MESSAG(YTITLE,36,0.5,2.0)
      CALL MESSAG(ZTITLE,36,0.5,2.5)
```

```
90 FORMAT( )
   CALL ENDPL(1)
   RETURN
   END
```

APPENDIX E

INSTANTANEOUS VELOCITY PROGRAM FOR GROUPS OF STATIONS

```
                        PROGRAM VLEG
C     PROGRAM FOR VEL/ONE WAY TRAVEL TIME PLOT BY LEG AND
C     SUBROUTINES LEGLST, LEGPAR AND LEGEXPO
      IMPLICIT DOUBLE PRECISION (S)
C     THIS CREATES STORAGE FOR QUANTITIES SUCH AS THICKNESS,
      VELOCITY AND TIME TO BE MANIPULATED LATER.
      DIMENSION THICK(100),
     *          VELOC(100),
     *          THIN(500),
     *          TIME(100)
      DIMENSION VLEG(500),
     *          TLEG(500)
      CHARACTER*6 SHIP,ACRUZ,ICRUZ,XTITLE*23,LEG*2,ILEG*2,
     *AREA*20,DLT*1,DLN*1
      CALL COMPRS
C     THIS READS A CARD WHICH INDICATES HOW MANY TIMES THE
C     PROGRAM  WILL BE RUN IE HOW MANY LEGS OF DATA
C     TO BE PROCESSED.
      READ(5,40)NUM
   40 FORMAT(I2)
      DO 4000 MM=1,NUM
C     SETS COUNTERS AT ZERO THESE ARE USED TO KEEP TRACK OF
C     NUMBER OF LAYERS AND NUMBER OF STATIONS.
      ITOTAL=1
      ICOUNT=0
C     SETS THE LIMITS FOR THE NUMBER OF STATIONS TO BE
C     PROCESSED IN ONE LEG.
      DO 5000 II=1,50
C     ON STATION NUMBER, AREA, SHIP, CRUISE,DAY AND YEAR,
C     POSITION, LEG ON WHICH STATION TAKEN AND NUMBER OF DATA
C     CARDS IN THIS STATION.
      READ(5,50)ISTANM,AREA,SHIP,ICRUZ,JD,IYR,ALAT,
     *DLT,ALON,DLN,NCDS,LEG,ITHTIM
C     GIVES THE FORMAT FOR PUTTING THE ABOVE DATA ON CARDS.
   50 FORMAT(I3,A20,A6,A6,I3,I2,F5.2,A1,F6.2,A1,I3,A2,6X,I1)
C     SAVE THE LEG AND CRUISE NUMBERS FOR LABELS
C     THIS SAVES THE CRUISE NUMBER AND LEG NUMBER FROM THE
C     FIRST HEADER  CARD  FOR USE IN LABELING THE PLOTS.
      IF(II.NE.1) GO TO 500
      ILEG=LEG
      ACRUZ=ICRUZ
  500 IF (ISTANM.EQ.999) GO TO 2550
C     INDICATES THAT A 999 CARD IS NEEDED AFTER THE LAST
C     STATION DATA CARD IN EACH LEG.
C     READ IN SEDIMENT SURFACE DATA
      IF(ITHTIM.LT.1)GO TO 51
C     THIS READS IN THE SEDIMENT SURFACE VELOCITY AND TIME
      DO 52 JJ=1,NCDS
   52 READ(5,60)TIME(JJ),VELOC(JJ)
```

```
      GO TO 2001
C     THIS READS THE SEDIMENT SURFACE VELOCITY AND THICKNESS
C     THIS IS THE FIRST DATA CARD FOR EACH STATION AND THE
C     THICKNESS WILL ALWAYS BE ZERO SINCE THIS IS
C     SEDIMENT SURFACE.
   51 READ(5,55) THICK(1),VELOC(1)
   55 FORMAT(F5.3,1X,F5.3)
C     INITIALIZES TIME AT ZERO.
      TIME(1)=0.0
C     READ IN SINGLE LAYER DATA AND CONVERT TO ONE
C     WAY TRAVEL TIME.  SINGLE LAYER DATA ARE STORED IN
C     THE ARRAYS THICK, VELOC, AND TIME FROM SUBSCRIPT
C     (2) TO SUBSCRIPT (LAYER)
C     THIS DETERMINES HOW MANY INDIVIDUAL LAYERS ARE TO BE
C     CALCULATED FOR A STATION.
      LAYER=NCDS/2+1
C     THIS TAKES CARE OF THE CASE OF ONLY A SEDIMENT SURFACE
C     VELOCITY.
      IF (LAYER.LE.1) GO TO 2001
C     INITIALIZE CTIME
      CTIME=0.0
C     THIS LOOP TAKES THE DATA READ IN ON INDIVIDUAL LAYERS
C     AND CALCULATES THE MIDPOINT TO THE LAYER IN TERMS OF ONE
C     WAY TRAVEL TIME FROM THE SEDIMENT SURFACE THESE ARE
C     STORED IN ARRAYS FOR FURTHER USE.
      DO 1000 JJ=2,LAYER
      READ(5,60) THICK(JJ),VELOC(JJ)
   60 FORMAT(F5.3,1X,F5.3)
      TIME(JJ)=CTIME+((THICK(JJ)*0.5)/VELOC(JJ))
      CTIME=CTIME+(THICK(JJ)/VELOC(JJ))
 1000 CONTINUE
C     READ IN AND PROCESS COMBINED LAYER DATA.
C     COMBINED LAYER VALUES ARE STORED IN ARRAYS FROM
C     SUBSCRIPT (ICOMB) TO SUBSCRIPT (NCDS)
C     SKIP THIS LOOP IF ONLY SEDIMENT SURFACE DATA IS
C     AVAILABLE OR ONLY SURFACE AND ONE SEDIMENT LAYER
C     DATA IS USED.
      IF(NCDS.LE.2) GO TO 2001
      CTIME=0.0
      ITALLY=2
      ICOMB=LAYER+1
      DO 2000 KK=ICOMB,NCDS
      READ(5,70) THICK(KK),VELOC(KK)
   70 FORMAT(F5.3,1X,F5.3)
      TIME(KK)=CTIME+((THICK(KK)*0.5)/VELOC(KK))
      CTIME=CTIME+(THICK(ITALLY)/VELOC(ITALLY))
      ITALLY=ITALLY+1
C     THIS SEQUENCE STORES THE CALCULATED TRAVEL TIMES, THE
C     THICKNESS AND VELOCITIES  FROM INDIVIDUAL STATIONS INTO
C     LARGE ARRAYS FOR THE ENTIRE  LEG.
 2000 CONTINUE
 2001 ICOUNT=ICOUNT+NCDS
      ITALLY=1
      DO 3000 NN=ITOTAL,ICOUNT
```

```
      VLEG(NN)=VELOC(ITALLY)
      TLEG(NN)=TIME(ITALLY)
      THIN(NN)=THICK(ITALLY)
      ITALLY=ITALLY+1
 3000 CONTINUE
      ITOTAL=ITOTAL+NCDS
 5000 CONTINUE
C     ESTABLISHES THE PLOT TITLE
 2550 WRITE(6,72) ILEG
   72 FORMAT(' DATA FOR LEG ',A2)
C     PRINTS OUT THICKNESS, TRAVEL TIME, AND VELOCITY
C     BY STATION.
      DO 350 LL=1,ICOUNT
      IF(ITHTIM.LT.1)WRITE(6,75) LL,THIN(LL),VLEG(LL),TLEG(LL)
   75 FORMAT(' POINT NUMBER ',I3,3X,'THICKNESS ',
     *   F5.3,3X,'VELOCITY= ',F5.3,3X,'TIME= ',F5.3)
      IF(ITHTIM.GE.1)WRITE(6,76)LL,VLEG(LL),TLEG(LL)
   76 FORMAT(' POINT NUMBER ',I3,3X,'VELOCITY= ',F5.3,3X,
     *'TIME= ',F5.3)
  350 CONTINUE
C     ESTABLISHES CRUISE AND LEG TITLE FOR PLOTS
 2500 ENCODE(80,XTITLE) ACRUZ,ILEG
   80 FORMAT(' CRUISE ',A6,2X,'LEG ',A2,'$')
C     CALLS THE LEAST SQUARE FIT SUBPROGRAMS.
      CALL LEGLST(VLEG,TLEG,ICOUNT,XTITLE)
      CALL LEGPAR(VLEG,TLEG,ICOUNT,XTITLE)
      CALL LEGEXP(VLEG,TLEG,ICOUNT,XTITLE)
 4000 CONTINUE
      CALL DONEPL
      STOP
      END
 EOF:124
```

```
C     SUBPROGRAM FOR LEAST SQUARE LINE OF VEL/TIME DATA BY LEG
C     SUMX=SUM OF THE XS (VLEG)
C     SUMY=SUM OF THE YS (TLEG)
C     SUMW=SUM OF THE WS (A WEIGHTING FACTOR)
C     SUMXW=SUM OF THE X * WS
C     SUMYW=SUM OF THE Y * WS
C     SUMXYW=SUM OF THE X * Y * WS
C     SUMYSW=SUM OF THE Y SQ. * WS
      SUBROUTINE LEGLST(VLEG,TLEG,ICOUNT,XTITLE)
C     SETS AND CREATES STORAGE FOR DATA TO BE MANIPULATED.
      DIMENSION VLEG(500),
     *          XEST(500),
     *          TLEG(500)
      DIMENSION X(80),
     *          Y(80),
     *          W(1000)
      CHARACTER XTITLE*23,
     *          YTITLE*36,
     *          ZTITLE*32
C     INITIALIZED THESE QUANTITIES AT ZERO.
      SUMW=0.
      SUMX=0.
      SUMXW=0.
      SUMY=0.
      SUMYW=0.
      SUMXYW=0.
      SUMYSW=0.
C     GIVES WEIGHTING TO FIRST DATA POINT THIS POINT SHOULD
C     BE THE SEDIMENT SURFACE VELOCITY VALUE DESIRED FOR THE
C     DATA GROUP AND THE SURFACE POINT THROUGH WHICH THE CURVE
C     FIT IS TO BE FORCED. WEIGHT FIRST POINT BY GIVING W(1)
C     A HIGH VALUE
      W(1)=5
      DO 500 LL=2,ICOUNT
  500 W(LL)=1.
C     TAKING THE VALUES CALCULATED AND STORED IN THE MAIN
C     PROGRAM, THE VARIOUS SUMS ARE CALCULATED FROM THE
C     VALUES. READ THROUGH VELOC AND TIME TO OBTAIN VARIABLES
C     FOR LEAST SQUARES EQUATION
      DO 1000 JJ=1,ICOUNT
      SUMX=SUMX+VLEG(JJ)
      SUMY=SUMY+TLEG(JJ)
      SUMW=SUMW+W(JJ)
      SUMXW=SUMXW+(VLEG(JJ)*W(JJ))
      SUMYW=SUMYW+(TLEG(JJ)*W(JJ))
      SUMXYW=SUMXYW+(VLEG(JJ)*TLEG(JJ)*W(JJ))
 1000 SUMYSW=SUMYSW+(TLEG(JJ)**2.*W(JJ))
      XAVE=SUMX/ICOUNT
C     USE THE CALCULATED SUMS TO OBTAIN CONSTANT "A" FOR
C     EQUATION OF BEST LEAST SQUARE FIT LINE X=A+BY
C     CREATE A0 VARIABLE FOR LEAST SQ EQUATION
      A0=((SUMXW*SUMYSW)-(SUMYW*SUMXYW))/
     * ((SUMW*SUMYSW)-SUMYW**2)
C     USE CALCULATED SUMS TO OBTAIN CONSTANT "B".
```

```
C     CREATE A1 VARIABLE FOR LEAST SQ EQUATION
      A1=((SUMW*SUMXYW)-(SUMXW*SUMYW))/
      * ((SUMW*SUMYSW)-SUMYW**2)
C     PRINT CONSTANTS A AND B.
      PRINT 90,A0,A1
C     DERIVE POINTS FOR BEST FIT LINE USING DETERMINED
C     CONSTANTS AND ITERATED VALUES OF Y.
C     DERIVE X AND Y POINTS FOR LINE BY USING
C     EQUATION FOR EVERY TICK MARK ON THE Y AXIS
      YORIG=0.0
      DO 2000 II=1,80
      Y(II)=YORIG
      YORIG=YORIG+0.05
      X(II)=A0+A1*Y(II)
 2000 CONTINUE
C     DETERMINE CORRELATION COEFFICIENT FOR THE BEST FIT LINE
C     USING DETERMINED COEFFICIENTS AND OTHER PREVIOUSLY
C     CALCULATED SUMS.
C     CORRELATION COEFFICIENT
C     FIND ESTIMATED YS BY USING FORMULA
C     ON EACH X VALUE
      SSR=0
      SST=0
      DO 1500 LL=1,ICOUNT
      XEST(LL)=A0+(A1*TLEG(LL))
      SSR=SSR+(VLEG(LL)-XEST(LL))**2
      SST=SST+(VLEG(LL)-XAVE)**2
 1500 CONTINUE
      COC=SQRT(ABS(1-(SSR/SST)))
C     PRINT THE DETERMINED CORRELATION COEFFICIENT.
      PRINT 90,COC
C     CALCULATES VARIANCE FOR BEST FIT LINE.
      SUMV=0.0
      DO 750 NN=1,ICOUNT
      SUMV=SUMV+((VLEG(NN)-XEST(NN))**2)
  750 CONTINUE
      VAR=SUMV/ICOUNT
C     PRINTS VARIANCE VALUES.
      PRINT 90,VAR
C     CALLS COMMANDS FOR DRAWING GRAPH, PLOTTING POINTS AND
C     CURVE AND LABELING PLOT AND AXES.
      ENCODE(70,ZTITLE) COC
   70 FORMAT(' CORRELATION COEFFICIENT= ',F5.3,'$')
      ENCODE(80,YTITLE) A1,A0
   80 FORMAT(' A1=',F5.3,2X,'A0=',F5.3,5X,'X=A0 + A1*Y$')
      CALL TITLE(' ',1,0,0,'ONE WAY TRAVEL TIME IN SECS.$',
      *  100,6.0,8.0)
      CALL XTICKS(1)
      CALL YTICKS(2)
      CALL GRAF(1.4,0.2,5.0,4.0,-0.5,0.0)
      CALL XGRAXS(1.4,0.2,5.0,6.0,'VELOCITY-KM/SEC$',
      *  -100,0.,8.)
      CALL MARKER(8)
      CALL CURVE(VLEG,TLEG,ICOUNT,-1)
```

```
      CALL CURVE(X,Y,19,0)
      CALL MESSAG(YTITLE,100,0.5,-0.5)
      CALL MESSAG(XTITLE,100,0.5,9.0)
      CALL MESSAG(ZTITLE,100,0.5,0.0)
   90 FORMAT( )
      RETURN
      END
```

```
C     SUBPROGRAM FOR PARABOLIC CURVE ON VEL/TIME DATA BY LEG
      SUBROUTINE LEGPAR(VLEG,TLEG,ICOUNT,XTITLE)
C     SUMX=SUM OF THE XS (VELOC)
C     SUMY=SUM OF THE YS (TIME)
C     SUMYSQ=SUM OF THE Y SQUAREDS
C     SUMYCU=SUM OF THE Y CUBEDS
C     SUMYFO=SUM OF THE Y TO THE FOURTHS
C     SUMXY=SUM OF THE X*YS
C     SUMYSX=SUM OF THE Y SQ. * XS
C     XAVE= AVERAGE OF XS (WITHOUT WEIGHTED PTS.)
C     ESTABLISH LIMIT AND STORAGE FOR DATA TO BE MANIPULATED.
      DIMENSION VLEG(500),
     *          TLEG(500)
      DIMENSION X(80),
     *          Y(80),
     *          A(3,3),
     *          B(3),
     *          WTVEL(5),
     *          WTTIM(5),
     *          XEST(500)
      CHARACTER XTITLE*23,
     *          YTITLE*30,
     *          ZTITLE*32
C     INITIALIZES SUMS TO ZERO.
      SUMX=0.
      SUMY=0.
      SUMYSQ=0.
      SUMYCU=0.
      SUMYFO=0.
      SUMXY=0.
      SUMYSX=0.
      ZERO=1.0E-06
C     THIS WEIGHTS THE INITIAL DATA POINT (SEDIMENT SURFACE
C     VELOCITY) WITH A WEIGHT AS SPECIFIED IN LINE 276 WHILE
C     ALL OTHER DATA POINTS HAVE A VALUE OF ONE.
C     WEIGHTING FOR SPECIFIC POINTS
C     VALUES TO BE WEIGHTED ARE ADDED ONTO THE END OF
C     EXISTING DATA ARRAYS AND PROCESSED AS ACTUAL POINTS
C     ISED=NUMBER OF POINTS BEING WEIGHTED
C     WTVEL AND WTTIM ARE ARRAYS THAT HOLD THE VALUES
C     THAT ARE TO BE WEIGHTED
C     IWT IS AN ARRAY WHICH HOLDS THE WEIGHT FACTOR
C     FOR THE WTVEL AND WTTIM VALUES OF THE CORRESPONDING
C     SUBSCRIPT.
C     NOTE: AN IWT VALUE OF 1 MEANS THAT A VALUE IS BEING
C     WEIGHTED BY 2 SINCE THE VALUE HAS ALREADY BEEN READ
C     INTO VLEG AND TLEG ARRAYS ON THE INITIAL READ
C     NUM= FINAL NUMBER OF POINTS AFTER WEIGHTING
      WTTIM(1)=0.000
      WTVEL(1)=VLEG(1)
      IWT=5
      ITALLY=ICOUNT+1
      NUM=ICOUNT+IWT
      DO 500 NN=ITALLY,NUM
```

```
      VLEG(NN)=WTVEL(1)
      TLEG(NN)=WTTIM(1)
  500 CONTINUE
C     THIS CALCULATES THE SUM OF THE VARIOUS SUMS NEEDED FOR
C     MAKING THE LEAST SQUARE PARABOLIC FIT TO THE DATA. DATA
C     IS PULLED FROM THE MAIN PROGRAM.
C     READ THROUH VELOC AND TIME TO OBTAIN SUMS
      DO 1000 JJ=1,NUM
      SUMX=SUMX+VLEG(JJ)
      SUMY=SUMY+TLEG(JJ)
      SUMYSQ=SUMYSQ+(TLEG(JJ)**2)
      SUMYCU=SUMYCU+(TLEG(JJ)**3)
      SUMYFO=SUMYFO+(TLEG(JJ)**4)
      SUMXY=SUMXY+(VLEG(JJ)*TLEG(JJ))
      SUMYSX=SUMYSX+((TLEG(JJ)**2)*VLEG(JJ))
 1000 CONTINUE
C     CALCULATES THE SUM OF THE VELOCITIES FOR USE LATER IN
C     THE COEFFICIENT OF CORRELATION COMPUTATION.
C     SUM THE XS WITHOUT THE WEIGHTED VALUES TO
C     FIND A TRUE AVERAGE FOR THE COC EQUATION
      XSUM=0.
      DO 1200 KK=1,ICOUNT
 1200 XSUM=XSUM+VLEG(KK)
      XAVE=XSUM/ICOUNT
C     DETERMINE COEFFICIENT OF LEAST SQUARE BEST FIT PARABOLA
C     CURVE X=A+BY+CY2 USING METHOD OF SIMULTANEOUS SOLUTION
C     OF THREE EQUATIONS BY MATRIX METHOD .  PRINT THE THREE
C     COEFFICIENTS. SOLVE SIMULTANEOUS EQUATIONS FOR
C     COEFFICIENTS OF PARABOLIC EQUATION
      A(1,1)=NUM
      A(1,2)=SUMY
      A(1,3)=SUMYSQ
      A(2,1)=SUMY
      A(2,2)=SUMYSQ
      A(2,3)=SUMYCU
      A(3,1)=SUMYSQ
      A(3,2)=SUMYCU
      A(3,3)=SUMYFO
      B(1)=SUMX
      B(2)=SUMXY
      B(3)=SUMYSX
      DO 100 I=1,3
      DIV=A(I,I)
      IF(ABS(DIV)-ZERO) 99,99,1
    1 DO 101 J=1,3
      A(I,J)=A(I,J)/DIV
  101 CONTINUE
      B(I)=B(I)/DIV
      DO 102 J=1,3
      IF(I-J) 2,102,2
    2 RATIO=A(J,I)
      DO 103 K=1,3
      A(J,K)=A(J,K)-RATIO*A(I,K)
  103 CONTINUE
```

```
      B(J)=B(J)-RATIO*B(I)
  102 CONTINUE
  100 CONTINUE
      PRINT 90,B(1),B(2),B(3)
C     USING  THE  THREE COEFFICIENTS JUST DETERMINED DERIVE
C     POINTS FOR THE CURVE  BY USING ITERATED VALUES OF Y
C     AND CALCULATING THE CORRESPONDING X VALUES.
   99 YORIG=0.0
C     DERIVE X AND Y POINTS FOR LINE BY USING
C     EQUATION FOR EVERY TICK MARK ON THE Y AXIS
      DO 2000 II=1,80
      Y(II)=YORIG
      YORIG=YORIG+0.05
      X(II)=B(1)+(B(2)*Y(II))+(B(3)*Y(II)**2)
 2000 CONTINUE
C     CALCULATES THE CORRELATION COEFFICIENT FOR THE BEST
C     FIT LEAST SQUARE PARABOLA TO THE DATA USING PREVIOUSLY
C     CALCULATED QUANTITIES.
C     CORRELATION COEFFICIENT
C     FIND ESTIMATED XS BY USING FORMULA ON EACH Y VALUE
      SSR=0
      SST=0
      DO 1500 LL=1,ICOUNT
      XEST(LL)=B(1)+(B(2)*TLEG(LL))+(B(3)*TLEG(LL)**2)
      SSR=SSR+(VLEG(LL)-XEST(LL))**2
      SST=SST+(VLEG(LL)-XAVE)**2
 1500 CONTINUE
      COC=SQRT(ABS(1-(SSR/SST)))
C     PRINT THE CORRELATION COEFFICIENT.
      PRINT 90,COC
C     USING PREVIOUSLY CALCULATED QUANTITIES CALCULATE AND
C     PRINT OUT THE VARIANCE FOR THE LEAST SQUARE FIT CURVE.
      SUMV=0.0
      DO 750 NN=1,ICOUNT
      SUMV=SUMV+((VLEG(NN)-XEST(NN))**2)
  750 CONTINUE
      VAR=SUMV/ICOUNT
      PRINT 90,VAR
C     ESTABLISH GRAPH PLOT HEADINGS AND CALL  PLOT ROUTINES
C     FOR THE GRAPH.
      ENCODE(70,ZTITLE) COC
   70 FORMAT(' CORRELATION COEFFICIENT= ',F5.3,'$')
      ENCODE(80,YTITLE) B(1),B(2),B(3)
   80 FORMAT(' B0=',F5.3,2X,'B1=',F5.3,2X,'B2=',F5.3,'$')
      CALL CURVE(X,Y,19,0)
      CALL MESSAG(YTITLE,100,0.5,1.0)
      CALL MESSAG(XTITLE,100,0.5,9.0)
      CALL MESSAG(ZTITLE,100,0.5,1.5)
      CALL MESSAG('  X= B0 + B1*Y + B2*Y**2$',100,0.5,0.5)
   90 FORMAT( )
      RETURN
```

```
C     SUBPROGRAM FOR EXPONENTIAL CURVE FIT OF VELOCITY/TIME
C     DATA BY LEG THE METHOD IS THE SAME AS THAT FOR THE FIT
C     TO DATA BY STATION
C     THE XS,YS,XYS AND YSQUARES ARE SUMMED AND A W WEIGHTING
C     FACTOR IS USED
      SUBROUTINE LEGEXP(VLEG,TLEG,ICOUNT,XTITLE)
C     ESTABLISHES STORAGE AND LIMITS FOR QUANTITIES TO BE
C     CALCULATED FOR LATER MANIPULATION.
      DIMENSION VLEG(500),
     *          TLEG(500),
     *          XEST(500)
      DIMENSION X(80),
     *          Y(80),
     *          W(500),
     *          LOGVEL(500)
      CHARACTER XTITLE*23,
     *          YTITLE*35,
     *          ZTITLE*37
      REAL LOGVEL
C     INITIALIZES THE QUANTITIES TO BE CALCULATED AT ZERO.
      SUMX=0.
      SUMY=0.
      SUMW=0.
      SUMXW=0.
      SUMYW=0.
      SUMXYW=0.
      SUMYSW=0.
C     TAKES THE LOG OF THE VELOCITY VALUES (VLEG) IN THE MAIN
C     PROGRAM AND PRINTS THE LOG VALUES AND THE BASIC VALUES.
C     LOG X VALUES(VLEG)
      DO 300 KK=1,ICOUNT
      LOGVEL(KK)=ALOG(VLEG(KK))
      PRINT 90,VLEG(KK),TLEG(KK),LOGVEL(KK)
  300 CONTINUE
C     GIVES THE SEDIMENT SURFACE VELOCITY AND THICKNESS A
C     WEIGHTING.
C     THIS IS THE FIRST DATA POINT READ IN THE MAIN PROGRAM.
C     WEIGHT FIRST POINT BY GIVING W(1) A HIGH VALUE
      W(1)=5
      DO 500 LL=2,ICOUNT
  500 W(LL)=1.
C     USING DATA QUANTITIES FROM MAIN PROGRAM AND CALCULATED
C     LOG VALUES ABOVE , CALCULATES THE VARIOUS  SUMS NEEDED
C     FOR THE LEAST SQUARES FIT TO THE DATA  AND PRINTS OUT
C     THE SUMS.
C     READ THROUGH LOGVEL AND TLEG TO OBTAIN VARIABLES
C     FOR LEAST SQUARES EQUATION
      DO 1000 JJ=1,ICOUNT
      SUMX=SUMX+VLEG(JJ)
      SUMY=SUMY+TLEG(JJ)
      SUMW=SUMW+W(JJ)
      SUMXW=SUMXW+(LOGVEL(JJ)*W(JJ))
      SUMYW=SUMYW+(TLEG(JJ)*W(JJ))
      SUMXYW=SUMXYW+(LOGVEL(JJ)*TLEG(JJ)*W(JJ))
```

```
 1000 SUMYSW=SUMYSW+(TLEG(JJ)**2*W(JJ))
      PRINT 90,SUMX,SUMY,SUMW,SUMXW,SUMYW,SUMXYW,SUMYSW
C     CALCULATES A SUM NEEDED IN DETERMINING THE CORRELATION
C     COEFFICIENT.
      XAVE=SUMX/ICOUNT
C     DETERMINES THE COEFFICIENT B0 IN THE LEAST SQUARE FIT
C     EQUATION LOGX=LOGA+LOGBY WHERE B0=LOGA.
C     CREATE B0 VARIABLE FOR LEAST SQUARES EQUATION
      B0=((SUMXW*SUMYSW)-(SUMYW*SUMXYW))/
      * ((SUMW*SUMYSW)-SUMYW**2)
C     DETERMINES THE COEFFICIENT B1 WHERE B1=LOGB
C     CREATE B1 VARIABLE FOR LEAST SQUARES EQUATION
      B1=((SUMW*SUMXYW)-(SUMXW*SUMYW))/
      * ((SUMW*SUMYSW)-SUMYW**2)
C     TAKE THE ANTILOG OF B0 AND B1 TO OBTAIN COEFFICIENTS
C     A0 AND A1 OF THE EQUATION X=AB**Y
C     PRINT THE COEFFICIENTS.
      A0=EXP(B0)
      A1=EXP(B1)
      PRINT 90,A0,A1
C     DERIVE THE POINTS FOR THE BEST FIT CURVE X=AB**Y USING
C     THE COEFFICIENTS JUST DETERMINED AND ITERATED VALUES OF
C     Y TO CALCULATE CORRESPONDING VALUES OF X.
C     DERIVE X AND Y POINTS FOR CURVE BY USING
C     EQUATION FOR EVERY 0.05 VALUE OF THE Y AXIS
      YORIG=0.0
      DO 2000 II=1,50
      Y(II)=YORIG
      YORIG=YORIG+0.05
      X(II)=A0*(A1**Y(II))
 2000 CONTINUE
C     CALCULATES CORRELATION COEFFICIENT USING DERIVED
C     EQUATION COEFFICIENTS AND PREVIOUSLY CALCULATED
C     QUANTITIES
C     PRINT COEFFICIENT.
C     CORRELATION COEFFICIENT
C     FIND ESTIMATED XS BY USING FORMULA ON
C     EACH ACTUAL Y VALUE
      SSR=0
      SST=0
      DO 1500 LL=1,ICOUNT
      XEST(LL)=A0*(A1**TLEG(LL))
      SSR=SSR+(VLEG(LL)-XEST(LL))**2
      SST=SST+(VLEG(LL)-XAVE)**2
 1500 CONTINUE
      COC=SQRT(ABS(1-(SSR/SST)))
      PRINT 90,COC
C     CALCULATES VARIANCE USING PREVIOUSLY DERIVED EQUATION
C     COEFFICIENTS AND PRINTS VARIANCE.
      SUMV=0.0
      DO 750 NN=1,ICOUNT
      SUMV=SUMV+((VLEG(NN)-XEST(NN))**2)
  750 CONTINUE
      VAR=SUMV/ICOUNT
```

```
      PRINT 90,VAR
C     CALL VARIOUS CURVE PLOTTING AND TITLE PLOTTING
C     ROUTINES, PLOT GRAPH AND BEST FIT CURVE WITH AXES
C     TITLES AND GRAPH TITLES.
      ENCODE(70,ZTITLE) COC
   70 FORMAT(' CORRELATION COEFFICIENT EXPO= ',F5.3,'$')
      ENCODE(80,YTITLE) A1,A0
   80 FORMAT(' A1=',F5.3,2X,'A0=',F5.3,5X,'X=A0*A1**Y$')
      CALL CURVE(X,Y,50,0)
      CALL MESSAG(YTITLE,100,0.5,2.0)
      CALL MESSAG(ZTITLE,100,0.5,2.5)
   90 FORMAT( )
      CALL ENDPL(1)
      RETURN
      END
```

APPENDIX F

PROGRAM FOR VELOCITY/DEPTH PLOT FOR GROUPS OF STATIONS

```
      IMPLICIT DOUBLE PRECISION(S)
C     ESTABLISHES STORAGE FOR THE VELOCITY, TIME, DEPTH,
C     AND TITLE QUANTITIES TO BE USED LATER IN
C     PLOTTING AND CURVE FITTING.
      DIMENSION VINST(50),
     * DEPTH(50),
     * TIM(50),
     * XTITLE(7)
      CALL COMPRS
C     READS IN COEFFICIENTS FOR THE VELOCITY FUNCTION
C     OBTAINED IN PROGRAM VLEG.
C     AN "END" CARD STOPS THE PROGRAM.
    5 READ(5,10,END=4000)A,B,IGROUP
   10 FORMAT(F7.4,1X,F7.4,1X,I2)
C     THE FOLLOWING FORTRAN STATEMENTS ARE COMMENTED OUT
C     BUT WHEN THE CUBED TERM IS NOT DESIRED THEY SHOULD
C     BE CONVERTED INTO LEGITIMATE STATEMENTS AND THE
C     PRECEEDING FORTRAN STATEMENTS SHOULD BE COMMENTED OUT.
C ************************************************************
C5    READ(5,10,END=4000)A,B,C,IGROUP
C10   FORMAT(F7.4,1X,F7.4,1X,F7.4,1X,I2)
C ************************************************************
C     ESTABLISHES THE GRAPH PLOT TITLE
C     (INSERT GROUP NUMBER DESIRED)
      ENCODE(15,XTITLE),IGROUP
   15 FORMAT(' DATA GROUP ',I2,'$')
C     INITIALIZES TIME AT ZERO.
      TIME=0.0
C     ESTABLISHES THE NUMBER OF DATA POINTS TO BE GENERATED.
      ICOUNT=9
C     GENERATES THE DATA POINTS FOR THE VELOCITY
C     VERSUS DEPTH PLOT.
      DO 300 MM=1,ICOUNT
      TIM(MM)=TIME
      VINST(MM)=A+(B*TIM(MM))
      DEPTH(MM)=A*TIM(MM)+((B*TIM(MM)**2)/2)
C     THE FOLLOWING FORTRAN STATEMENTS ARE COMMENTED
C     OUT ALSO; BUT WHEN THE CUBFD TERM IS NOT DESIRED THEY,
C     TOO, SHOULD BE CONVERTED INTO LEGITIMATE STATEMENTS AND
C     THE TWO PRECEEDING  STATEMENTS SHOULD BE COMMENTED OUT.
C ************************************************************
C     VINST(MM)=A+(B*TIM(MM))+(C*(TIM(MM))**2)
C     DEPTH(MM)=A*TIM(MM)+((B*(TIM(MM))**2)/2)+
      *((C*(TIM(MM))**3)/3)
C ************************************************************
      TIME=TIME+0.05
  300 CONTINUE
C     PRINTS OUT THE HEADING FOR THE
C     TABULATION OF PLOT VALUES.
      WRITE(6,72)IGROUP
```

```
   72 FORMAT(' DATA FOR GROUP ',I2)
C     PRINTS OUT THE PLOT VALUES.
      DO 350 LL=1,ICOUNT
      WRITE(6,75)LL,DEPTH(LL),VINST(LL),TIM(LL)
   75 FORMAT(' POINT NUMBER ',I3,3X,' DEPTH ',
     *   F6.4,3X,' VELOCITY= ',F5.3,3X,' TIME= ',F4.2)
  350 CONTINUE
C     CALLS THE PARABOLIC LEAST SQUARES CURVE
C     FITTING SUB PROGRAM.
      CALL LEGPAX(VINST,DEPTH,ICOUNT,XTITLE)
C     CALL LSTPAX(VINST,DEPTH,ICOUNT,XTITLE)
C     CALLS THE PLOTTING ROUTINE.
      CALL ENDPL(1)
C     RETURNS TO THE START OF THE PROGRAM TO PROCESS
C     ANOTHER SET OF DATA.
      GO TO 5
 4000 CONTINUE
C     ENDS THE PROGRAM.
      CALL DONEPL
      STOP
      END
```

DISTRIBUTION LIST

NUSC		1
NRL/Stennis Space Center		2
DTIC (Code OCC)		2
NAVOCEANO Code	CO	1
	CJL	15
	CJTP	1
	M	1
	O	1
	OA	1
	OAP	1
	OAPC	2
	OW	1
	P	1
	TD	1
SAI		1
University of Hawaii		8